

METAL-DOPED RARE EARTH OXIDE CATALYSTS FOR CONDENSATIONS TO KETONES

A Thesis,

Submitted to the Graduate Faculty of the
Louisiana State University and
Agricultural and Mechanical College
in partial fulfillment of the
requirements for the degree of
Master of Science in Chemical Engineering

In

The Department of Chemical Engineering

by
Arvind Karkal Bhat
B.E., Mangalore University, 1995
August 2004

ACKNOWLEDGEMENTS

I would like to thank Dr. Kerry M. Dooley, my advisor. He has been an inspiration; his endless knowledge and motivation were irreplaceable. Thanks to EagleView Technologies, Inc and MGK Co. for providing the funding for my research. My thanks to Dr. Elizabeth J. Podlaha and Dr. F. Carl Knopf, for serving on my thesis committee. I would also like to thank Dr. Amitava Roy for assisting me with my XAS work at CAMD. I would like to thank the assistance provided by Mr. Paul Rodriguez, Mr. Frederick McKenzie, Mr. Joe Bell and Mr. Robert Perkins from the Chemical Engineering Workshop. Lastly, I would like to thank my family, and friends for their continual support and advice over the past three years.

TABLE OF CONTENTS

ACKNOWLEDGEMENTS	ii
LIST OF TABLES	iv
LIST OF FIGURES	v
ABSTRACT	vii
CHAPTER 1. INTRODUCTION AND REVIEW OF LITERATURE	1
1.1 Goals and Project Summary	1
1.2 Effect of Dopants on the Catalytic Activity of the Active Metal Oxide	2
1.3 Effect of Dopants on the Structure of the Active Metal Oxide	6
1.4 Study of Doped Metal Oxides by X-ray Absorption Spectroscopy	7
CHAPTER 2. EXPERIMENTAL	11
2.1 Catalyst Preparation	11
2.2 Continuous Flow Reactor Experiments	12
2.3 Analysis of Feed and Product Samples	16
2.4 Catalyst Characterization	17
CHAPTER 3. RESULTS AND DISCUSSION	21
3.1 Continuous Reactor Experiments	21
3.1.1 IBA feed – CeO ₂ /Al ₂ O ₃ Catalysts	22
3.1.2 IBA Feed – Modified CeO ₂ /Al ₂ O ₃ Catalysts	31
3.1.3 IBA Feed – Metal-Doped CeO ₂ /Al ₂ O ₃ Catalysts	31
3.1.4 3/1 HOAc/DOAc Feeds – CeO ₂ /Al ₂ O ₃ Catalysts	34
3.1.5 3/1 HOAc/DOAc feeds – Metal-Doped CeO ₂ /Al ₂ O ₃ Catalysts	40
3.2 Catalyst Characterization	41
CHAPTER 4. CONCLUSIONS	58
REFERENCES	63
APPENDIX A. GAS CHROMATOGRAPHY (GC) DETAILS	66
APPENDIX B. MASS BALANCE CALCULATIONS AND RESULTS FOR REACTOR EXPERIMENTS	69
VITA	104

LIST OF TABLES

2.1: Composition, Size and Shape of Catalysts Used	11
2.2: XAS – Experimental Details.....	19
3.1: Surface areas for CeO ₂ /Al ₂ O ₃ Catalysts	22
3.2: Summary of Results of Isobutyric Acid Condensation on CeO ₂ /Al ₂ O ₃ Catalysts ...	28
3.3: Summary of Results of Isobutyric Acid Condensation on Modified CeO ₂ /Al ₂ O ₃ Catalysts.....	33
3.4: Summary of Results of Isobutyric Acid Condensation on Metal-Doped CeO ₂ /Al ₂ O ₃ Catalysts.....	33
3.5: Summary of Results of 3/1 HOAc/DOAc Condensation on CeO ₂ /Al ₂ O ₃ Catalysts	41
3.6: Metal Dispersion for Catalysts at 0 °C.....	43
3.7: Metal Dispersion for Catalysts at 150 °C.....	43
3.8: Results of TGA Experiments –Unused vs. Used Catalysts	45
3.9: Fitted parameters of the Takahashi model for Ce(III) acetate and CeO ₂	51
3.10: Fitted parameter, method of Takahashi et al., for 15 wt.% CeO ₂ /Al ₂ O ₃ treated in H ₂ at 420 °C.....	51
3.11: Comparison of method of Takahashi et al. (2002) with least-squares refinement, WinXAS, for Ce L _{III} -edge XANES spectra.....	54
A.1: GC Settings for IBA Product Analysis	66
A.2: Retention Times for IBA Products	66
A.3: GC Settings for HOAc/DOAc Product Analysis.....	67
A.4: Retention Times for HOAc/DOAc Products using GC, Analysis of Liquid Phases	67
A.5: GC Settings for HOAc/DOAc Products, Gas Phase Analysis.....	68
A.6: Retention Times for HOAc/DOAc Products, Gas Phase Analysis.....	68

LIST OF FIGURES

2.1: Schematic of Low Pressure Continuous Flow Reactor system	13
2.2: Schematic of High Pressure Continuous Flow Reactor system.....	14
3.1: Run M-126, 20% CeO ₂ /Al ₂ O ₃ , 1.27 mm extrudate, IBA feed, WHSV ~5, P (IBA)=0.41 atm.....	25
3.2: Run M-115, 17% CeO ₂ /Al ₂ O ₃ , 1.59 mm extrudate, IBA feed, WHSV ~5, P (IBA)=0.41 atm.....	25
3.3: Data fit for a zero-order reaction, IBA feed, P (IBA)=0.41atm, X=IBA fractional conversion.....	26
3.4: Data fit for a first-order reaction, IBA feed, P (IBA)=0.41atm, X=IBA fractional conversion, ε = volumetric expansion factor	26
3.5: Effect of Catalyst Particle Size on Effectiveness Factor, IBA feed, P (IBA)=0.41atm, T=440 °C.....	27
3.6: Product Distribution, Run M-126, 20% CeO ₂ /Al ₂ O ₃ , 1.27 mm extrudate	27
3.7: Product Distribution, Run M-126, 20% CeO ₂ /Al ₂ O ₃ , 1.27 mm extrudate	28
3.8: Run M-124, 17% CeO ₂ /0.8% Co/Al ₂ O ₃ , 1.59 mm extrudate, IBA feed, WHSV ~5, P (IBA) = 0.41 atm.....	32
3.9: Product Distribution, Metal Doped CeO ₂ /Al ₂ O ₃ , 1.59 mm extrudate, 440 °C	35
3.10: Kinetics results, organic layer GC analysis. On the X-axis, “M” means in the morning, “A” in the late afternoon, and “D” denotes days during which there was no catalyst regeneration	36
3.11: Kinetics results, gas phase analysis, and overall mass balance	36
3.12: Data fit for a first-order reaction, 3/1 HOAc/DOAc feed, 400 °C, X=DOAc fractional conversion, ε = volumetric expansion factor.....	39
3.13: Data fit for a zero-order reaction, 3/1 HOAc/DOAc feed, 400 °C, X=DOAc fractional conversion.....	40
3.14: Comparison of Product Distributions at 400 °C for Pure/Doped 17% CeO ₂ /Al ₂ O ₃ at different WHSV	42
3.15: TGA analysis, fresh 18.4% CeO ₂ /Al ₂ O ₃ , 3.18 mm extrudate.....	45

3.16: TGA analysis, 18.4% CeO ₂ /Al ₂ O ₃ used in Run M-139, 3.18 mm extrudate.....	46
3.17: TGA analysis, 15% CeO ₂ /0.1% K ₂ O/Al ₂ O ₃ used in Run M-74, 1.27 mm extrudate.....	46
3.18: TGA analysis, 17% CeO ₂ /Al ₂ O ₃ used in Run M-81, 1.59 mm extrudate.....	47
3.19: Ce L _{III} -edge XANES spectra for Ce(III) acetate	51
3.20: Ce L _{III} -edge XANES spectra for CeO ₂	52
3.21: Ce L _{III} -edge XANES spectra for 15 wt.% CeO ₂ /Al ₂ O ₃ treated in H ₂ at 420 °C	52
3.22: Ce L _{III} -edge XANES spectra for 0.8 wt.% Co/17 wt.% CeO ₂ /Al ₂ O ₃ , treated in H ₂ at 420 °C.....	53
3.23: Comparison of Ce ³⁺ content for doped-CeO ₂ /Al ₂ O ₃ with CeO ₂ /Al ₂ O ₃ , 420 °C	53
3.24: Comparison of Co K-edge XANES spectra of various Co-doped CeO ₂ /Al ₂ O ₃ with standards, ambient conditions.....	55
3.25: Comparison of PRDF of 2.4 wt.% Co/CeO ₂ /Al ₂ O ₃ with Co and Co oxides, ambient conditions.....	56
3.26: Comparison of Pd L _{III} -edge XANES spectra, 0.8 wt.% Pd/17 wt.% CeO ₂ /Al ₂ O ₃ and standards, ambient conditions (PdO spectra courtesy of H. Modrow, Bonn University, Germany)	57

ABSTRACT

Metal-doped supported rare earth oxide catalysts were examined to determine their suitability for the decarboxylative condensation of two carboxylic acids to produce ketones. The catalysts were characterized based on chemisorption tests, coke analysis using thermo-gravimetric analysis and X-ray absorption spectroscopy. Effect of catalyst particle size on rate of reaction was studied for various supported cerium oxide catalysts. Catalysts were tested for activity, selectivity, and stability using isothermal fixed bed reactors. Optimal operating conditions for the production of diisopropyl ketone and methyl nonyl ketone were determined.

It was found that supported cerium oxide catalysts effectively catalyzed the condensation of isobutyric acid to diisopropyl ketone for up to 12 hours of operation at weight hourly space velocities of ~4-5. On most occasions these catalysts showed no sign of deactivation at the end of 12 hours. Reactivation with air at 540 °C was sufficient to maintain long-term activity. The optimal temperature range was 470-480 °C. Activity could be improved by using catalyst particle sizes < 1 mm. Doping (0.1 - 2.4 wt.%) a supported cerium oxide catalyst with a transition metal such as Mn or Pd deactivated the catalyst but the addition of 0.8 wt.% Co increased the molar yield to diisopropyl ketone.

For methylnonyl ketone production from acetic acid and decanoic acid the optimal operating conditions using supported cerium oxide catalysts were 400-420 °C at weight hourly space velocities of ~4-6. Buildup of coke on the catalyst was observed. However, yield loss due to this coke formation was negligible, and the coke was easily removed by reactivation with air at 520 °C. Doping a supported cerium oxide catalyst with a transition metal such as Co or Pd increased both the activity and selectivity.

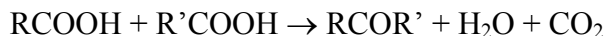
Reaction results indicate a ketene-like surface intermediate is involved in the mechanism. The role of the transition metal dopants may be to facilitate the recombination of atomic hydrogen, produced during the formation of a ketene-like intermediate, with surface $-OH$ groups, thereby increasing the reaction rate of ketone formation.

CHAPTER 1

INTRODUCTION AND REVIEW OF LITERATURE

1.1 Goals and Project Summary

Asymmetric (non-symmetric) ketones are known to be produced by the decarboxylative condensation of carboxylic acids (Rajadurai, 1994). The general reaction is:



Asymmetric ketones are useful as solvents for elastomers, polyvinyl acetate and other plastics. They are also used as reaction/extraction solvents and intermediates in making pesticides, herbicides, and pharmaceuticals. In this project, catalysts to make two such ketones of industrial interest, methylnonylketone (MNK) and diisopropyl ketone (DIPK) were studied. MNK is made by the decarboxylative condensation of acetic acid (HOAc) and decanoic acid (DOAc) (Randery, 1999), while DIPK is made by the decarboxylative coupling of isobutyric acid (IBA). MNK is useful as a raw material for herbicides and pharmaceutical products; also it can also be used as a dog and cat repellent. DIPK is used in nutrients, fragrances and flavorings.

From previous work of Randery (1999) and Hendren (2001) it was shown that CeO₂-based catalysts selectively catalyzed the acid/acid condensation reaction to non-symmetric ketones, up to high conversions. For the MNK product using 3/1 molar HOAc/DOAc feed the DOAc conversion at 420 °C was 94±2% using a 17 wt.% CeO₂/Al₂O₃ catalyst at weight hourly space velocities (WHSVs) ~4.8-7.4 (Hendren et al., 2003). The aim of this project was to further improve the activity and selectivity of these CeO₂-based catalysts by the addition of dopant metals like Co, Pd and Mn, in amounts

from 0.1 to 2.4 wt.%. Another goal was to reduce deactivation due to coking. For MNK product using 3/1 molar HOAc/DOAc feed a 15 wt.% CeO₂/3% K₂O/Al₂O₃ catalyst showed no signs of deactivation for up to 36 h of operation at WHSVs ~2.2-4.7 (Hendren, 2001). There are no comparable data for DIPK.

1.2 Effect of Dopants on the Catalytic Activity of the Active Metal Oxide

Catalysts containing Mn, Ce and Zr oxides deposited on Al₂O₃, SiO₂ and TiO₂ were studied by Glinski et al. (2000) for the ketonization of heptanoic acid. They observed that the effect of an alumina support on promotion of catalytic activity was pronounced. The catalysts supported on Al₂O₃ were the most active and the most selective of the group of catalysts containing supported MnO₂ and CeO₂. A ZrO₂/SiO₂ catalyst was the most selective among ZrO₂/support catalysts. Cryberg et al. (1986) had found that catalysts containing CeO₂ and ZrO₂ were viable for pinacolone synthesis from acetic acid and pivalic acid. Both these oxides have an amphoteric or a weak base nature (Brunelle, 1978; Lippert et al., 1991; Zhang et al., 1995; Yamanaka et al., 1975; Auroux et al., 1990). The activity of supported oxide phases in ketonization of heptanoic acid was in the following order: MnO₂ > CeO₂ > ZrO₂. Of all the catalysts studied, the MnO₂/support (Al₂O₃, SiO₂ or TiO₂) systems were the most active and selective catalysts. Of these, the MnO₂/Al₂O₃ system and in particular the 20 wt.% MnO₂/Al₂O₃ catalyst was the most active and selective catalyst, although at 375 °C the catalysts with an MnO₂ concentration of 10, 15 and 25 wt.% showed similar activity. This suggests the existence of an optimal value of MnO₂ loading on any conventional support. Assuming that the (1 1 1) plane of MnO₂ was exposed, from unit cell dimensions and atom density, the MnO₂ surface density is $1.14 \times 10^{-3} \text{ g/m}^2$. The surface density of MnO₂ for the 10 wt.%

MnO₂/Al₂O₃ catalyst was calculated to be $1.04 \times 10^{-3} \text{ g/m}^2$ (Glinski et al., 2000). Therefore the optimum MnO₂ loading corresponds to ~1-2.5 times theoretical monolayer coverage of MnO₂ on the Al₂O₃ support. The 20 wt.% MnO₂/Al₂O₃ catalyst also showed good stability during long-time experiments at 350 °C and 400 °C. For this catalyst, at 350 °C, LHSV~2 cm³/(g.h), the heptanoic acid conversion was found to decrease from a high of 84% after 4 h of time onstream to 59% after 20 h. Randery (1999), in his studies of the decarboxylative condensation of HOAc and cyclopropanecarboxylic acid (CCA) to methylcyclopropylketone (MCPK), had observed that TiO₂-supported CeO₂ was more selective than Al₂O₃-supported CeO₂, but was slightly less active. The lower activity was attributed to lower surface area as it was observed that high conversions could be achieved at low WHSVs.

The effect of alkali as promoters for zirconia-supported catalysts was studied by Parida et al. (1999), for ketonization of acetic acid. Except for Li, all the alkali metal cations were capable of enhancing the catalytic activity, in the order Na > K > Cs > Li. ZrO₂, being moderately basic (as observed by surface basicity measurements using phenol and acrylic acid), shows appreciable activity for ketonization. However, Randery et al. (2002) had observed that the addition of ZrO₂, in 1/1 to 3.5/1 molar ratio (Ce/Zr), to CeO₂/Al₂O₃ reduced the selectivity to MCPK. The surface interaction pathway of two carboxylates, for acetone from acetic acid, is favored by oxides of high lattice energy (Pestman et al., 1997); ZrO₂ is an oxide of high lattice energy. Sodium stabilizes the tetragonal phase of zirconia, and alkali metals, specifically sodium, favor the formation of surface carbonate groups. Both modifications appear to promote ketonization (Parida et al., 1999). A decrease in activity in the case of the Li-doped sample may have been due

to the drastic decrease in surface area of this catalyst. Therefore the alkali metal can have unexpected effects on the surface structure.

Doping with alkaline earth oxides was found to deactivate the catalyst towards ketonization of acetic acid (Parida et al., 1999). Blackening of the samples at the end of the reaction indicated coke formation. Transition metals were also observed to be good promoters for unsupported ZrO_2 , but rapid deactivation also took place. Samarium doping (0.5 mol%) of ZrO_2 was found to increase catalytic activity, whereas cerium (0.5 mol%) and yttrium (0.5 mol%) doping reduced the catalytic activity.

Supporting 10 wt.% of relatively acidic oxides (B_2O_3 , P_2O_5 , MoO_3 , V_2O_5 and WO_3) on SiO_2 gave low activities for the ketonization of acetic acid when compared to MnO_2/SiO_2 or CeO_2/SiO_2 (Glinski et al., 1995). Methane and CO were detected as major side products in the stream of CO_2 leaving the reactor. For catalysts containing 10 wt.% of either B_2O_3 , P_2O_5 , Al_2O_3 , or Fe_2O_3 supported on SiO_2 , there is rapid formation of coke deposits at temperatures higher than 350 °C.

The addition of Group VIII metals (Pd, Pt, Rh) to the activity of metal oxides was studied by Yee et al. (1999) and He et al. (2002). Yee et al. (1999) have studied the reaction of ethanol to acetaldehyde, acetone and benzene on unreduced and H_2 -reduced CeO_2 and 1 wt.% Pd/ CeO_2 by TPD, IR, and steady-state kinetics. They have suggested that the synthesis of acetone was via two different reaction mechanisms, one on the oxide (acetate coupling) and another in the presence of Pd (acetyl disproportionation). Idriss et.al. (1995), in their studies of reactions of acetaldehyde on the surfaces of CeO_2 , 3 wt.% Pd/ CeO_2 , 3 wt.% Co/ CeO_2 , and 3 wt.% Pd-3 wt.% Co/ CeO_2 , have observed ketonization to occur at lower temperatures for the metal-doped catalysts. Other reactions which were

observed were reduction to ethanol, oxidation to acetates, β – aldolization to crotonaldehyde and crotyl alcohol, carboxylate ketonization, an acetyl reaction with an adsorbed methyl group to give, also, acetone (this reaction observed only on Pd/CeO₂, Co/CeO₂ and Pd-Co/CeO₂ catalysts) and reductive coupling of two molecules of acetaldehyde to form butenes and butadiene. However the fractional yield (carbon basis) of acetone was generally lower for all the metal-doped catalysts (0.02-0.04) when compared to CeO₂ (0.06), except for Co (0.09). He et al. (2002) investigated the catalytic performance and redox properties of 0.5 wt.% Pd-, Pt- or Rh-doped Ce_{0.6}Zr_{0.4}O₂ (CZ) and Ce_{0.6}Zr_{0.05}Y_{0.05}O₂ (CZY) catalysts. Redox behavior can be affected by both the formation of surface oxygen vacancies and modified lattice oxygen mobility. The metals were loaded by wet impregnation and calcined at 550 °C. The addition of Pd slightly reduced the oxygen mobility of the CZY catalyst. However the presence of metal particles facilitated the reduction of Ce⁴⁺ to Ce³⁺ by facile adsorption and spillover of CO and hydrogen to the CZY interface, increasing the oxygen uptake capacity as a result.

The deactivation mechanism for a Pd/CeO₂ catalyst has been studied by Wang et al. (2002) for the water-gas shift (WGS) reaction. It was observed that for a 1 wt.% Pd/CeO₂ catalyst, heating in pure H₂O had no effect on the catalyst, heating in pure H₂ caused a slight increase in WGS activity, heating in pure CO₂ caused a slight decrease, and heating in pure CO caused a significant decrease, which could be partially recovered by oxidation with O₂. CO treatment (400 °C, 10 h) of 1 wt.% Pd/CeO₂ catalyst reduced Pd dispersion from 23% to 3%; calcination in O₂ increased the dispersion to 10%. For a 6 wt.% Pd/CeO₂ catalyst, an increase in Pd particle size from ~3 to 8 nm was observed after identical treatment. Since for the WGS reaction the rate depends greatly on the

metal surface area, the deactivation of the Pd/CeO₂ catalyst is likely due to loss of metal surface area. The growth of Pd particles can be due to several mechanisms. First, it is known that CO adsorption on Pd single crystals can cause the diffusion of surface Pd atoms at temperatures even less than 250 °C (Behm et al., 1979). Second, reduction of Pd/CeO₂ catalysts in CO has been shown to lead to carbonates on the CeO₂ surface; these carbonates could be removed by reoxidation in either O₂ or H₂O (Hilaire et al, 2001). The restructuring of the CeO₂ could cause Pd particle growth.

1.3 Effect of Dopants on the Structure of the Active Metal Oxide

The structural effects of the addition of dopants to rare earth oxides has been studied by Dong et al. (2001), Cousin et al. (2001), He et al. (2002), Idriss et al. (1995), Trovarelli et al. (1997), and Parida et al. (1999). Cousin et al. (2001) observed that when Cu²⁺ was added to CeO₂ and calcined in air, monomers, dimers, and clusters of Cu²⁺ were formed in the solid. Cu²⁺ dimers were located in distorted octahedral sites. Mobile oxygen was responsible for the coupling between two Cu²⁺. When the Cu/Ce atomic ratio is >0.5, two phases, CeO₂ and CuO, were formed. Dong et al. (2001) have shown that for a mechanical mixture of CeO₂ and Al₂O₃, upon calcination at 450 °C, CuO dispersed preferentially on the CeO₂ decreasing the surface area and being incorporated in the vacancies of CeO₂. The doping of Pd, Pt or Rh (0.5 wt.%) into Ce_{0.6}Zr_{0.05}Y_{0.05}O₂ (CZY) caused a decrease in surface area, a decrease in surface Ce/Zr ratio, an increase in average pore size, and a broadening of the pore size distribution (He et al., 2002). From TPR experiments (Pd/CZY) they observed a decrease in reducible oxygen from 0.84 to 0.53 mmol/g over the course of four successive reduction/oxidation cycles; there was no significant change in the TPR for the undoped or the Pt-, or Rh-doped catalysts.

Idriss et al. (1995) have observed in their studies of CeO₂ and supported CeO₂ catalysts that while there was no difference in surface area between 3 wt.% Pd/CeO₂ and CeO₂, impregnation of 3 wt.% Co or 3 wt.% Pd + 3 wt.% Co decreased the surface area by a factor of 2 to 3. But in all these catalysts the fluorite structure of CeO₂ was maintained and no diffraction lines related to Pd or Co compounds were observed.

It has been suggested by Trovarelli et al. (1997), that the addition of alkaline earth oxides to CeO₂ would result in the generation of defect sites that would promote the reduction of Ce⁴⁺ to Ce³⁺. Such doping can also lead to phase change. Parida et al. (1999) have shown from XRD of catalyst samples that the addition of 0.5 mol% Na to ZrO₂ leads to a predominantly tetragonal phase, whereas doping with Li, K and Cs caused little change in phase from the normal monoclinic phase. The surface areas of samples doped with 0.5 mol % Na, K and Cs were almost unchanged.

1.4 Study of Doped Metal Oxides by X-ray Absorption Spectroscopy

The techniques of Extended X-ray Absorption Fine Structure Spectroscopy (EXAFS) and X-ray Absorption Near Edge Spectroscopy (XANES) are together called X-ray Absorption Spectroscopy (XAS). EXAFS can be used for ex-situ and in-situ study of the electronic and structural properties of oxides. Apart from yielding distances that separate an arbitrarily selected central atom from other atoms in its first and successive neighboring shells, EXAFS can also yield the coordination numbers for the atom and a measure of the atomic rigidity in those shells. It is also a very sensitive technique, being capable of probing the behavior of less than 10¹² atoms, which is equivalent to one-thousandth of a monolayer of a typical metal of 1 cm² surface area. XANES is a sensitive probe for electronic properties, e.g. the valence, the symmetry of the unoccupied

electronic states, and the effective charge of a chosen atom within a molecule or in a solid. It can also be used to determine the coordination geometry around the excited atom. In contrast to classical scattering techniques, XANES does not require long range ordering. Thus, XANES is a suitable technique for the investigation of doped rare earth oxides as both the rare earth ion and the corresponding dopant ion can be investigated separately.

Hormes et al. (2000) have applied XANES spectroscopy to investigate changes in the electronic and geometric structure of dopants in CeO₂. For their study, the XANES spectra of a series of CeO₂ samples doped with trivalent rare earth oxides (10 mol % of the elements of the lanthanide series) were measured at the L_{III}-edges of the dopants and the Ce. By comparing XANES spectra of the pure dopant oxides with those of the oxides in CeO₂, it was possible to observe how the dopants are incorporated into the CeO₂ lattice. The Ce L_{III} XANES spectra of Ce(IV)O₂ and Ce(III)-oxalate are typical examples for the L_{III} spectra of lanthanides with valence +4 and +3, respectively. For Ce³⁺, the spectrum is dominated by one intense white line at about 5728.3 eV. For Ce⁴⁺, the entire spectrum is shifted to higher energies in accordance with the general rule correlating valence and the position of the edge. Furthermore, the white line is now split into two well-separated peaks at about 5732.9 and 5739.7 eV with about the same intensity. For Ce⁴⁺, this intensity is about 50% lower compared to the white line for the Ce³⁺. Wan et al. (1997) have shown the height of the second peak to increase proportionally with CeO₂ content. Thus by direct observation of the edge shape of the spectra, information on the relative amounts of Ce³⁺ and Ce⁴⁺ in the sample may be obtained.

When the spectrum of Pr_6O_{11} – the most stable oxide of Pr – is compared to $\text{Pr}_2\text{O}_3/\text{CeO}_2$ (Hormes et al., 2000), it was observed that the low energy Pr peak was reduced in intensity, suggesting that most of the Pr in CeO_2 is oxidized to Pr^{4+} upon sintering. Thus a much lower number of oxygen vacancies are created in the sample than would be expected from the initial stoichiometry. In the case of $\text{La}_2\text{O}_3/\text{CeO}_2$ (Hormes et al., 2000), the La L_{III} spectrum obtained is similar to that of pure La_2O_3 , dominated by a single white line indicating a valence of +3 for La in both samples. However, two differences were noted. The amplitude of the white line was reduced by about 20 %, and there were significant differences in the fine structure on the high-energy side of the white line. This suggests structural changes in the surroundings of the La atoms when dissolved into CeO_2 . In several cases a correlation of $\Delta E \propto 1/R^2$ has been observed with ΔE = the energy difference between a shape resonance and the white line and R = the distance between the excited atom and its coordination shell (Sette et al., 1984; Kasrai et al., 1991; Kueper et al., 1992). Applying this correlation to $\text{La}_2\text{O}_3/\text{CeO}_2$, it was observed that the first two peaks on the high energy side in the fine structure of the La L_{III} spectrum have shifted to higher energies, suggesting that both the La-O and La-Ce distances are decreasing.

Skarman et al. (2002) have used XANES and EXAFS to characterize nonstoichiometric $\text{CuO}_x/\text{CeO}_2$ composite particles, 4.9-29.4% Cu. The pre-edge in the XANES spectrum, specific to Cu(I) species (Kau et al., 1987), was used to evaluate the ratio of Cu^{+1} to Cu^{2+} , which varied from 0.36 in fresh samples to less than 0.05 in the activated samples. EXAFS showed a Cu-Cu distance varying from 2.89 to 2.85 Å, corresponding to a low coordination number between 0.4 and 0.3. This showed that the

copper was very dispersed. Also the EXAFS analysis showed that in the activated catalysts the Cu species were generally in lower coordination, suggesting that Cu ions migrate to the surface.

CHAPTER 2

EXPERIMENTAL

2.1 Catalyst Preparation

In this work eighteen different catalysts were used. The composition, size and shape are shown in Table 2.1.

Table 2.1: Composition, Size and Shape of Catalysts Used

Composition	Size (mm)	Shape
20 wt.% CeO ₂ /Al ₂ O ₃	0.42-0.84	Powder
20 wt.% CeO ₂ /Al ₂ O ₃	1.27	Cylindrical
17 wt.% CeO ₂ /Al ₂ O ₃	1.59	Cylindrical
18.4 wt.% CeO ₂ /Al ₂ O ₃	3.18	Cylindrical
19.9 wt.% CeO ₂ /Al ₂ O ₃	3.18	Cylindrical
22.3 wt.% CeO ₂ /Al ₂ O ₃	2.18	Tri-lobed
15 wt.% CeO ₂ /3 wt.% K ₂ O/Al ₂ O ₃	1.19	Cylindrical
17 wt.% CeO ₂ /0.1 wt.% Co/Al ₂ O ₃	1.59	Cylindrical
17 wt.% CeO ₂ /0.8 wt.% Co/Al ₂ O ₃	1.59	Cylindrical
17 wt.% CeO ₂ /2.4 wt.% Co/Al ₂ O ₃	1.59	Cylindrical
17 wt.% CeO ₂ /0.1 wt.% Pd/Al ₂ O ₃	1.59	Cylindrical
17 wt.% CeO ₂ /0.8 wt.% Pd/Al ₂ O ₃	1.59	Cylindrical
17 wt.% CeO ₂ /0.8 wt.% Mn/Al ₂ O ₃	1.59	Cylindrical
17 wt.% CeO ₂ /2.4 wt.% Mn/Al ₂ O ₃	1.59	Cylindrical
11.8 wt.% PrO _{1.83} /9.8 wt.% CeO ₂ /Al ₂ O ₃	2.38	Spherical
20 wt.% MgO/ZrO ₂	3.18	Cylindrical
4 wt.% CeO ₂ on KOH doped ZrO ₂	3.18	Cylindrical
33 wt.% CeO ₂ MCM-41	0.84-1.68	Powder

All the metal-doped CeO₂/Al₂O₃ catalysts (Sud-Chemie) were prepared by a dropwise incipient wetness impregnation method. For the Pd-doped catalysts, the desired amount of the precursor salt PdCl₂ was dissolved in a solution of 1 M HCl. Before impregnation the catalyst was dried in a high temperature oven at 450-500 °C. The catalyst was impregnated after it had cooled down to about 150-200 °C, then dried in air (~100 °C) overnight, then calcined in flowing air (~150 cm³/min) at 500 °C for 6 h, then in He at 450 °C for at least 1 h. Finally, it was reduced using 30-40% H₂ in He at 450 °C

for at least 2 h. For the Co-doped catalysts, the precursor salt was $\text{Co}(\text{NO}_3)_2 \cdot 6\text{H}_2\text{O}$; for the Mn-doped catalysts, it was $\text{Mn}(\text{NO}_3)_2$. Both precursors were dissolved in DI water and subsequent procedures were identical to those of the Pd-doped catalysts.

Prior to performing any kinetics studies, the catalysts were calcined in the reactor in flowing air ($\sim 55 \text{ cm}^3/\text{min}$)/He ($\sim 5 \text{ cm}^3/\text{min}$) mixture at 500-520 °C.

2.2 Continuous Flow Reactor Experiments

The experiments were performed in fixed bed reactors. Two types of reactors were used, a quartz tube reactor (1.25 cm ID, 38 cm length) and a high pressure, Autoclave Engineers 316 stainless steel tube reactor (1.75 cm ID, 61 cm length) with “slimline” high-pressure fittings at inlet and outlet.

For the low pressure, quartz reactor system, typical catalyst loads were 0.5 g. Quartz wool was placed above and below the catalyst bed. The reactor was heated by means of an external clamshell furnace (Teco F5, 350 W, 6” length). Reactor temperatures were varied between 350 °C and 495 °C. A 1/16” internal K thermocouple, located in a quartz thermowell in contact with the catalyst bed, measured the temperature, which was controlled by a PID controller (Love Series 2600). The temperature was typically within ± 1 °C of the set point. A schematic of the flow reactor is shown in Fig. 2.1.

The reactor was operated in upflow mode with a vaporized feed. A syringe pump (Sage Instruments model 341 A) using a 25.0 cm^3 syringe (Hamilton 82520) was used to feed the reactants. Flow rate was set using a selection knob on the syringe pump. For a given knob position the flow rate was determined by displacement of DI water vs. time. All gases were supplied to the reactor system by means of flow controllers (Brooks MFC

5850). The flow control valves were interfaced to a Data Translation 2805/5716 board running under QuickBasic. The feed stream, from the vaporizer to the reactor inlet, was heated using electrical heating tapes kept at ~ 200 °C. The product from the reactor was collected in a sample bottle, which was cooled in an ice-bath

Prior to starting the feed pump, the reactor was purged with He for 15 min. Typical feed consisted of 40 mol% acid mixture in He. Samples were collected twice over a 9 h period. When shutting down the reactor, the system was purged with He for 15 min. While purging, the temperature of the reactor was raised to 520-540 °C. Then He was replaced by an air/He mixture to regenerate the catalyst overnight. The startup, shutdown, and regeneration procedures were developed in previous work (Randery, 1999).

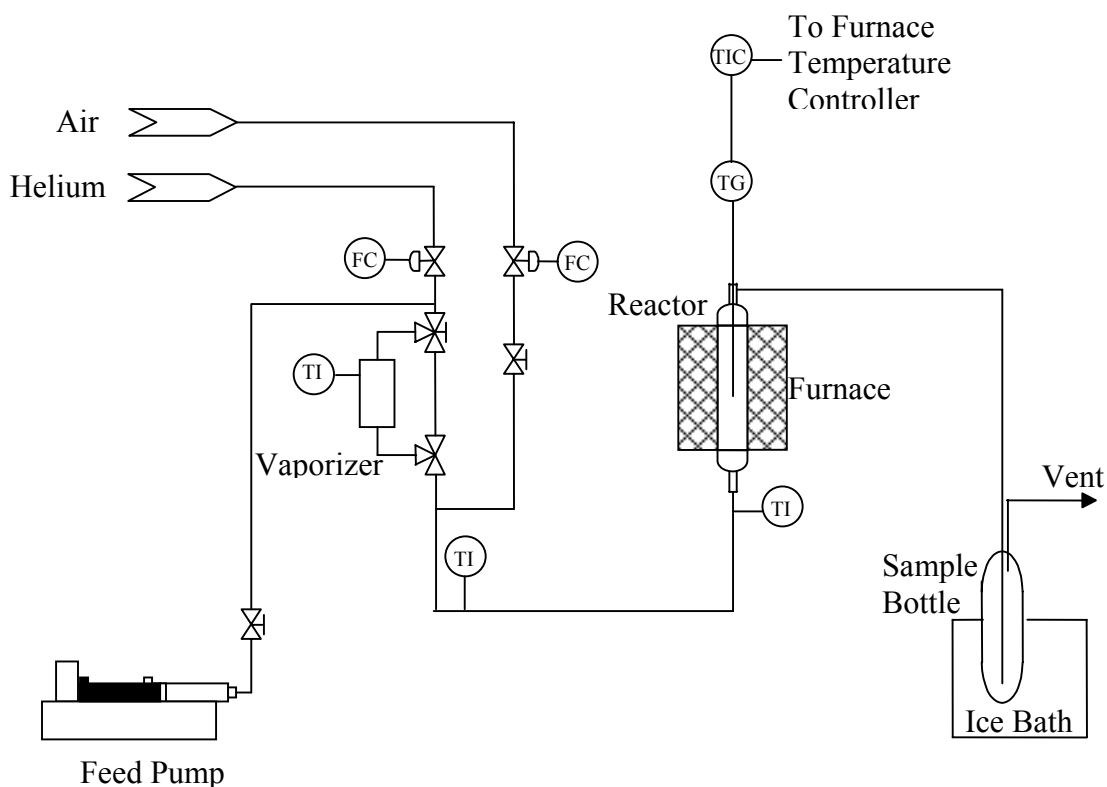


Figure 2.1: Schematic of Low Pressure Continuous Flow Reactor system

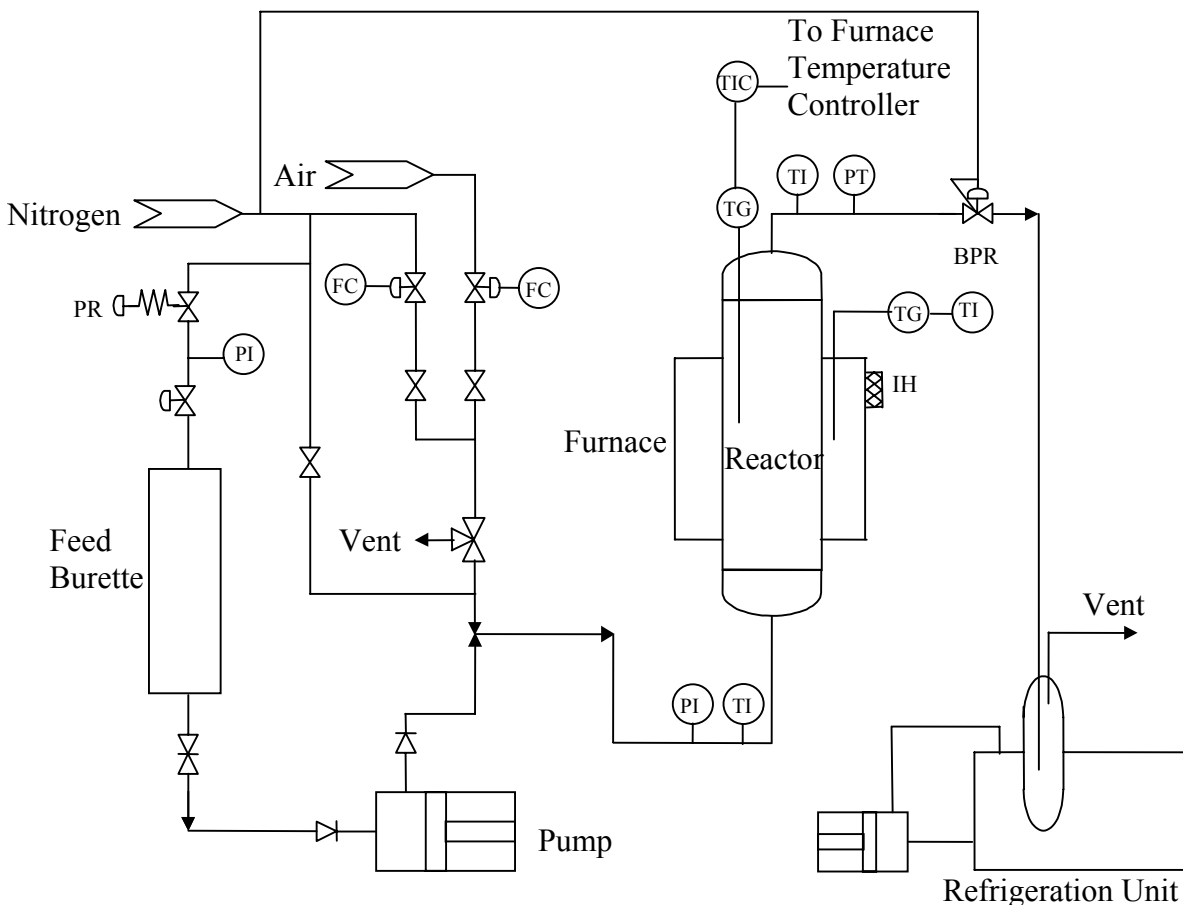


Figure 2.2: Schematic of High Pressure Continuous Flow Reactor system

For larger scale experiments, using the stainless steel tube reactor, typical catalyst loads were 25 g. Quartz wool and glass beads were placed above and below the catalyst bed. The reactor was heated by means of an external clamshell furnace (Hevi-Duty, MU-2018). Reactor temperatures were varied between 430 °C and 450 °C. The temperature was controlled using a 1/16 in. internal K thermocouple in contact with the catalyst bed, by a PID controller (Love Series 2600), and was held within ± 1 °C of the set point. The reactor pressure was controlled with a diaphragm-type backpressure regulator (Grove Mitey Mite). A schematic of the flow reactor is shown in Fig. 2.2.

The reactor was operated in upflow mode with a vaporized feed. A stainless steel plunger pump (Milton Royal MiniPump model 1-C-29R) was used to feed the reactants from a calibrated feed burette. Adjusting the stroke length of the pump controlled the flow rate. The feed stream, from pump discharge line to reactor inlet, was heated using electrical heating tapes kept at ~ 270 °C. The feed burette was kept under a slight nitrogen purge. The pressure at the reactor outlet was measured using a pressure transducer (Tem Controlli TP 867-1D/M, 150 psi/1.5mV/V); there was also a Bourdon pressure gauge at the inlet to the reactor.

The products from the reactor were collected in a glass receiver cooled to ice temperature by means of a cooling bath. The exit line between the reactor outlet and the backpressure regulator was heated using heating tapes kept at ~ 230 °C.

Gases could be supplied to the reactor system through a three-way valve. Prior to starting the feed pump, the reactor was purged with N₂ for 15 min. Upon observation of liquid exiting the reactor, backpressure was applied. It took the reactor approximately 20 min to reach a pressure of 30 psi. Samples of product were taken throughout the day from the exit line at the cooling bath.

To shut down the reactor, the pump was stopped and the inlet heating tape was turned off. The contents of the reactor were vented through the three-way valve. The system was then purged with N₂ for at least 15 min. While purging, the temperature of the reactor was raised to 520 °C. After purging, the N₂ was replaced by air through the three-way valve to regenerate the catalyst. This was done overnight. The start up, shutdown, and regeneration procedures were developed in previous work (Randery, 1999).

2.3 Analysis of Feed and Product Samples

Feeds were prepared from isobutyric acid (IBA, Aldrich, 99%), decanoic acid (DOAc, Henkel, 98.8%) and acetic acid (HOAc, glacial, 99.9%). Feed mixtures were prepared in the correct molar ratios and then charged to the feed burette/syringe for the continuous experiments.

For the continuous experiments, the products collected in sample bottles were stored in a refrigerator until they could be analyzed by gas chromatography (GC). The organic phase was analyzed using an HP5890A gas chromatograph fitted with a flame ionization detector (FID). A Supelco SPB 1000 column (0.32 mm ID, 30 m length) was used. Methanol was the internal standard; 0.1 cm³ of the IBA or HOAc/DOAc samples were diluted with 2 cm³ of 2% methanol in pentane. The aqueous layer was analyzed similarly. Gaseous product samples were collected in Tedlar bags with syringe ports, and 0.5 cm³ samples were analyzed using a Carbosieve SII packed column (Alltech, 1/8 in. diameter, 6 ft length) on an HP 5890A gas chromatograph with a thermal conductivity detector (TCD). Details of the GC analyses are given in Appendix A.

The IBA reaction calibration curves (three points) were prepared for 2,4-dimethyl-3-pentanone (diisopropyl ketone, DIPK), 4-methyl-2-pentanone, isobutyraldehyde and IBA. Calibration slopes for propanoic acid, 2-methyl anhydride and the isomers of DIPK were assigned the same values as DIPK. The slopes for 2-pentanone and 3-methyl-2-butanone were assigned the same value as 4-methyl-2-pentanone. For the heavier products an average of the slopes for DIPK and IBA was used. All peak identifications for the IBA reactions were made using a GC-MS (HP 5972) fitted with a similar column and operated under similar conditions.

For the HOAc/DOAc feeds there were either one or two product phases. The second (aqueous) phase was at least 55% water. Calibration curves (three points) were prepared for 2-undecanone (methylonyl ketone, MNK), HOAc, DOAc, 4-methyl,2-pentanone and acetone. Calibration slopes for heptadecane, dodecanones, tridecanones, and dinonyl ketones (DNK) were assigned the same values as MNK. The same slope for DOAc was used for dodecanoic acid. The same slope as methylpentanone was used for all C5-C10 ketones. All peak identifications for the HOAc/DOAc runs had been done prior to this work using a GC-MS fitted with a similar column and operated under similar conditions (Randery, 1999).

2.4 Catalyst Characterization

For thermogravimetric analysis (TGA), the catalyst was ground to a fine powder. A 12-17 mg of the catalyst sample was reduced using 50 mL/min of 30% H₂/70% He from 50 °C to 450 °C using a 5 °C/min ramp and held for 2 h. The catalyst was then purged with He before oxidizing it in 50 cm³/min of air at 450-540 °C using a 5 °C/min ramp and a final hold of 1 h. For coke analysis the sample was calcined in 50 cm³/min of air from 50 °C to 250 °C using a 10 °C/min ramp and held for 1 h. Then the temperature was increased to 600 °C using a 10 °C/min ramp and held for 1 h. All experiments were performed in a Perkin-Elmer TGA 7 Thermogravimetric Analyzer. Data was acquired using a LabView 4.0 (National Instruments) program. The raw data were then differentiated using a C++ program (Massgraph).

Chemisorption tests were conducted to determine the metal dispersion of the catalysts. A Micromeritics Pulse Chemisorb 2700 apparatus was used. Samples were first dried in the quartz sample holder at from ambient temperature to 520 °C in He at 50

cm³/min, then oxidized in air (50 cm³/min) for 4 h, then purged at 450 °C in He for 1 h. Then the catalyst sample was reduced in H₂ (50 cm³/min) for 4 h at 450 °C, purged at 450 °C in He (10 cm³/min) and then switched to Ar (20 cm³/min). The samples were pulsed with H₂ (52/97/206/500 uL loops) at 0 °C until no further adsorption occurred and then at 150 °C. Approximately 0.5-3.0 g of catalyst was used in the experiments. All samples were weighed immediately after the dispersion measurements were obtained.

XAS (X-ray Absorption Spectroscopy) measurements were conducted on various supported CeO₂ catalysts, both pure and doped (1-3 wt.% K, Co, and Pd) using synchrotron radiation emitted by the electron storage ring of the LSU Center for Advanced Microstructures and Devices (CAMD). Measurements were done at the Ce L_{III}-edge and Co K-edge in transmission mode and at the K K-edge, Co K-edge and Pd L_{III}-edge in fluorescence mode. XANES and EXAFS spectra for Ce were collected at ambient temperature in air and at 420 °C in both He and 10% H₂/N₂ environments. All other spectra were collected at ambient temperature, in air for Co and in He for Pd and K. In fluorescence mode, the EXAFS spectra were recorded at least three times.

The reference materials included Ce(III) acetate (Aldrich, 99.9%), Ce(IV) oxide (Aldrich, 99.9%), Co foil, Co(II) oxide, Co(II, III) oxide (Aldrich), Pd foil and KCl. The spectra in transmission mode were obtained using ionization chambers measuring the incident beam intensity before and the transmitted beam intensity after the sample cell. In fluorescence mode, a 13-element Ge detector array and Si (111) double-crystal monochromator were used to obtain K K-edge, Pd L_{III}-edge, and Ce L_{III}-edge spectra, while a Si (311) monochromator was used for Co K-edge spectra.

The XANES and EXAFS spectra at ambient conditions were taken by coating the finely powdered catalyst samples onto Kapton tape. The spectra at 420 °C were taken by pressing the catalyst samples into self-supporting wafers, which were loaded into a XAS cell. The wafer was heated from room temperature to ~420 °C in 50 cm³/min He. For the experiments in H₂, the temperature was brought to ~420°C in He, then the gas was switched to 10% H₂ for 15 min. The details of the energy ranges and resolutions used for various spectra are given in Table 2.2. The resolution corresponds to a single step in energy during a scan.

The raw data were first reduced to $\mu(E)$, the absorption coefficient. It was calculated using the following equations.

$$\mu(E) = \log(I_0 / I) \quad - \text{Transmission mode,}$$

$$\mu(E) = I_f / I_0 \quad - \text{Fluorescence mode,}$$

where I_0 is the incident X-ray intensity, I the transmitted intensity, and I_f the averaged intensity of a fluorescence line.

Table 2.2: XAS – Experimental Details

	Resolution (eV)	Range (eV)
Cerium L _{III} -edge (Transmission)		
XANES	3	5525-5710
	0.3	5710-5785
	3	5785-5985
EXAFS	3	5525-5710
	2	5710-6145
XANES + EXAFS	3	5525-5710
	0.3	5710-5785
	2	5785-6164

(Table 2.2 cont.)

Cobalt K-edge (Transmission)		
XANES + EXAFS	3	7550-7695
	0.3	7695-7770
	2	7770-8700
Cobalt K-edge (Fluorescence)		
XANES	3	7559-7689
	0.3	7689-7739
	3	7739-8000
EXAFS	3	7559-7690
	2	7690-8700
Palladium L _{III} -edge (Fluorescence)		
XANES	3	3050-3160
	0.3	3160-3240
	3	3240-3400
Potassium K-edge (Fluorescence)		
XANES + EXAFS	3	3450-3590
	0.2	3590-3680
	2	3680-4200

CHAPTER 3

RESULTS AND DISCUSSION

3.1 Continuous Reactor Experiments

Complete data sets for all reaction experiments are given in Appendix B. The terminology used to describe the results here and in the spreadsheets is as follows:

$$\% \text{ Conversion IBA/DOAc} = 100 * (\text{mols IBA/DOAc reacted}) / (\text{mols IBA/DOAc fed})$$

$$\% \text{ Weight selectivity DIPK/MNK} = 100 * (\text{weight of DIPK/MNK}) / (\Sigma \text{weight of products})$$

$$\% \text{ Molar Yield DIPK} = 100 * (2 * \text{mols DIPK}) / (\text{mols IBA fed})$$

$$\% \text{ Molar Yield MNK} = 100 * (\text{mols MNK}) / (\text{mols DOAc fed})$$

$$\text{WHSV (Weight Hourly Space Velocity)} = (\text{weight of feed}) / (\text{weight of catalyst-h})$$

In these equations, acetone is omitted as a product in the summations because it is formed from the ketonization of HOAc only.

Experiments were performed using different catalysts (Table 2.1, Table 3.1) at various temperatures and WHSVs to determine the optimal range for obtaining the highest conversion of IBA and DOAc (3/1 HOAc/DOAc feed) and weight selectivity to DIPK and MNK respectively. For the IBA feed, the average values of IBA conversion, wt.% selectivity to DIPK, and molar yield to DIPK are shown in Tables 3.2-3.4. For the 3/1 HOAc/DOAc feed, the average values of DOAc conversion, wt.% selectivity to MNK, and molar yield to MNK are shown in Table 3.5. On most occasions, the catalysts were regenerated in high temperature air at the end of the working day (~9-12 h), even if no signs of deactivation were apparent. The regeneration cycles are indicated by vertical broken lines in subsequent figures. A typical regeneration consisted of 55 cm³/min air at 520/540 °C for 12-15 h. Experiments were carried out using two different size reactors

(Chapter 2). In the smaller quartz tube reactor the feed partial pressure was maintained at 0.34-0.41 atm (balance He to 1 atm), while no He was used in the larger stainless steel tube reactor.

3.1.1 IBA feed – CeO₂/Al₂O₃ Catalysts

Experiments were performed using five different CeO₂/Al₂O₃ catalysts (Table 3.1). Table 3.2 shows a summary of the results of these studies. The CeO₂ loading for these catalysts varied from 17-22.3 wt.%, which corresponds to approximately theoretical monolayer (1.0×10^{-3} g CeO₂/m²) coverage of CeO₂ on the Al₂O₃ support (Randery et al., 2002).

Table 3.1: Surface Areas for CeO₂/Al₂O₃ Catalysts

Catalyst	Surface area (m ² /g)	Wt.% CeO ₂	CeO ₂ density (g CeO ₂ /m ²)
20 wt.% CeO ₂ /Al ₂ O ₃ , Engelhard, 1.27 mm extrudate	152 ¹	19.8	1.3×10^{-3}
17 wt.% CeO ₂ /Al ₂ O ₃ , Sud-Chemie, 1.59 mm extrudate	158 ²	16.7	1.1×10^{-3}
19.9 wt.% CeO ₂ /Al ₂ O ₃ , Sud-Chemie, 3.18 mm extrudate	170 ³	19.9	1.2×10^{-3}
18.4 wt.% CeO ₂ /Al ₂ O ₃ , Sud-Chemie, 3.18 mm extrudate	165 ³	18.4	1.1×10^{-3}
22.3 wt.% CeO ₂ /Al ₂ O ₃ , Sud-Chemie, 2.18 mm tri-lobed extrudate	182 ³	22.3	1.2×10^{-3}

¹ Randery et al., (2002)

² Hendren et al., (2003)

³ From Sud-Chemie

The 17 wt.% and similar CeO₂/Al₂O₃ catalysts were not as active for this reaction as for MCPK (~99% conversion at 430 °C, WHSV~4-5) or MNK (~93% conversion at 400 °C, WHSV~3-5) formation (Hendren, 1999). At 430 °C, conversions for the 1.59 mm catalyst were only ~32% in long-term operation at WHSV~4-5 (Run M-115).

Selectivities were good, however, comparable to or better than for MNK formation (~90 wt.%).

The temperature/conversion/selectivity developments for runs M-126 and M-115 are shown in Fig. 3.1 and Fig. 3.2 respectively. In both these runs WHSVs of ~5 were maintained. Comparing these two runs, it is seen at identical temperatures the smaller sized catalyst (1.27 mm extrudate) used in run M-126 was more active than the larger catalyst (1.59 mm extrudate) used in run M-115. In run M-113, a 0.42-0.84 mm (20-40 mesh) powder of the 20 wt.% CeO₂/Al₂O₃ (1.27 mm extrudate) was used. The powdered catalyst was slightly more active than the 1.27 mm extrudate. Obviously there are diffusional limitations on the IBA condensation reaction. The best activities were obtained with the smaller diameter CeO₂/Al₂O₃ extrudates or powders. Unlike previous acid condensations studied by Randery (1999) and Hendren (2001), this reaction is diffusion-limited, with an obvious particle size effect. The critical diffusion length for the tri-lobed catalyst (Runs M-121, M-119) is <1 mm, accounting for its high activity as well. The 3.18 mm catalysts (Runs M-117, M-120) were clearly less active, and deactivated faster, probably due to pore mouth poisoning, which is common in diffusion-limited reactions where coking products are formed. Using data from Runs M-110 and M-116, a good fit (Fig. 3.3) is obtained assuming a zero-order reaction. Other orders were also examined. Assuming a first-order reaction, a poorer fit is obtained (Fig. 3.4). The rate of disappearance of IBA is given by,

$$r_{\text{IBA}} = k_1 \quad \text{- Zero-order reaction}$$

$$r_{\text{IBA}} = k_2 C_0 \quad \text{- First-order reaction}$$

The equations used in the fits are as follows:

$$X = \underbrace{\frac{k_1 \eta MW_{IBA}}{\rho_c}}_{\text{Slope}} \left(\frac{1}{\text{WHSV}} \right) \quad \text{- Zero-order reaction}$$

$$(1 + \varepsilon) \ln \left(\frac{1}{1 - X} \right) - \varepsilon X = \underbrace{\frac{k_2 \eta MW_{IBA} C_0}{\rho_c}}_{\text{Slope}} \left(\frac{1}{\text{WHSV}} \right) \quad \text{- First-order reaction}$$

where k_1 and k_2 are the rate constants, mol/(cm³ catalyst.h) and h⁻¹, respectively, η is the effectiveness factor, ρ_c is the density of the catalyst, g/cm³, C_0 is the concentration of IBA feed, mol/cm³, X is the IBA fractional conversion, and ε is the volumetric expansion factor. The observed zero-order rate constants ($k_1 \eta$) obtained from the regressed data are 0.0096 mol/(cm³.h) and 0.015 mol/(cm³.h) at 440 °C and 450 °C, respectively. The effect of catalyst particle size on reaction rate was studied at 440 °C, P_{IBA} =0.41 atm, $\text{WHSV} \sim 5.0$. The η 's for the 1.27-3.18 mm extrudate catalysts were calculated assuming $\eta=1$ for the powdered catalyst (Run M-113). The value of k obtained was 0.020 mol/(cm³.h) at 440 °C. Fig. 3.5 shows the results of the calculations of η .

From Fig. 3.1 it is seen that both conversion and selectivity are low in the temperature range 380-390 °C. Typical product distributions at these temperatures and at 440 °C are plotted in Figs. 3.6-3.7. It is seen that the major side products at low temperature are isobutyraldehyde, 2-pentanone and 3-methyl-2-butanone. Other side products include the anhydride of IBA, some isomers of DIPK (e.g., 3-methyl,2-hexanone) and a small amount of heavies. Working at higher temperatures proved more successful. The optimal temperature range for maximum yield was ~470-480 °C. Conversions of ~70% with >90 wt.% selectivity to DIPK were obtained in this temperature range. At higher temperatures selectivity was seen to decrease.

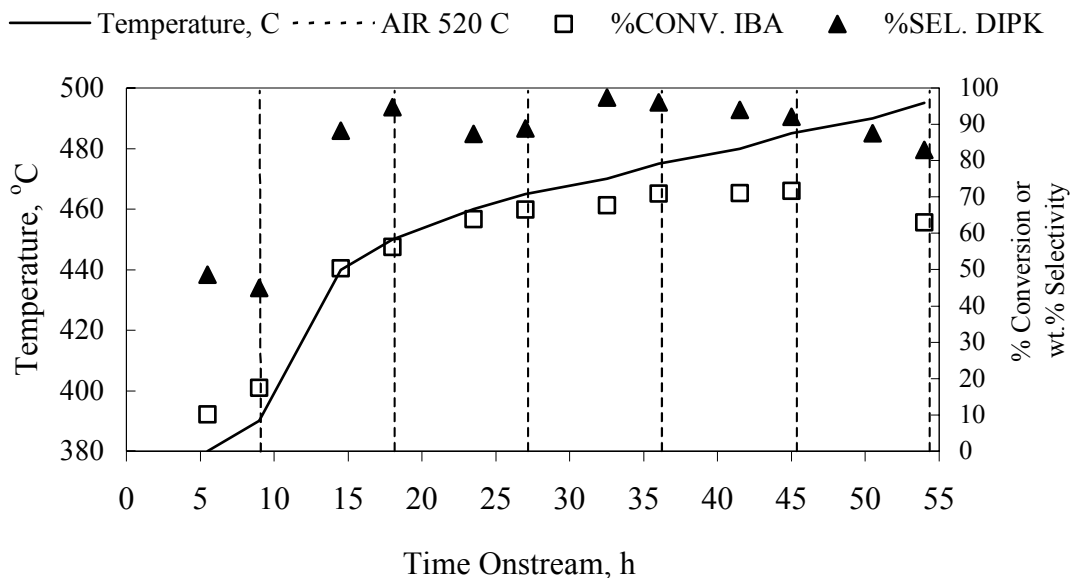


Figure 3.1: Run M-126, 20% CeO₂/Al₂O₃, 1.27 mm extrudate, IBA feed, WHSV ~5, P (IBA)=0.41 atm

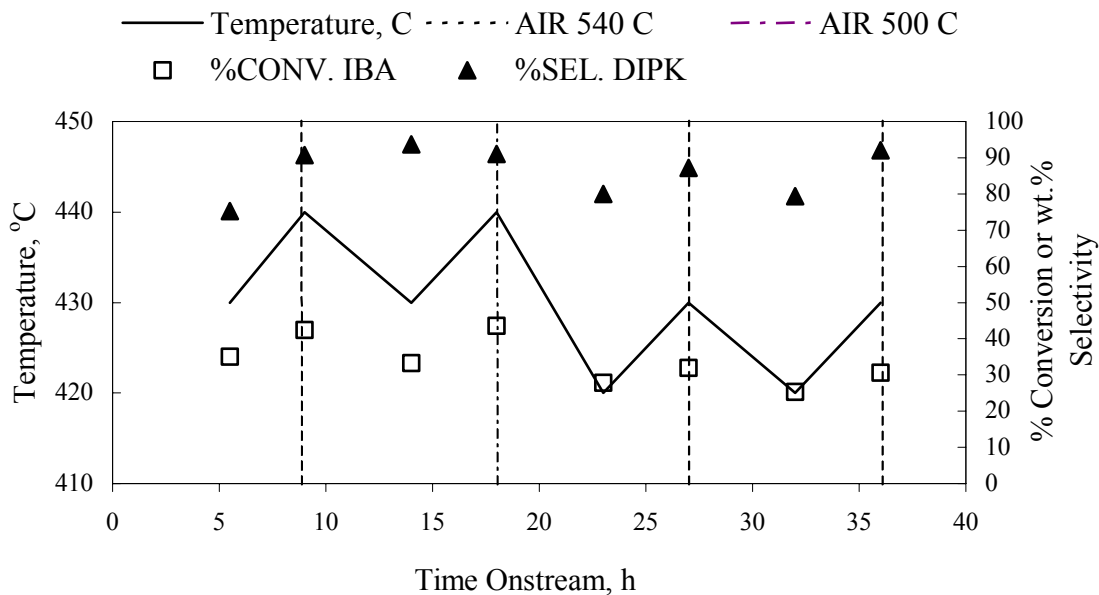


Figure 3.2: Run M-115, 17% CeO₂/Al₂O₃, 1.59 mm extrudate, IBA feed, WHSV ~5, P (IBA)=0.41 atm

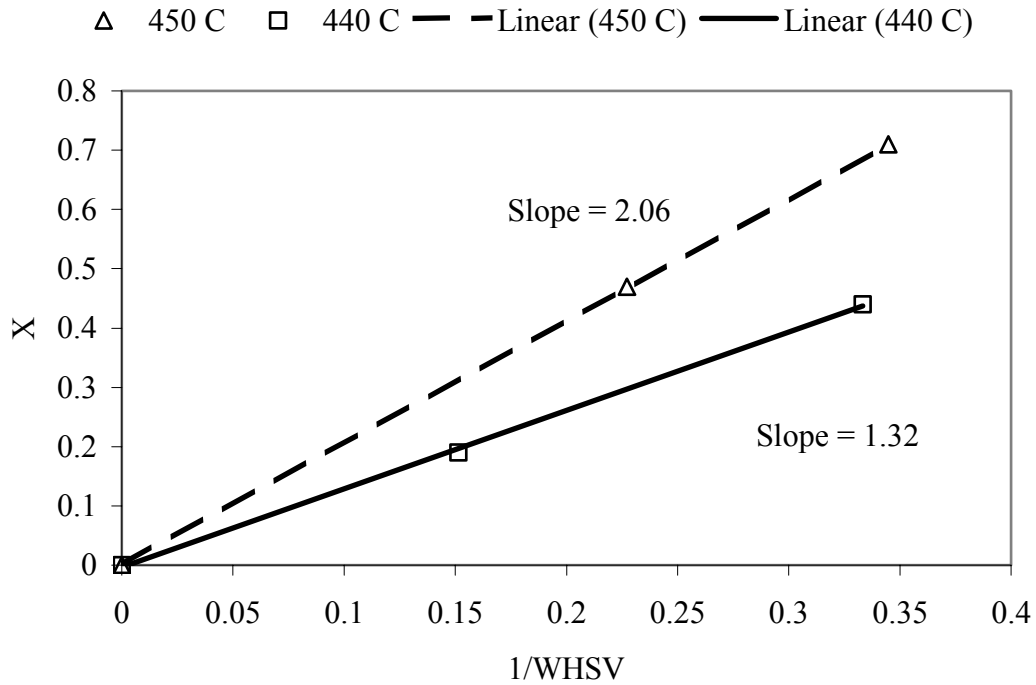


Figure 3.3: Data fit for a zero-order reaction, IBA feed, $P(\text{IBA}) = 0.41\text{atm}$, $X = \text{IBA}$ fractional conversion

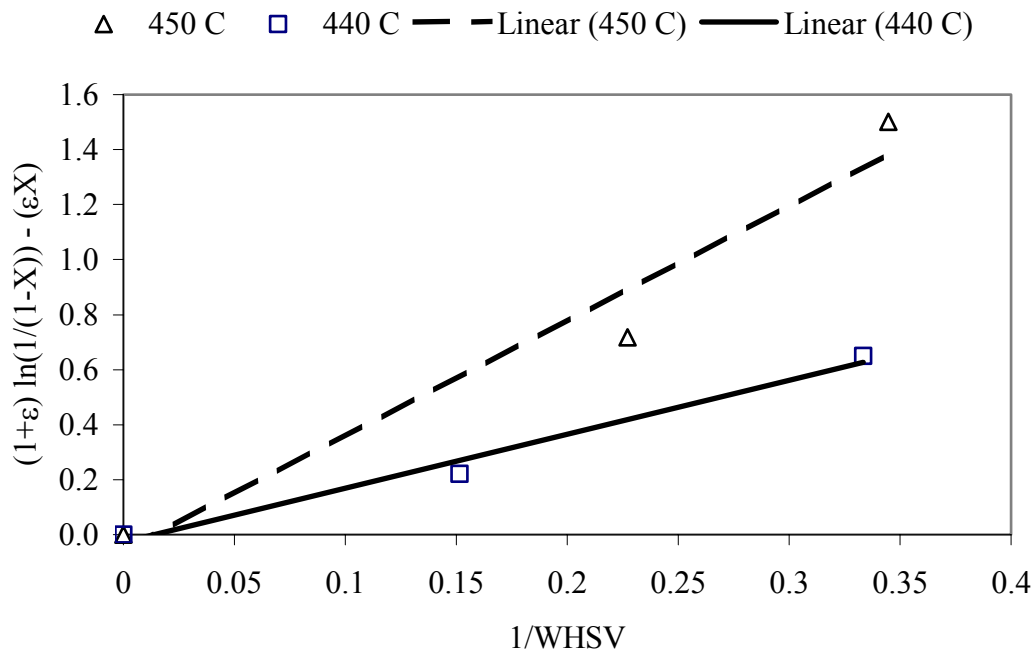


Figure 3.4: Data fit for a first-order reaction, IBA feed, $P(\text{IBA}) = 0.41\text{atm}$, $X = \text{IBA}$ fractional conversion, $\epsilon = \text{volumetric expansion factor}$

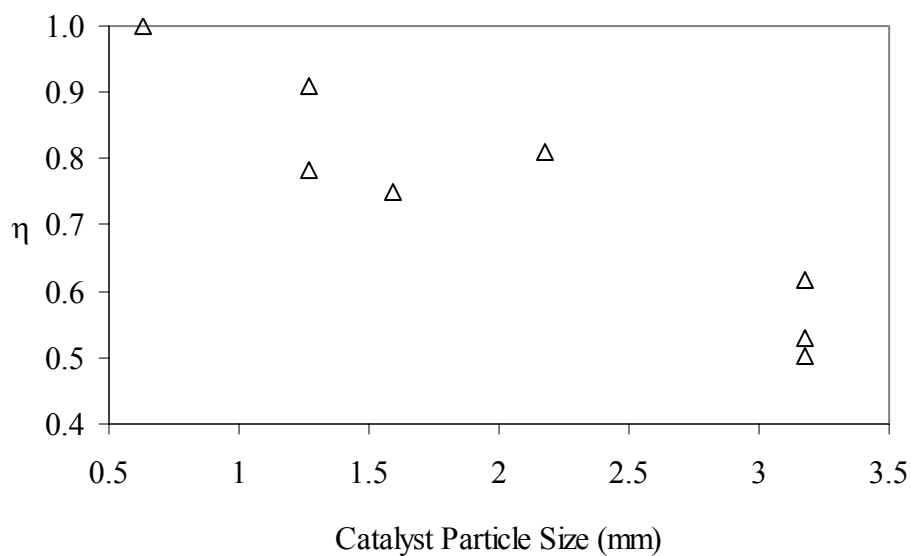


Figure 3.5: Effect of Catalyst Particle Size on Effectiveness Factor, IBA feed, P (IBA) = 0.41atm, T = 440 °C

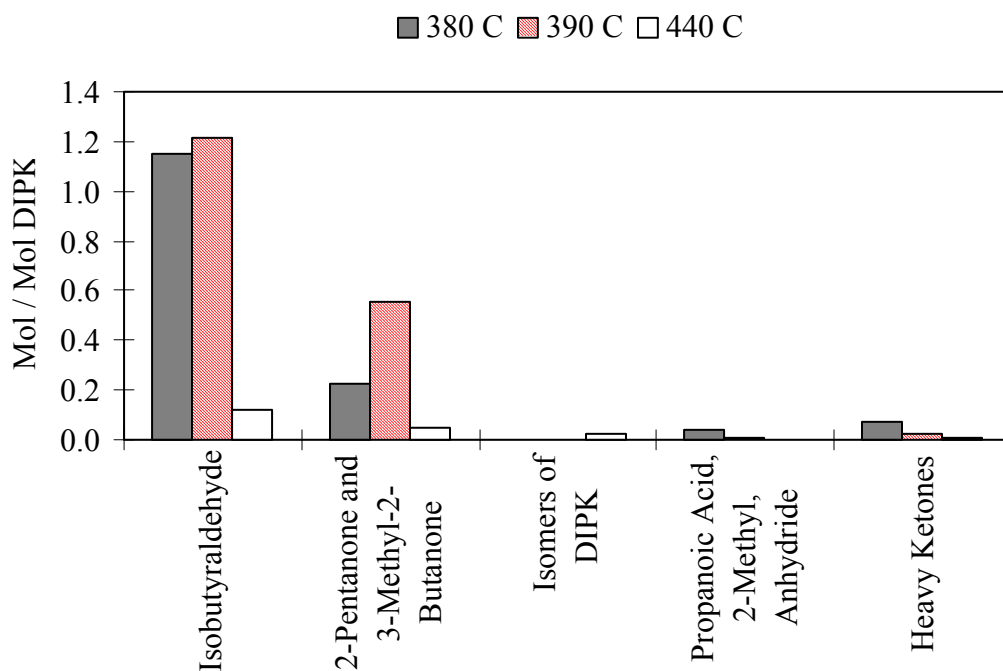


Figure 3.6: Product Distribution, Run M-126, 20% CeO₂/Al₂O₃, 1.27 mm extrudate

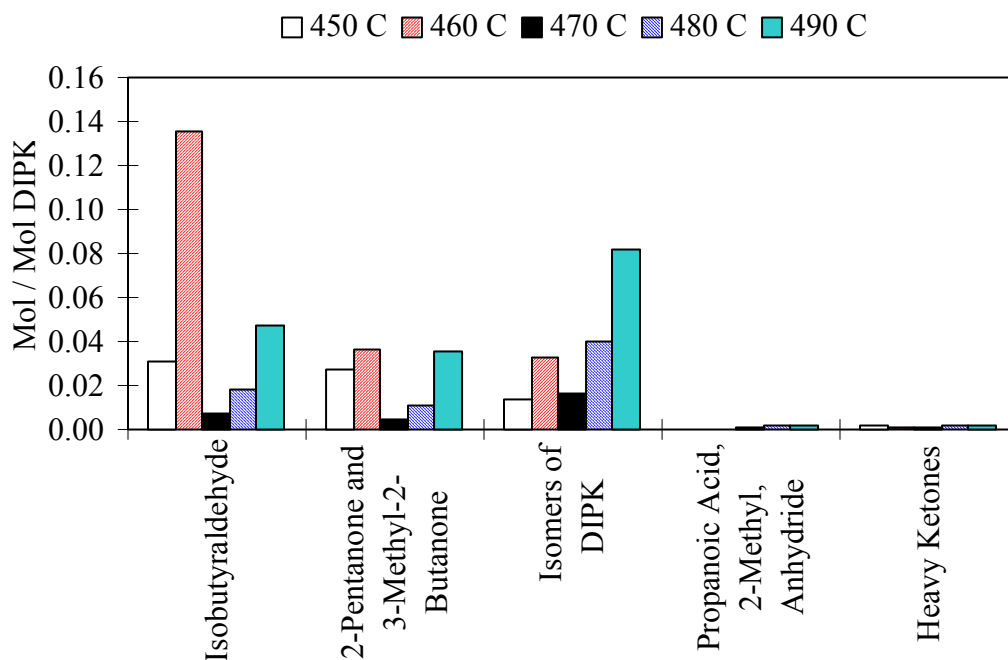


Figure 3.7: Product Distribution, Run M-126, 20% CeO₂/Al₂O₃, 1.27 mm extrudate

Table 3.2: Summary of Results of Isobutyric Acid Condensation on CeO₂/Al₂O₃ Catalysts

Day #	Temp. Range, °C	WHSV	% IBA Conversion	% Wt. Selectivity	% Molar Yield
Run M-113, 20% CeO ₂ /Al ₂ O ₃ , Engelhard, 0.42 - 0.84 mm (40 - 20 mesh) powder					
1-2	440	4.8-5.0	55±1	90±2	49±1
3	430	4.7-4.9	44±2	87±5	37±1
Run M-126, 20% CeO ₂ /Al ₂ O ₃ , Engelhard, 1.27 mm extrudate ¹					
1	380-390	4.7-5.0	14±4	47±3	7±1
2	440	4.9	50±1	88±2	45±0
2	450	4.9	56±0	95±0	53±0
3	460-465	4.7-5.2	65±1	88±1	58±2
4	470-475	4.9-5.0	69±2	97±1	67±1
5	480-485	4.8-5.2	71±1	93±1	66±1
6	490-495	4.7-4.9	66±3	85±3	56±4

(Table 3.2 cont.)

Run M-125, 20% CeO ₂ /Al ₂ O ₃ , Engelhard, 1.27 mm extrudate					
1-2	440	4.7-4.9	44±1	91±3	40±1
Run M-110, 20% CeO ₂ /Al ₂ O ₃ , Engelhard, 1.27 mm extrudate ²					
1	430	4.1	55	40	24
1	430	4.5	25	92	23
1	440	4	29	88	26
2 ³	450	2.9	71	56	41
2	450	4.4	47	67	32
2	450	4.7	35	84	30
2	440	3.6	43	92	40
2 ⁴	440	2.1-3.8	56±10	97±2	55±9
3	440	2.8-3.7	47±3	89±6	42±4
3 ⁵	440	2.9-3.1	56±2	95±0	53±1
4 ⁴	440	4.1	56	85	48
4 ⁴	440	2.8-3.0	78±2	95±3	74±4
Run M-116, 20% CeO ₂ /Al ₂ O ₃ , Engelhard, 1.27 mm extrudate ²					
1	440	11.5	24	27	6
1	440	6.6	19	72	13
1-2	440	2.3-3.7	44±4	82±7	35±6
2-3 ⁴	440-450	2.5-3.0	62±4	93±2	57±4
4-5	450	2.6-3.3	47±8	90±3	42±9
5-6 ⁴	450	2.8-2.9	73±3	94±2	69±3
7-8	450	2.8-2.9	36±6	92±7	33±5
8-9 ⁴	450	2.7-3.2	61±4	94±3	58±5
10	450	2.7	36	92	32
10	450	4.5	14	98	14
10	450	3.0	31	29	9
11-12 ⁴	450	2.3-2.9	42±5	82±6	34±2
12-13 ⁵	450	2.2-2.4	57±8	85±2	48±6
13-14 ⁶	450	2.4	72±5	93±2	67±6
14	450	2.4-2.8	32±9	82±0	26±7

(Table 3.2 cont.)

Run M-121, 22.3% CeO ₂ /Al ₂ O ₃ , Sud-Chemie, 2.18 mm tri-lobed extrudate					
1-3	440	4.7-4.9	48 _{±1}	79 _{±3}	38 _{±1}
4-6	450	4.6-5.2	60 _{±1}	88 _{±3}	52 _{±2}
7-8	455	4.7-4.9	64 _{±1}	85 _{±1}	55 _{±1}
Run M-119, 22.3% CeO ₂ /Al ₂ O ₃ , Sud-Chemie, 2.18 mm tri-lobed extrudate					
1-3	440	4.7-4.8	46 _{±3}	89 _{±4}	41 _{±2}
Run M-115, 17% CeO ₂ /Al ₂ O ₃ , Sud-Chemie, 1.59 mm extrudate					
1	430	4.8	37	66 _{±1}	25 _{±1}
1	440	4.7	44 _{±1}	82 _{±1}	37
2	430	4.7	36	82	30
2	440	4.7	46 _{±1}	82 _{±1}	38
3 ⁷	420	4.7	31	68 _{±1}	21 _{±1}
3	430	4.7	34	76 _{±1}	26
4	420	4.5	28	66 _{±1}	19
4	430	4.7	33 _{±1}	80 _{±1}	27
Run M-117, 19.9% CeO ₂ /Al ₂ O ₃ , Sud-Chemie, 3.18 mm extrudate					
1	440	4.5-4.9	41 _{±2}	65 _{±3}	27 _{±1}
2	440	4.3-4.7	37 _{±5}	80 _{±14}	29 _{±1}
Run M-120, 19.9% CeO ₂ /Al ₂ O ₃ , Sud-Chemie, 3.18 mm extrudate					
1	440	4.8-4.9	28 _{±3}	75 _{±11}	21 _{±1}
3	440	4.6-4.9	30 _{±3}	83 _{±11}	25 _{±1}

Pretreatment and regeneration of catalyst with air at 520 °C and 540 °C, respectively, unless otherwise specified.

¹ Pretreatment with air at 500 °C, regeneration with air at 520 °C.

² Large reactor.

³ Regeneration with air at 520 °C.

⁴ Product recycled through reactor once.

⁵ Product recycled through reactor twice.

⁶ Product recycled through reactor three times; during this time the catalyst was not regenerated.

⁷ Regeneration with air at 500 °C.

On most occasions, the CeO₂/Al₂O₃ catalysts showed little or no sign of deactivation at the end of the working day. When deactivation occurred, reactivation with air at 520-540 °C was sufficient to maintain long-term activity. Comparing M-126 with

M-110 or M-116 (Table 3.2), or M-128 with M-122 (Table 3.4), it appears as if there is no effect of using the lower regeneration temperature for catalysts where rapid deactivation is not a problem.

With the larger reactor (23 g catalyst, 1.75 cm diameter, 61 cm length, stainless steel) the $\text{CeO}_2/\text{Al}_2\text{O}_3$ catalyst showed lower activities but selectivities similar to those obtained with the smaller reactor. The WHSV in the larger reactor was halved (~ 2.5) to obtain the same molar yield of DIPK at the same temperature (Table 3.2, runs M-110 and M-116). This result was probably due to the more complex flow pattern in the larger reactor. It was almost impossible to vaporize all of the pure IBA in the feed lines at atmospheric pressure (IBA BP = 155 °C). Two phase flow, even if only at the bottom of the reactor, would result in more channeling of flow, and poorer contact with the catalyst particles. This problem was avoided in the smaller reactor because He was mixed with the feed. Another cause could be greater reactant inhibition at 1.0 atm vs. 0.41 atm IBA.

3.1.2 IBA Feed – Modified $\text{CeO}_2/\text{Al}_2\text{O}_3$ Catalysts

Of the modified (more acidic or basic) $\text{CeO}_2/\text{Al}_2\text{O}_3$ Catalysts (Table 3.3), the 15% $\text{CeO}_2/3\% \text{K}_2\text{O}/\text{Al}_2\text{O}_3$ catalyst showed the best activity and selectivity, although there was no advantage over plain $\text{CeO}_2/\text{Al}_2\text{O}_3$. The rest of these catalysts showed much lower conversion, or selectivity, or both. This was especially true when CeO_2 was impregnated onto a more acidic support, MCM-41 mesoporous silica.

3.1.3 IBA Feed – Metal-Doped $\text{CeO}_2/\text{Al}_2\text{O}_3$ Catalysts

The metal-doped catalysts (Table 3.4) were prepared by drop-wise impregnation of the solution of the precursor salt onto the base catalyst - 17 wt.% $\text{CeO}_2/\text{Al}_2\text{O}_3$, Sud-Chemie, 1.59 mm extrudate, Lot # SPP-1443-101. Final calcinations were at 540 °C.

The goal here was to obtain higher activity through transition metal activation of the acid to a dehydrogenated “ketene”-type intermediate (Imanaka et al., 1973; Kim and Barteau, 1990; Pestman et al., 1997). The metal could serve as sites for the initial dehydrogenation, or for recombination of hydrogen atoms with –OH groups from the oxide to form water. From the results it is seen that the 0.8 wt.% Co-doped catalyst showed slightly better activity and selectivity (Table 3.4, Fig. 3.8) when compared to the base catalyst (Table 3.2, Run M-115) at 440 °C. This was not true for the other metal-doped catalysts, especially those containing 0.8 wt.% Pd and 2.4 wt.% Mn, which deactivated rapidly. Fig. 3.9 shows a comparison of product distributions of metal-doped catalysts of similar loadings with the base catalyst. It is seen that the Co-doped catalyst gave fewer side products than the undoped catalyst. The catalysts were regenerated at the end of a day using air at 540 °C.

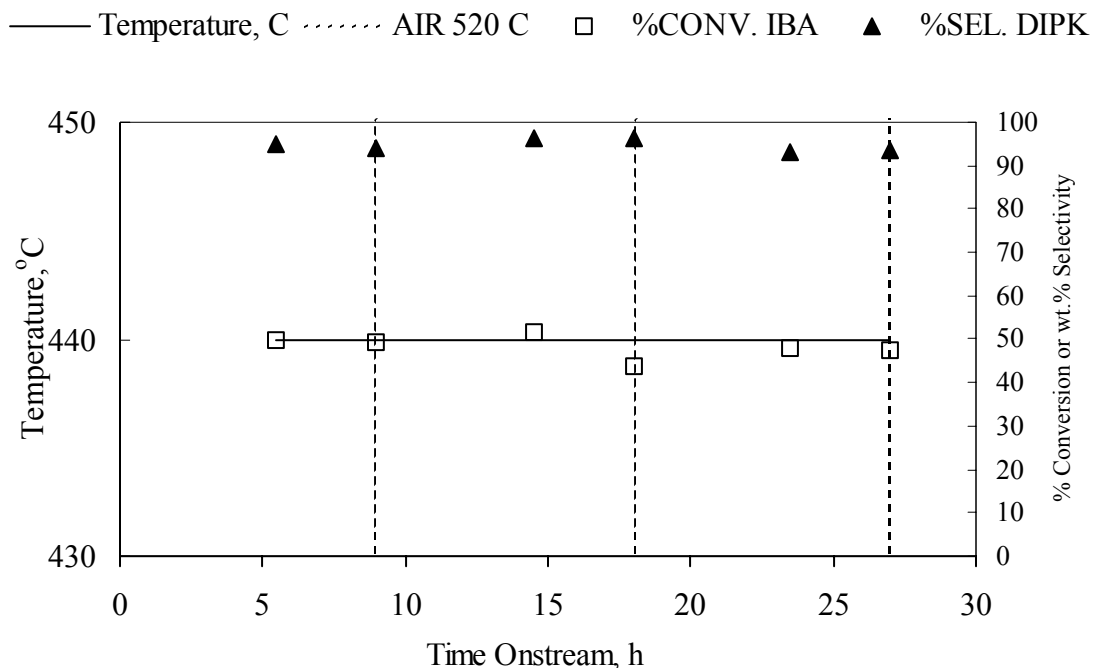


Figure 3.8: Run M-124, 17% CeO₂/0.8% Co/Al₂O₃, 1.59 mm extrudate, IBA feed, WHSV ~5, P (IBA) = 0.41 atm

Table 3.3: Summary of Results of Isobutyric Acid Condensation on Modified CeO₂/Al₂O₃ Catalysts

Day #	Temp. Range, °C	WHSV	% IBA Conversion	% Wt. Selectivity	% Molar Yield
Run M-111, 15% CeO ₂ /3% K ₂ O/Al ₂ O ₃ , Engelhard, 1.27 mm extrudate					
1	440	4.7-5.1	47 _{±1}	86 _{±4}	41 _{±3}
2	440	4.8-5.0	54 _{±1}	75 _{±5}	41 _{±2}
Run M-106/107, 20% MgO/ZrO ₂ , Engelhard, 3.18 mm extrudate					
1 ¹	430-440	3.1-3.4	31 _{±4}	84 _{±5}	27 _{±3}
2 ²	440-450	4.7-5.0	31 _{±2}	71 _{±11}	23 _{±3}
Run M-118, 4% CeO ₂ /KOH doped/ZrO ₂ , Engelhard, 3.18 mm extrudate					
1-2	440	4.5-5.0	28 _{±1}	69 _{±8}	20 _{±2}
Run M-112, 11.8% PrO _{1.83} /9.8% CeO ₂ /Al ₂ O ₃ , 2.38 mm sphere					
1	440	4.6-5.1	36 _{±5}	35 _{±8}	12 _{±1}
2	440	4.9-5.0	26 _{±2}	52 _{±6}	14 _{±1}
Run M-114, 33% CeO ₂ , MCM-41, 0.84 - 1.68 mm (20 – 12 mesh) powder					
1	440	4.7-4.8	9 _{±1}	42 _{±4}	4 _{±0}
2	440	4.9-5.2	7 _{±2}	24 _{±4}	2 _{±0}

Pretreatment and Regeneration of catalyst were done with air at 520 °C and 540 °C respectively unless otherwise specified.

¹ No pretreatment for this catalyst.

² Regeneration with air at 520 °C.

Table 3.4: Summary of Results of Isobutyric Acid Condensation on Metal-Doped CeO₂/Al₂O₃ Catalysts¹

Day #	Temp. Range, °C	WHSV	% IBA Conversion	% Wt. Selectivity	% Molar Yield
Run M-124, 0.8% Co					
1-3	440	4.5-5.1	48 _{±3}	95 _{±2}	46 _{±2}
Run M-127, 0.1% Co					
1-2	440	4.7-5.3	36 _{±2}	85 _{±4}	31 _{±1}

(Table 3.4 cont.)

Run M-131, 2.4% Co ²					
1	440	4.7-5.0	37 _{±1}	84 _{±4}	32 _{±2}
2 ³	440	4.6-5.1	39 _{±0}	87 _{±1}	34 _{±1}
3	440	4.7-5.0	42 _{±1}	80 _{±2}	34 _{±1}
Run M-132, 0.8% Mn ^{2,4}					
1-3	440	4.6-5.7	32 _{±1}	90 _{±4}	29 _{±2}
Run M-133, 2.4% Mn ^{2,4}					
1	440	4.8-5.3	29 _{±1}	84 _{±4}	24 _{±0}
2	440	4.7-5.1	23 _{±1}	82 _{±2}	19 _{±0}
3	440	4.7	5 _{±0}	52 _{±3}	3 _{±0}
Run M-123, 0.1% Pd					
1	440	3.8	43 _{±2}	72 _{±5}	31 _{±3}
2-3	440	4.7-4.9	32 _{±5}	69 _{±10}	22 _{±1}
Run M-122, 0.8% Pd					
1-3	440	4.6-5.0	29 _{±4}	66 _{±6}	20 _{±3}
Run M-128, 0.8% Pd					
1 ⁵	440	4.5-4.9	23 _{±2}	71 _{±2}	17 _{±1}
2 ⁴	440	4.9	22 _{±3}	66 _{±5}	14 _{±3}
3 ⁴	420	4.5-5.0	15 _{±1}	66 _{±3}	10 _{±1}
4	440	4.7	23 _{±1}	71 _{±2}	16 _{±0}
4	450	4.9	25 _{±0}	76 _{±0}	19 _{±0}

¹ 17 wt.% CeO₂/Al₂O₃, Sud-Chemie, 1.59 mm extrudate, P (IBA) = 0.41 atm. Pretreatment and regeneration of catalyst with air at 520 °C and 540 °C, respectively, unless otherwise specified.

² Pretreatment with air at 500 °C.

³ Regeneration with air at 500 °C.

⁴ Regeneration with air at 520 °C.

⁵ Pretreatment with air at 520 °C for 4 h followed by H₂ at 450 °C for 4 h.

3.1.4 3/1 HOAc/DOAc Feeds – CeO₂/Al₂O₃ Catalysts

Kinetics experiments for the MNK reaction were conducted, at temperatures from 400-440 °C and WHSVs from 4-8. A Sud-Chemie 3.18 mm extrudate catalyst, 18.4 wt.% CeO₂/Al₂O₃, surface area 165 m²/g, was used throughout. The primary goal was to determine a satisfactory window of operating temperatures to avoid formation of close

boiling impurities which cannot be separated from the MNK product, and to optimize MNK selectivity at high conversion.

The mass balances (equations in Appendix B) were >94% based on the GC results, except one day at 440 °C, see Figs. 3.10-3.11. The conversions were all high, and the selectivities started at ~70% (wt. basis) and increased to the 80-90% range as the catalyst spent more time on stream, and as the temperatures were reduced. Accounting for some loss in handling and sampling, and the difficulty in trapping all of the acetone, the observed recoveries suggest that everything of lower volatility was being collected.

The GC results showed that the primary side products were dinonylketone and other heavier (than MNK) and lighter (than MNK) ketones. GC-MS analysis showed that there were also some hydrocarbons such as heptadecane, methylundecenes, undecenes, nonane and nonene (K. Dooley, 2003, personal communication). These specific compounds were detected in multiple samples, by GC-MS. These hydrocarbons are products from the decomposition of DOAc on the catalyst surface.

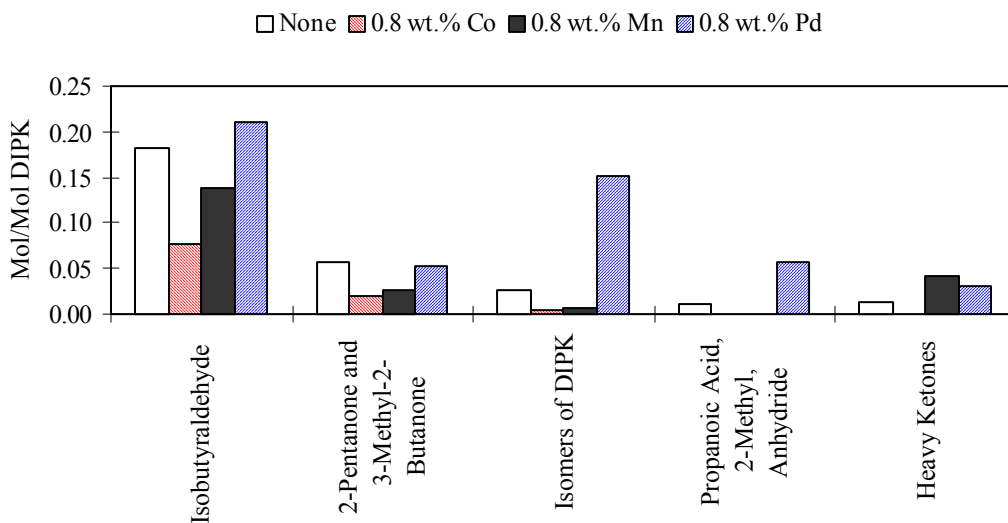


Figure 3.9: Product Distribution, Metal Doped CeO₂/Al₂O₃, 1.59 mm extrudate, 440 °C

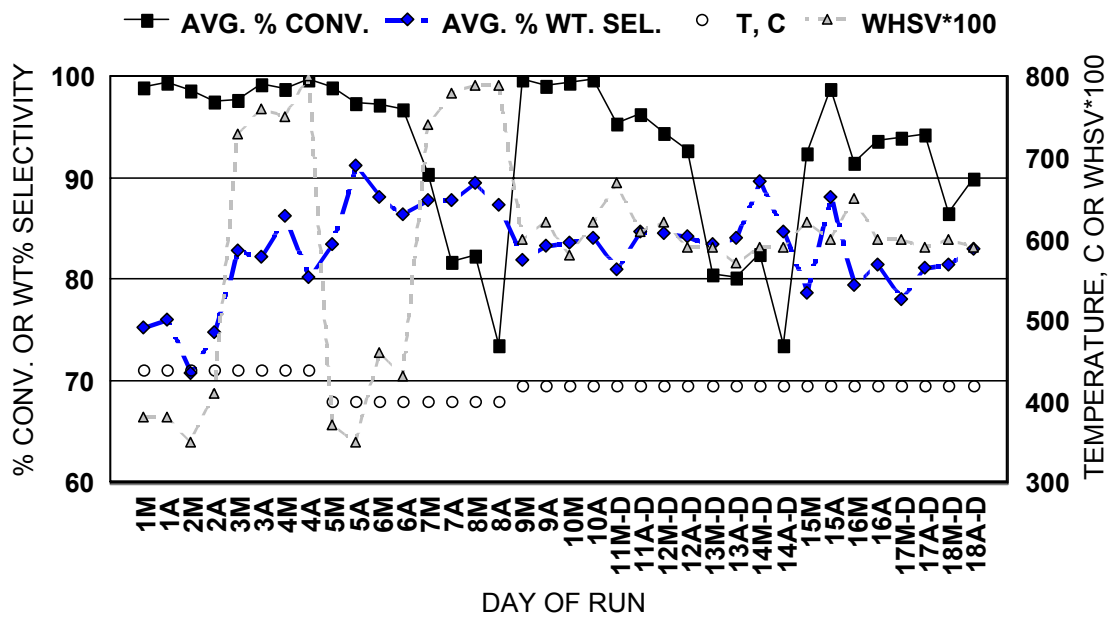


Figure 3.10: Kinetics results, organic layer GC analysis. On the X-axis, “M” means in the morning, “A” in the late afternoon, and “D” denotes days during which there was no catalyst regeneration.

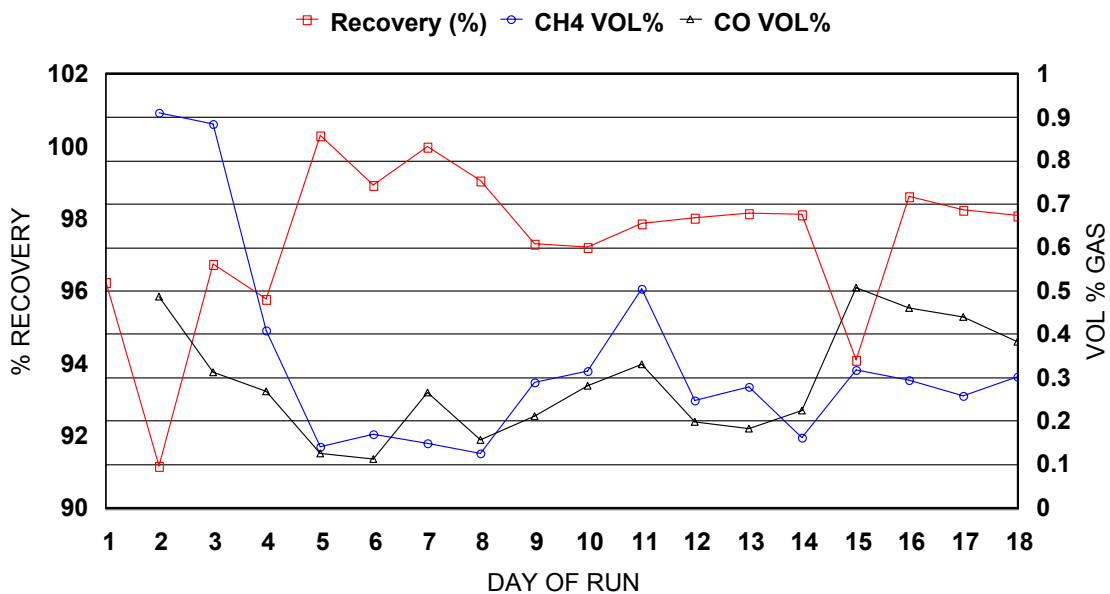


Figure 3.11: Kinetics results, gas phase analysis, and overall mass balance

A typical “day” in the above results was 11.5-12 h run time. The typical procedure was to regenerate the catalyst overnight, with air at 520 °C. However, for days 12-14 and day 18 the reactor was operated with unregenerated catalyst. It is evident that some deactivation took place during these times, but it was gradual. There was no noticeable change in the selectivity. There was no obvious buildup of coke during this time, because neither the pressure drop nor the radial temperature gradient across the reactor increased. Two tests of alternative regeneration conditions were conducted. Comparing day 15 to days 9-11 it appears that regeneration at 470 °C is essentially equivalent to regeneration at 520 °C. Comparing days 16-17 to days 9-11 it is apparent that regeneration at 570 °C does result in a slight penalty in both activity and selectivity. Previous work suggests that this is due to the formation of some inactive CeAlO₃ phase at the higher temperatures (Shyu et al., 1988).

In the gas phase analysis CO₂ was the primary product; the amounts of methane and CO are given in Fig. 3.11. Traces (<0.1% total) of N₂, O₂, ketene, ethane, ethylene and water were also observed. Most of the water was trapped in the liquid phase product. According to Child and Hay (1964) and Knopp et al. (1962) the primary low temperature (<350 °C), noncatalytic reactions of HOAc are dehydration to ketene and condensation to acetic anhydride. Virtually none of either product was found in these experiments. According to Nguyen et al. (1995) and Blake and Jackson (1968, 1969) the primary high temperature (>450 °C), noncatalytic reactions are dehydration to ketene and decarboxylation to methane and CO₂. Of course, ketene itself decomposes at high temperatures to form methylene radicals and CO (Mackie and Doolan, 1984). There are also indications that the decarboxylation reaction can produce CO at high temperatures,

from the reaction of methylene radicals and CO₂ (Mackie and Doolan, 1984). The results here suggest that such decarboxylation could be occurring, because from Fig. 3.11 it appears that the methane and CO concentrations are almost equivalent, except at startup conditions (T = 440 °C). But even at these startup conditions there is very little gas-phase decomposition compared to the liquid phase reactions.

Based on previous work (Randery et al., 1999), it is not unusual to observe the selectivity of the catalyst increase some in the first few days of operation, regardless of what conditions are used. However, the above results clearly show that 440 °C, WHSV ~4 is a severe operating condition that leads to loss of selectivity and HOAc decomposition. On the other hand, operation at 400 °C, WHSV ~8 leads to low conversions and excessive amounts of HOAc and other organics (mostly DOAc and MNK) in the aqueous product. In all cases except at 400 °C, WHSV ~8, only small amounts of HOAc are present in any organic layer sample.

Experiments were also conducted in the smaller quartz reactor using the 3/1 HOAc/DOAc feed. Results are summarized in Table 3.5. The conversions obtained here are lower than those in run M-139 because the partial pressure of the feed components is only 0.34 atm; this reaction is obviously overall positive order.

Using the 400 °C data from runs M-137 and M-139, a good fit for the observed rate constant ($k_2\eta$) (Fig. 3.12) is obtained assuming a first order reaction. The rate of disappearance of DOAc is given by,

$$r_{\text{DOAc}} = k_1 \quad \text{- Zero-order reaction}$$

$$r_{\text{DOAc}} = k_2 C_0 \quad \text{- First-order reaction}$$

The equations used in the fits are as follows:

$$X = \underbrace{\frac{k_1 \eta MW_{\text{DOAc}}}{\rho_c}}_{\text{Slope}} \left(\frac{1}{\text{WHSV}} \right) \quad \text{- Zero-order reaction}$$

$$(1 + \varepsilon) \ln \left(\frac{1}{1 - X} \right) - \varepsilon X = \underbrace{\frac{k_2 \eta MW_{\text{DOAc}} C_0}{\rho_c}}_{\text{Slope}} \left(\frac{1}{\text{WHSV}} \right) \quad \text{- First-order reaction}$$

where k_1 and k_2 are the rate constants, $\text{mol}/(\text{cm}^3 \text{ catalyst} \cdot \text{h})$ and h^{-1} , respectively, η is the effectiveness factor, ρ_c is the density of the catalyst, g/cm^3 , C_0 is the concentration of DOAc in feed, mol/cm^3 , X is the IBA fractional conversion, and ε is the volumetric expansion factor. The observed rate constants ($k_2 \eta$) obtained from the regressed data are 0.010 h^{-1} and 0.018 h^{-1} for the DOAc partial pressures of 0.09 atm and 0.25 atm respectively.

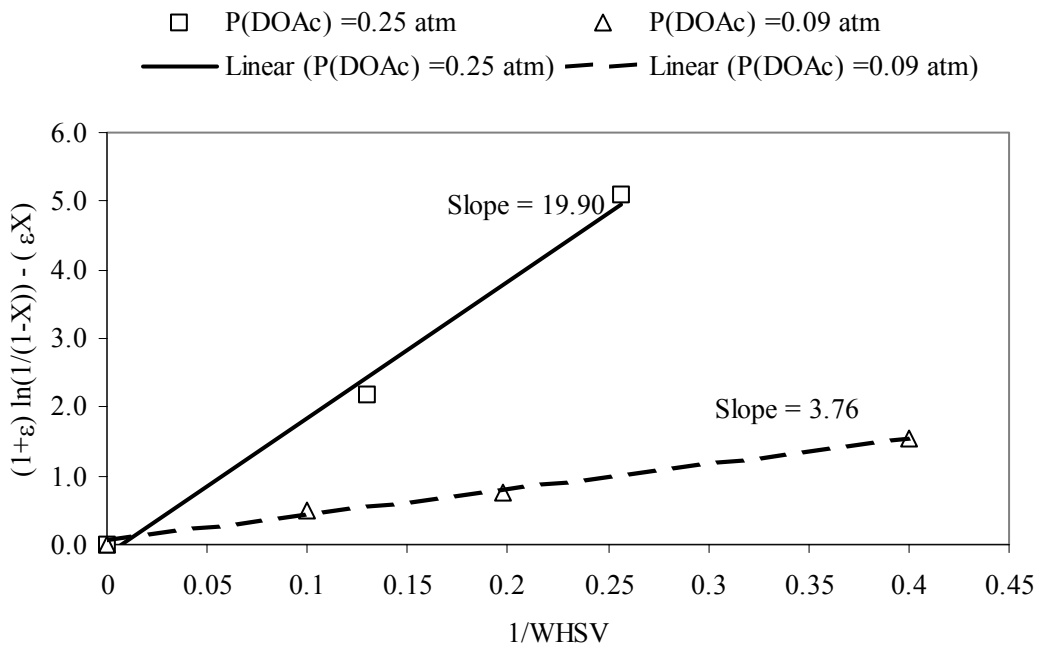


Figure 3.12: Data fit for a first-order reaction, 3/1 HOAc/DOAc feed, 400 °C, X=DOAc fractional conversion, ε = volumetric expansion factor

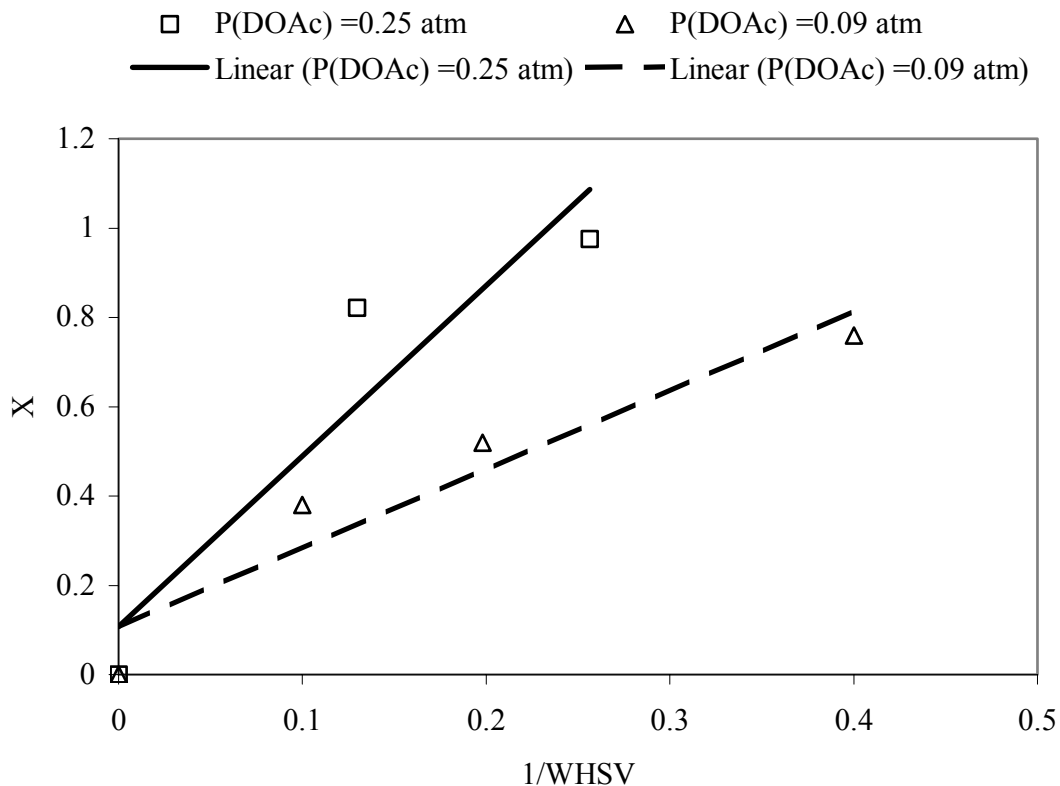


Figure 3.13: Data fit for a zero-order reaction, 3/1 HOAc/DOAc feed, 400 °C, X = DOAc fractional conversion

3.1.5 3/1 HOAc/DOAc feeds – Metal-Doped CeO₂/Al₂O₃ Catalysts

Comparing runs M-137, M-138 and M-135 (Table 3.5) it is seen that both of the metal-doped catalysts, were more active than the base catalyst. Fig. 3.14 gives a comparison for the product distributions for runs M-137 and M-135 at 400 °C and three different WHSVs. It is seen that at WHSV~5 the 2.4 wt.% Co-doped and base catalysts gave similar product distributions. At other WHSVs (2.5 and ≥ 10) the selectivities were lower than the base catalyst. The 0.8 wt.% Pd doped catalyst gave a better selectivity at comparable conditions, in limited testing.

Table 3.5: Summary of Results of 3/1 HOAc/DOAc Condensation on CeO₂/Al₂O₃ Catalysts¹

Day #	Temp. Range, °C	WHSV	% DOAc Conversion	% Wt. Selectivity	% Molar Yield
Run M-137 ²					
1	400	5.2-5.4	60±5	84±1	50±5
2	400	4.8-5.2	38±4	79±1	30±4
3-6	400	4.7-5.2	54±7	82±2	44±7
7	400	10	38±2	92±0	35±1
7	400	2.5	76±1	86±0	64±1
8	350	4.7	27±1	91±0	24±1
8	375	5.3	35±2	93±0	33±2
Run M-138, 0.8% Pd					
1-4	400	4.7-5.0	65±7	91±2	59±7
Run M-135, 2.4% Co					
1-2	400	4.8-5.1	65±3	84±1	55±3
3	400	12.3	33±0	86±1	29±0
3	400	2.5	91±0	71±3	66±0
4	350	4.8	18±0	85±1	16±1
4	375	4.9	45±1	88±0	39±1

¹ 17% CeO₂/Al₂O₃, Sud-Chemie, 1.59 mm extrudate, pressure of reactants = 0.34 atm, pretreatment and regeneration with air at 500 °C and 520 °C, respectively, unless otherwise specified.

² Regeneration with air at 540 °C except on day #2 (520 °C).

3.2 Catalyst Characterization

Hydrogen chemisorption of the metal-doped catalysts was used to determine the metal dispersion and catalyst reduction behavior using H₂ gas at 0 °C and at 150 °C. Tables 3.6-3.7 give the results of these tests. Dispersion is defined as the ratio of the number of metal atoms exposed at a particle surface to the total number of metal atoms present. In these calculations it was assumed that one H atom is adsorbed for each exposed metal atom.

The amount of H₂ adsorbed on CeO₂/Al₂O₃ at both 0 °C and at 150 °C was negligible. This was expected, because for pure CeO₂ reduction by H₂ begins near 200 °C (Laachir et al., 1991). Bensalem et al. (1995) obtained a dispersion of 270% at 100 °C for 1.58% Pd/CeO₂. They ascribed this result to H₂ spillover from Pd to CeO₂; in other words, the Pd remained a separate phase. From Table 3.7 it is clear that spillover is possible for the 0.8% Pd, but not the 0.1% Pd, catalyst. It can be concluded that the addition of Pd to CeO₂/Al₂O₃ does not result in complete dissolution of Pd, and therefore could increase Ce reduction through a spillover process at higher temperatures. Gatica et al. (2001) have observed (HRTEM, SEM) from studies of 0.55 wt.% Pd supported on Ce_{0.68}Zr_{0.32}O₂ mixed oxide that the Pd particles on the oxide surface are heterogeneously distributed with high concentrations at certain locations.

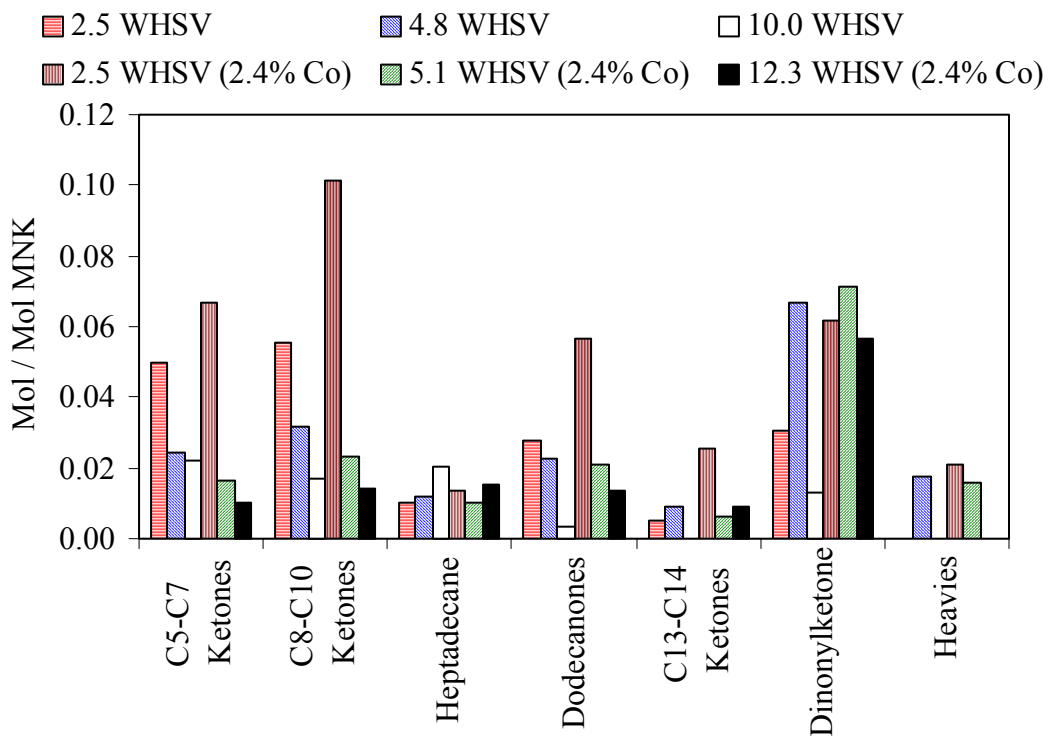


Figure 3.14: Comparison of Product Distributions at 400 °C for Pure/Doped 17% CeO₂/Al₂O₃ at different WHSV

It is clear that while the Co in Co/CeO₂ is not as heterogeneous as Pd, there is some metallic phase capable of H₂ spillover to CeO₂, for the 2.4% Co catalyst. Ho et al. (1992) observed similar behavior for Co/TiO₂ catalysts (Co > 1 wt.%). It was observed that upon increasing the temperature from ambient to 185 °C the hydrogen uptake increases twofold.

Table 3.6: Metal Dispersion for Catalysts at 0 °C

Catalyst	% Dispersion	Mol H ₂ / g Cat	Mol H ₂ / Mol Ce
17% CeO ₂ /Al ₂ O ₃	0	0	0
20% CeO ₂ /Al ₂ O ₃	0	0	0
17% CeO ₂ /0.1% Co/Al ₂ O ₃	0	0	0
17% CeO ₂ /0.8% Co/Al ₂ O ₃	0	0	0
17% CeO ₂ /2.4% Co/Al ₂ O ₃	0	0	0
17% CeO ₂ /0.1% Pd/Al ₂ O ₃	0	0	0
17% CeO ₂ /0.8% Pd/Al ₂ O ₃	42	1.6 x 10 ⁻⁵	0.016
17% CeO ₂ /0.8% Mn/Al ₂ O ₃	0	0	0
17% CeO ₂ /2.4% Mn/Al ₂ O ₃	0	0	0

Table 3.7: Metal Dispersion for Catalysts at 150 °C

Catalyst	% Dispersion	Mol H ₂ / g Cat	Mol H ₂ / Mol Ce
17% CeO ₂ /Al ₂ O ₃	0	0	0
20% CeO ₂ /Al ₂ O ₃	0	0	0
17% CeO ₂ /0.1% Co/Al ₂ O ₃	0	0	0
17% CeO ₂ /0.8% Co/Al ₂ O ₃	0	0	0
17% CeO ₂ /2.4% Co/Al ₂ O ₃	29	5.9 x 10 ⁻⁵	0.061
17% CeO ₂ /0.1% Pd/Al ₂ O ₃	6.2	0.029 x 10 ⁻⁵	0.0003
17% CeO ₂ /0.8% Pd/Al ₂ O ₃	160	5.8 x 10 ⁻⁵	0.060
17% CeO ₂ /0.8% Mn/Al ₂ O ₃	0	0	0
17% CeO ₂ /2.4% Mn/Al ₂ O ₃	0	0	0

TGA experiments were conducted to determine the amount of coke on used catalysts both with and without regeneration. The results are summarized in Table 3.8 while Figs. 3.15-3.18 show typical TGA plots. A few of the catalysts analyzed here were from previous experiments by Randery (1999) and Hendren (2001). Their work showed no evidence of residual coke on used catalysts that had been calcined in air at 520 °C. Obviously coke or oligomeric carbon-rich material does build up on the catalysts during reaction, because they deactivate somewhat over a few days of operation, as shown in Fig. 3.10. But coke or other heavy material does not seem to be present in large amounts after just one day of usage, and it appears to be easily removed. Used catalyst from run M-139 (results in Fig. 3.8) was examined. Note that this catalyst underwent 2 days of reaction (23-24 h) prior to removal from the reactor, without any regeneration. Assuming that the weight losses in air below 300 °C are primarily associated with water (based on work with fresh catalysts, e.g., Fig. 3.15), we found that the used catalyst lost 0.071 g/g at 300-520 °C while the fresh catalyst lost only 0.009 g/g. This suggests deposition of 0.062 g/g coke and oligomeric carbon-rich material on the used catalyst, which corresponds to a recovery (mass balance) loss of 0.022% over the course of a typical day at WHSV = 6, and a lost yield of 0.011%. The TGA results (Figs. 3.13-3.15) showed that almost all of the heavy material was removed by 470 °C. Comparing the TGA's from the catalysts of runs M-70 and M-139, the lower amount of heavy material production in run M-70 is probably due to a lower reaction temperature employed there (400 °C vs. 420 °C in run M-139). However, neither amount is significant in terms of lost yield.

Table 3.8: Results of TGA Experiments –Unused vs. Used Catalysts

CATALYST / RUN	LOSS (g/g of catalyst)	
	50-520 °C	300-520 °C
15% CeO ₂ / Basic Al ₂ O ₃	0.051	0.012
15% CeO ₂ / Basic Al ₂ O ₃ / run M-55C ¹	0.026	0.007
15% CeO ₂ / Al ₂ O ₃	0.062	0.013
15% CeO ₂ / Al ₂ O ₃ / run M-70 ²	0.053	0.029
17% CeO ₂ / Al ₂ O ₃	0.044	0.012
17% CeO ₂ / Al ₂ O ₃ / run M-81 ¹	0.054	0.014
18.4 % CeO ₂ / Al ₂ O ₃	0.040	0.009
18.4 % CeO ₂ / Al ₂ O ₃ / run M-139 ³	0.093	0.071
20% CeO ₂ / Al ₂ O ₃	0.005	0.008
20% CeO ₂ / Al ₂ O ₃ / run M-103 ¹	0.045	0.013

¹ Used catalyst but regenerated with air at 520 °C prior to removal from reactor.

² Used catalyst, ~31 h time on stream.

³ Used catalyst, ~24 h time on stream.

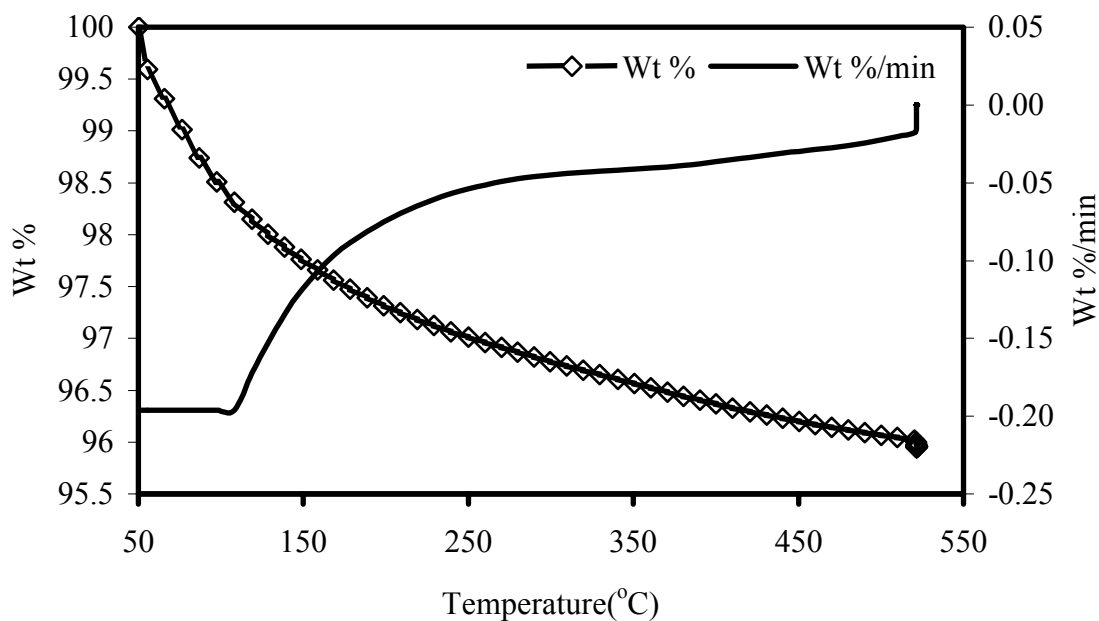


Figure 3.15: TGA analysis, fresh 18.4% CeO₂/Al₂O₃, 3.18 mm extrudate

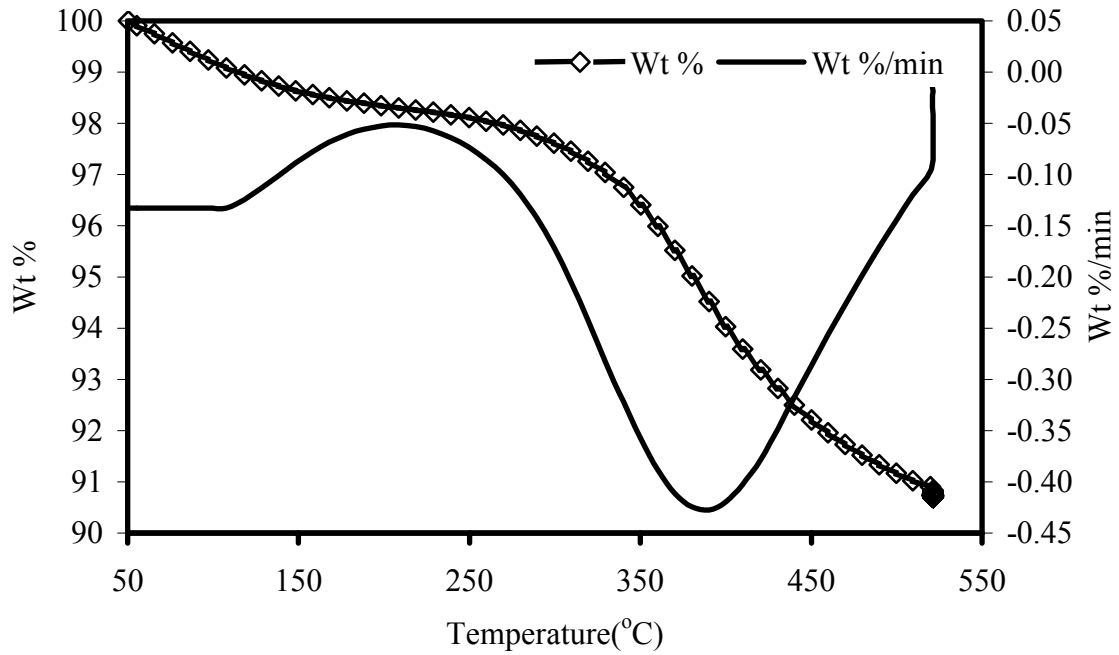


Figure 3.16: TGA analysis, 18.4% CeO₂/Al₂O₃ used in Run M-139, 3.18 mm extrudate

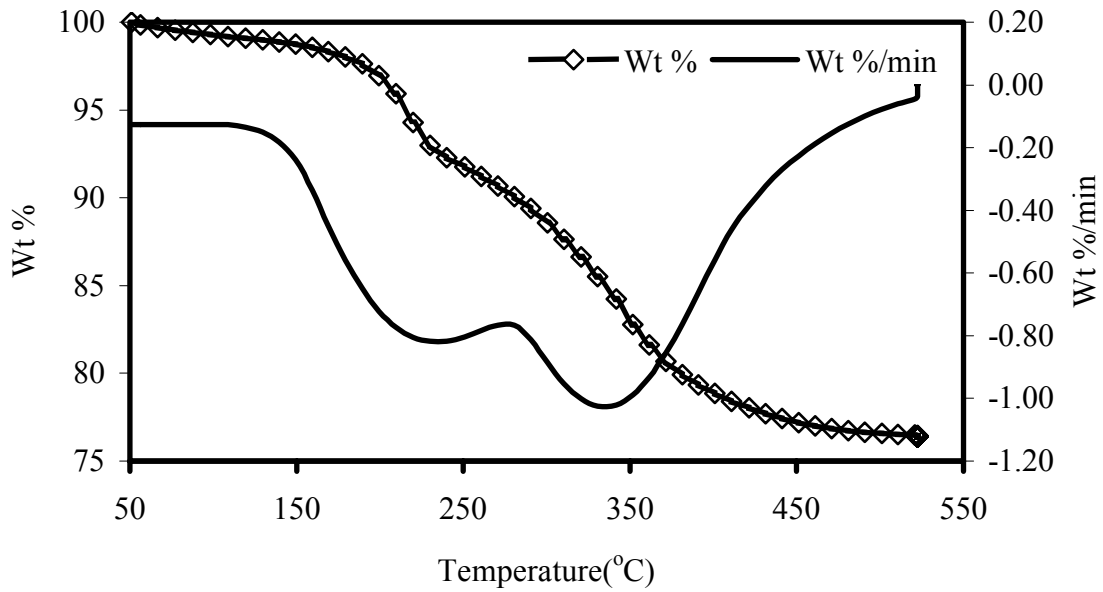


Figure 3.17: TGA analysis, 15% CeO₂/0.1%K₂O/Al₂O₃ used in Run M-74, 1.27 mm extrudate

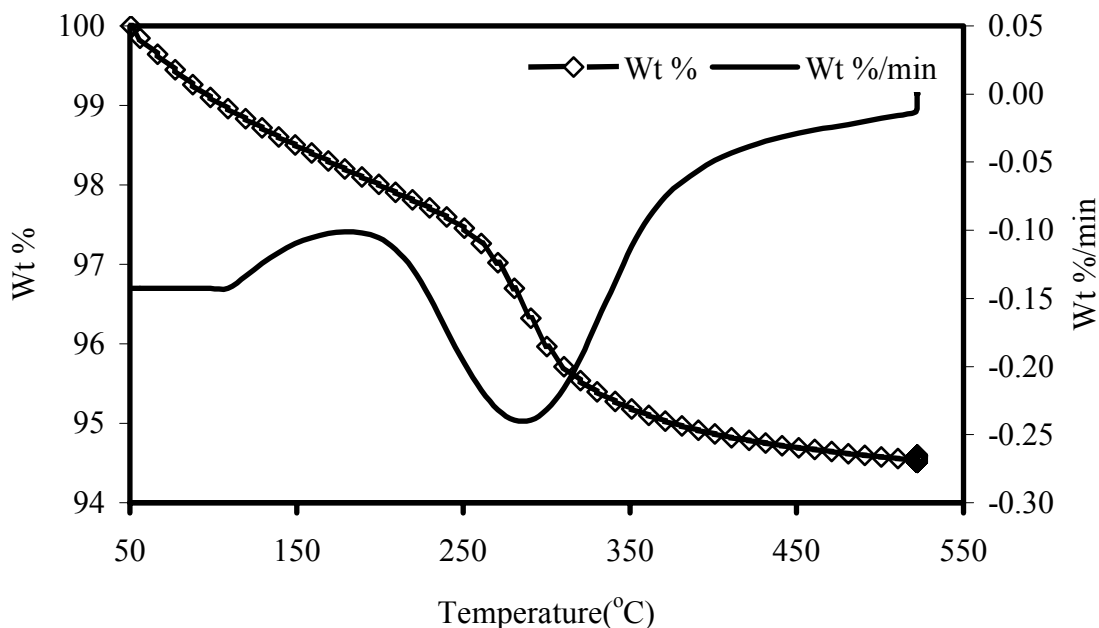


Figure 3.18: TGA analysis, 17% CeO₂/Al₂O₃ used in Run M-81, 1.59 mm extrudate

The coordination environment of Ce for certain catalysts was explored using XANES at both ambient temperature and at 420 °C (a typical reaction temperature) using either 10% H₂/N₂ (to simulate the reducing atmosphere of the carboxylic acid reactants) or He as the gas phase. The Ce³⁺/Ce⁴⁺ ratio was estimated by the method of Takahashi et al. (2002) and using the software package WinXAS 97(version 1.3, Ressler, 1998). Normalized XANES spectra at the Ce L_{III}-edge were used for these analyses. The data processing software Athena (version 0.8.024, Ravel, 2003) was used for normalization and background removal; the Cromer-Lieberman algorithm was used for normalization. When using WinXAS 97, background removal was done using a first order polynomial function. The threshold energy E₀ was identified as the energy of maximum derivative of $\mu(E)$. The spectra were then normalized by dividing by the actual absorption at 100 eV above the edge.

XANES spectra for the standards Ce(III) acetate and CeO₂ are shown in Figs. 3.19-3.20. For Ce(III) acetate a single peak, denoted A1, is observed at 5.7261 keV. For CeO₂, two main peaks, denoted B and C, are observed at 5.7298 and 5.7376 keV respectively, and a feature denoted A2 is observed around 5.7261 keV as a shoulder to peak B. Based on previous works, the peak A1 is attributed to Ce³⁺ and the peaks B and C are attributed to Ce⁴⁺ (Kaindl et al., 1987, Takahashi et al., 2000). Kaindl et al. (1987) assigned the feature A2 in CeO₂ to Ce³⁺ impurities. However, this assignment was disputed by Fallah et al. (1994), who observed that the A2 feature of CeO₂ persisted upon prolonged oxidation at 400 °C where the presence of Ce³⁺ impurities was highly improbable. Soldatov et al. (1994) ascribed this shoulder as being due to the crystal-field splitting of Ce 5d states when multiple-scattering is taken into account.

Using the method of Takahashi et al. (2002), one Lorentzian function and one arctangent function was assigned to each of the three peaks A1, B, and C, or A2, B, and C. The following equation was used to fit the data,

$$Y(E) = \underbrace{a \arctan[(b)(E - c)] + \frac{a\pi}{2}}_{\text{arctangent}} + \underbrace{\frac{de^2}{[(E - f)^2 + e^2]}}_{\text{Lorentzian}}$$

where E (keV) is the energy of the incident X-ray, and a, d (amplitude), b, e (width) and c, f (peak center) are the unknown parameters.

The following procedure was followed for peak-fitting. Calculations were done in an Excel spreadsheet.

1. For each arctangent/Lorentzian combination, the center positions were fixed relative to each other at values given by Takahashi et al. (2002).

2. Peak fitting was first done for the Ce(III) acetate reference using one arctangent/Lorentzian combination.
3. For the two arctangent and Lorentzian functions associated with Ce⁴⁺, the ratio of amplitudes (d/a) was kept fixed at 8.9, as in Ce(SO₄)₂.
4. The area of the Lorentzian (R) was calculated using the relation $R = \pi de$.
5. The area ratio of the two Lorentzians associated with Ce⁴⁺ was kept fixed at 1.4, as in Ce(SO₄)₂.
6. The widths (e) of the two Lorentzians associated with Ce⁴⁺ were set equal, as required theoretically.
7. The peak area ratio of the Lorentzian functions for Ce⁴⁺ and Ce³⁺, denoted R⁴⁺ and R³⁺, was used to estimate Ce⁴⁺/Ce³⁺ using the relationship developed by Takahashi et al. (2002).

$$X^{4+} (\%) = 100 \left[\frac{C^{4+}}{C^{3+} + C^{4+}} \right] = 100 \left[\frac{R^{4+}}{kR^{3+} + R^{4+}} \right]$$

where $k = 1.09 \pm 0.05$.

8. The CeO₂ reference spectra were fitted using the peak center locations and amplitude ratios (arctangent/Lorentzian) obtained for Ce(III) acetate to describe the A2 feature in CeO₂. By least squares fitting, a value of 10 atom% could be mistakenly assigned to Ce³⁺ even in CeO₂, if the A2 feature is taken as A1. Thus it is possible that the Ce⁴⁺ estimated by the method of Takahashi et al. is smaller than the actual value by as much as 10%. The fitted parameters for Ce(III) acetate and CeO₂ from the standards themselves are in Table 3.9, the fits are shown in Figs. 3.19-3.20. Here L1 and L2 represent the low (5720 eV) and high (5740 eV) limits of the fitting domain.

9. The spectra of the other samples were fitted as a linear combination of Ce^{4+} and Ce^{3+} spectra using least squares fitting. The parameter f associated with the second Lorentzian of Ce^{4+} was left unconstrained, while all other parameters associated with peak center locations were fixed relative to it using values obtained from the fits of the reference standards, taking into account slight changes in energy calibration. Also the widths b and e were kept fixed at the reference standard values.

Figs. 3.21-3.22 show typical peak-fitting results. Table 3.10 gives the results of the fitting parameters for 15 wt.% $\text{CeO}_2/\text{Al}_2\text{O}_3$ reduced in 10% H_2 at 420 °C. From Table 3.11, it is seen that the addition of K or Pd to the base catalyst may slightly increase the Ce^{3+} content at ambient conditions, although the change is probably not significant given the difficulty in resolving the A1 and A2 peaks – note that even CeO_2 shows 10% Ce^{3+} according to this method. In Fig. 3.23 the Ce^{3+} content is compared for several $\text{CeO}_2/\text{Al}_2\text{O}_3$ catalysts at 420 °C. It is seen that all three catalysts showed an increase in Ce^{3+} content even when heated in He; the differences in estimated Ce^{3+} content were slight. Under reducing conditions, the 0.8 wt.% Co showed the highest amount of Ce^{3+} .

Table 3.11 also shows a comparison of results obtained here using the method of Takahashi et al. (2002) with simple least-squares refinement based on selected reference compounds (Ce(III) acetate and CeO_2) using WinXAS 97. A good match is observed at high Ce^{3+} content, where there is less interference due to the A2 peak. The negative values in WinXAS are due to ascribing some of the A1+A2 peak to Ce^{4+} by WinXAS. Clearly this is incorrect at low Ce^{3+} contents in supported monolayer catalysts, where A1 dominates in the A1+A2 peak.

Table 3.9: Fitted parameters of the Takahashi model for Ce(III) acetate and CeO₂

	Arctangent			Lorentzian		
	a	b	c	d	e	f
Ce(III) acetate	0.2535	766	5.7237	2.5845	0.0026	5.7261
CeO ₂	0.0291	766	5.7237	0.2970	0.0026	5.7261
	0.1311	837	5.7253	1.1672	0.0034	5.7298
	0.0939	840	5.7320	0.8337	0.0034	5.7376

Table 3.10: Fitted parameter, method of Takahashi et al., for 15 wt.% CeO₂/Al₂O₃ treated in H₂ at 420 °C

	Arctangent			Lorentzian		
	a	b	c	d	e	f
Ce ³⁺	0.1114	766	5.7212	1.1359	0.0026	5.7236
Ce ⁴⁺	0.0849	837	5.7227	0.7556	0.0034	5.7272
	0.0608	840	5.7294	0.5397	0.0034	5.7350

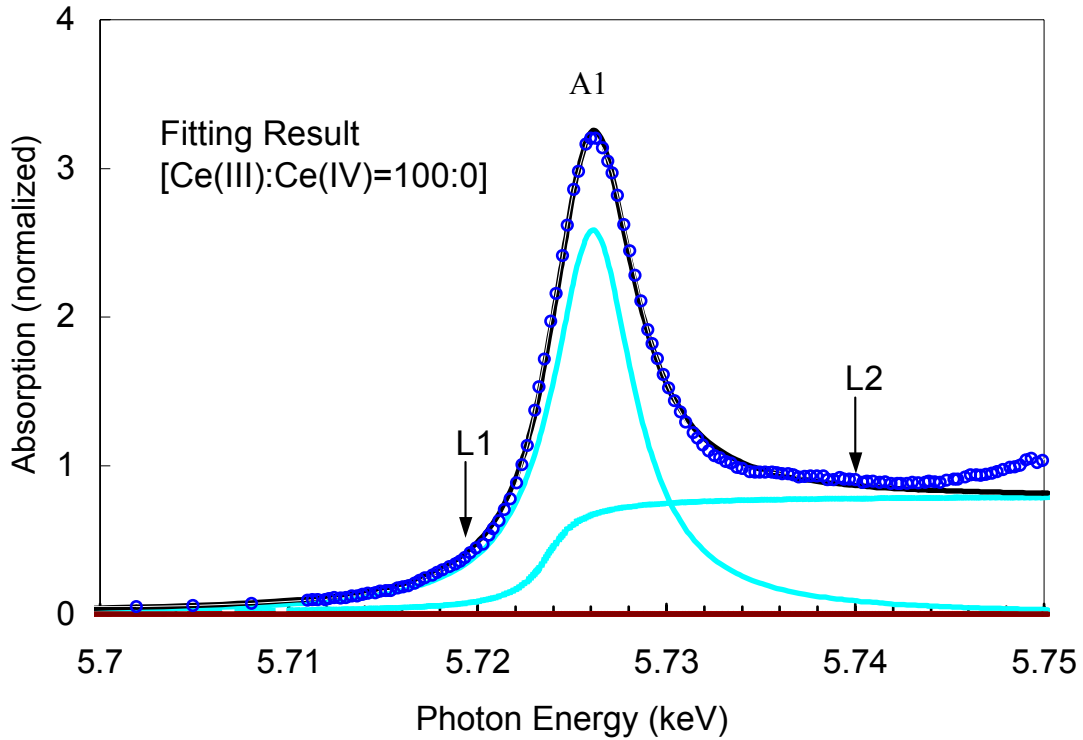


Figure 3.19: Ce L_{III}-edge XANES spectra for Ce(III) acetate

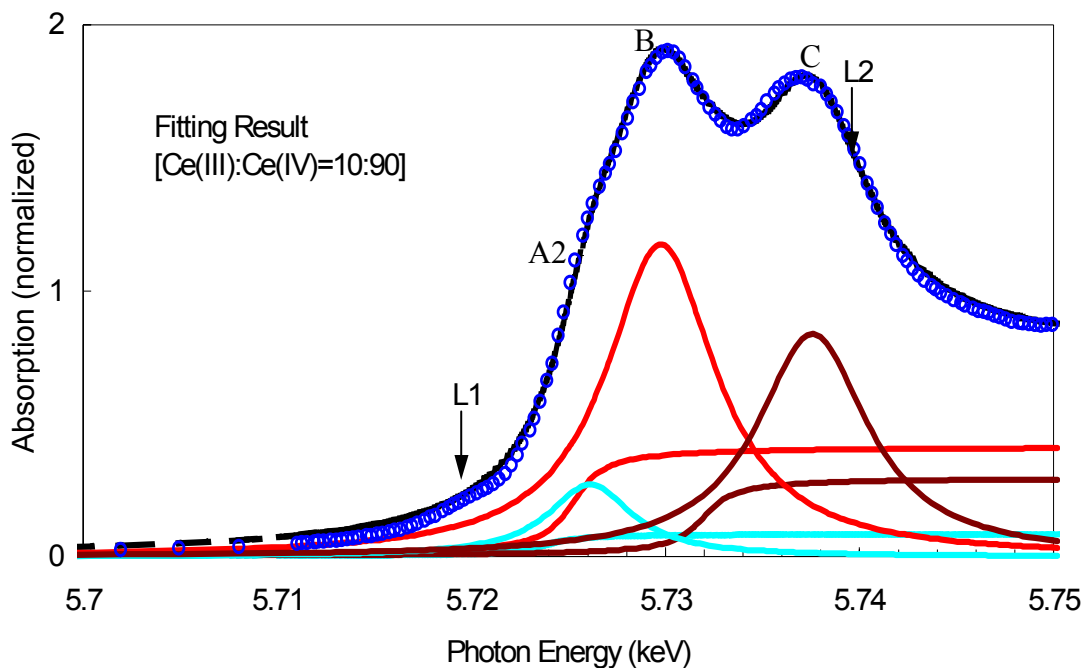


Figure 3.20: Ce L_{III}-edge XANES spectra for CeO₂

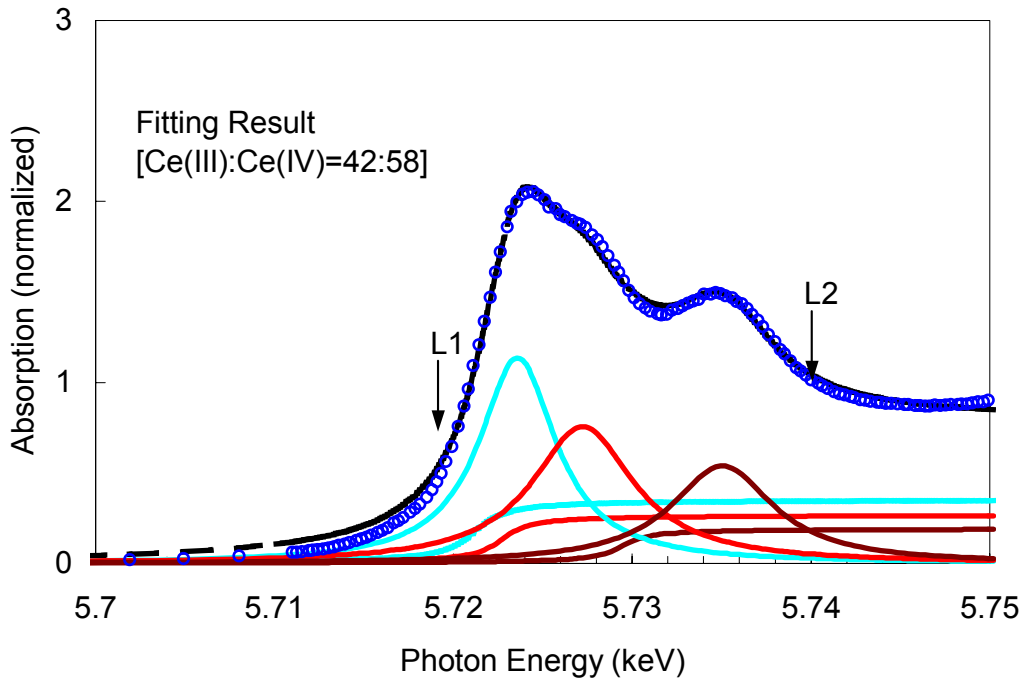


Figure 3.21: Ce L_{III}-edge XANES spectra for 15 wt.% CeO₂/Al₂O₃ treated in H₂ at 420 °C

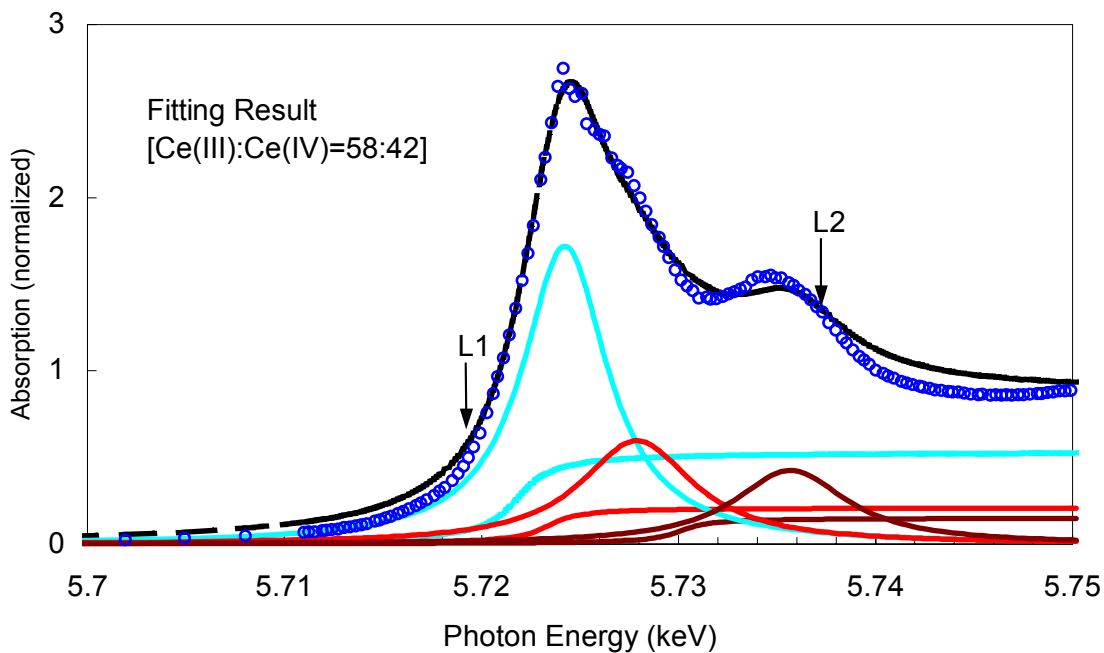


Figure 3.22: Ce L_{III}-edge XANES spectra for 0.8 wt.% Co/17 wt.% CeO₂/Al₂O₃, treated in H₂ at 420 °C

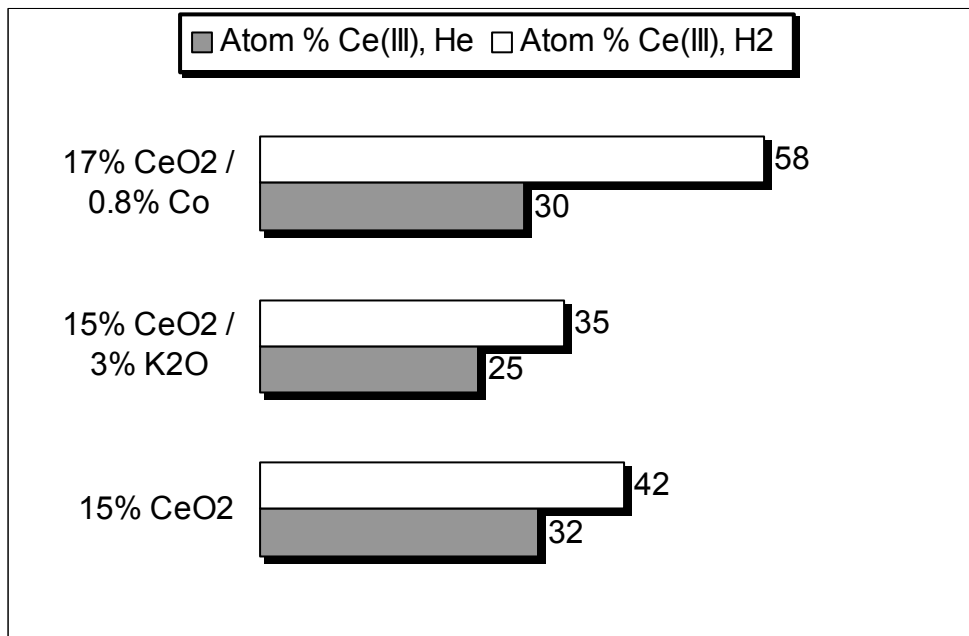


Figure 3.23: Comparison of Ce³⁺ content for doped-CeO₂/Al₂O₃ with CeO₂/Al₂O₃, 420 °C

Table 3.11: Comparison of method of Takahashi et al. (2002) with least-squares refinement, WinXAS, for Ce L_{III}-edge XANES spectra

	WinXAS	Method of Takahashi et al.
	Atom% Ce(III)	Atom% Ce(III)
Ce(III) acetate, ambient	Standard 1	100
CeO ₂ , ambient	Standard 2	10
17% CeO ₂ /0.8% Co/Al ₂ O ₃ , ambient	3	10
17% CeO ₂ /0.8% Co/Al ₂ O ₃ , He, 420 °C	37	30
17% CeO ₂ /0.8% Co/Al ₂ O ₃ , H ₂ , 420 °C	58	58
15% CeO ₂ /Al ₂ O ₃ , ambient	-8	4
15% CeO ₂ /Al ₂ O ₃ , He, 420 °C	38	32
15% CeO ₂ /Al ₂ O ₃ , H ₂ , 420 °C	43	42
15% CeO ₂ /3% K ₂ O/Al ₂ O ₃ , ambient	-7	13
15% CeO ₂ /3% K ₂ O/Al ₂ O ₃ , He, 420 °C	26	25
15% CeO ₂ /3% K ₂ O/Al ₂ O ₃ , H ₂ , 420 °C	35	35
17% CeO ₂ /2.4% Co/Al ₂ O ₃ , ambient	0	10
17% CeO ₂ /0.1% Pd/Al ₂ O ₃ , ambient	4	13
17% CeO ₂ /0.8% Pd/Al ₂ O ₃ , ambient	17	17

The Co K-edge spectra were analyzed using WinXAS 97. First, $\mu(E)$ was background-corrected by subtracting a first order polynomial function. The threshold energy E_0 was identified as the energy at the maximum derivative of $\mu(E)$. The spectra were then normalized at 50 eV above the edge. Since each spectrum was repeated a number of times, the average was taken after normalizing all spectra. From Fig. 3.24 it is seen that Co in the Co-doped catalysts is present as a mixture of Co(II) oxide and Co(II,III) oxide, with the amount of Co(II,III) oxide increasing slightly with increasing Co content, as determined from the shift in edge position to higher energies.

A smooth background function, $\mu_0(E)$, approximated by a cubic spline function, was subtracted from the averaged normalized spectra to obtain the EXAFS fine-structure function $\chi(E)$. Then $\chi(E)$ was transformed to $\chi(k)$, which was weighted by k^3 . Data from 2–10 \AA^{-1} were selected using a Hanning filter and Fourier transformed into R-space to

produce a pseudo radial distribution function, PRDF(r'). From Fig. 3.25 it is seen that the magnitude of the Fourier transform (FT) for the Co-doped catalyst is much smaller when compared to the standards. The magnitude of the first Co shell for the Co-containing catalyst is smaller by a factor of 3.6 when compared to the first Co shell of Co(II,III) oxide, suggesting a lower coordination number (Sinfelt et al., 1977) and so concentration at the surface. The identification of the various shells for reference standards was done by comparison of the PRDFs with those of Huffman et al. (1995).

Finally a qualitative analysis of Pd L_{III}-edge XANES (Fig. 3.26) shows that Pd in the Pd-doped catalysts is present as PdO.

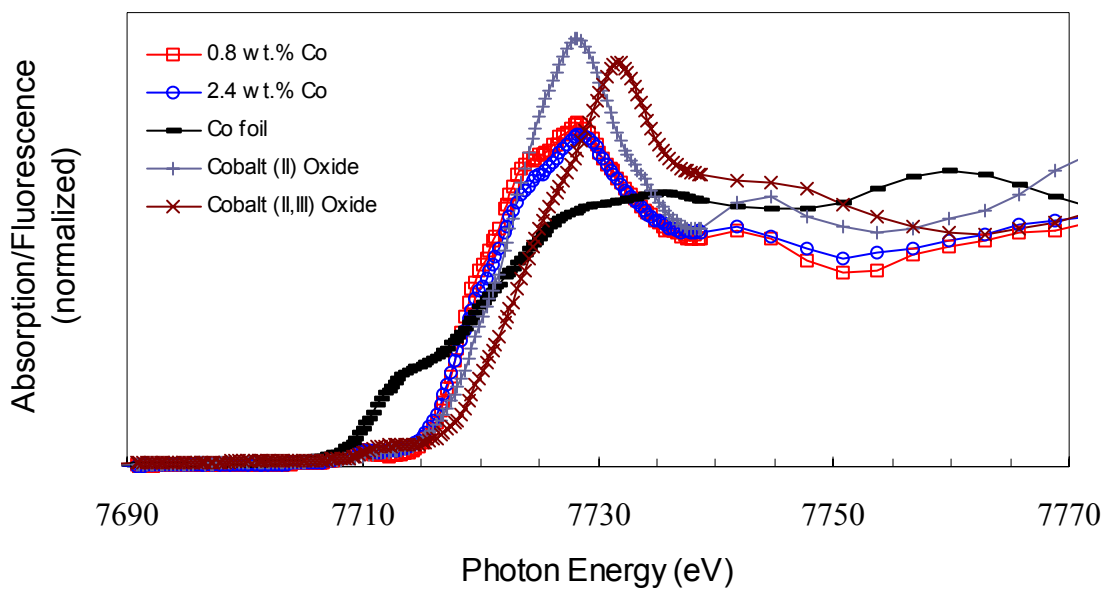


Figure 3.24: Comparison of Co K-edge XANES spectra of various Co-doped $\text{CeO}_2/\text{Al}_2\text{O}_3$ with standards, ambient conditions

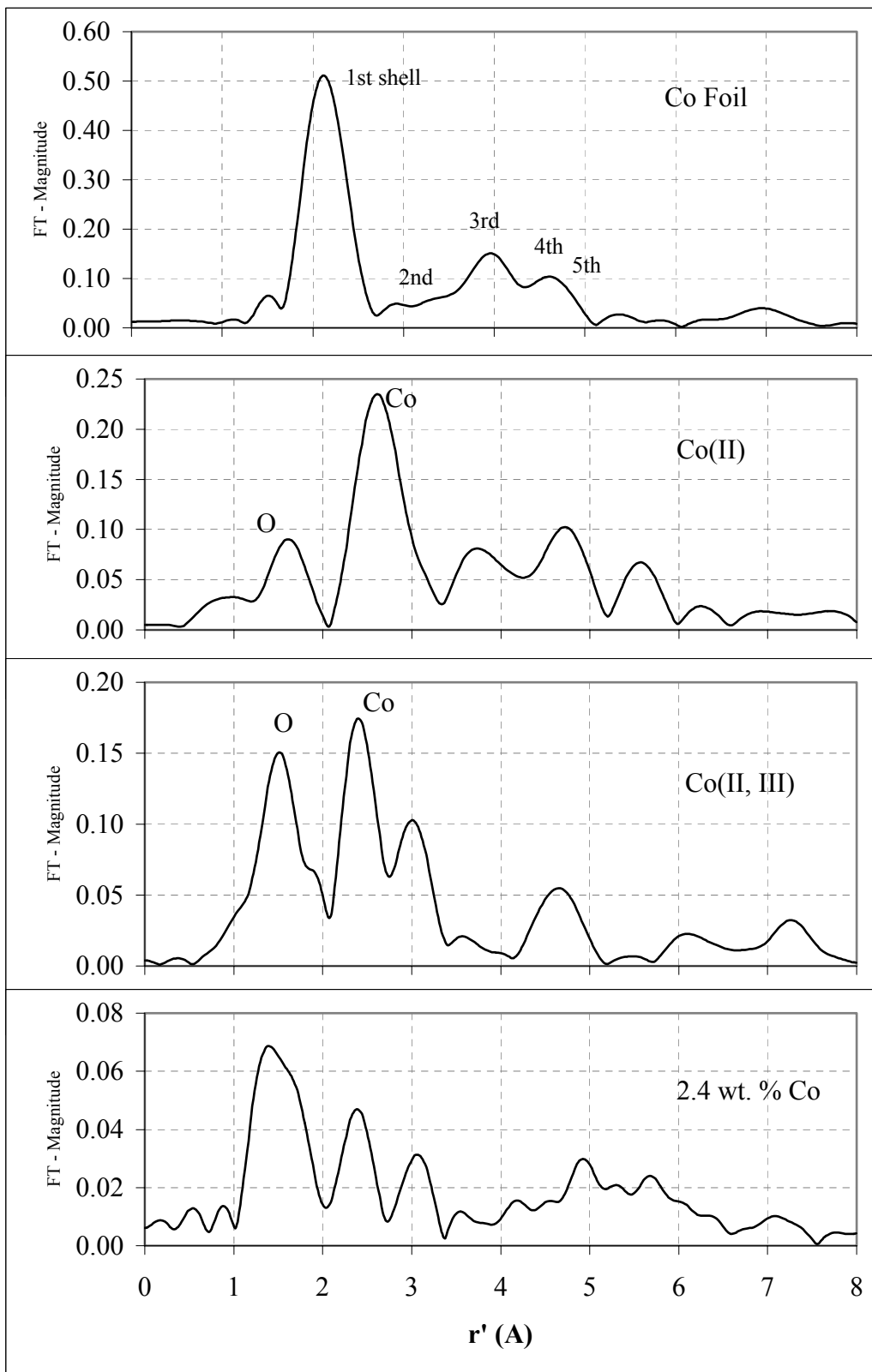


Figure 3.25: Comparison of PRDF of 2.4 wt.% Co/CeO₂/Al₂O₃ with Co and Co oxides, ambient conditions

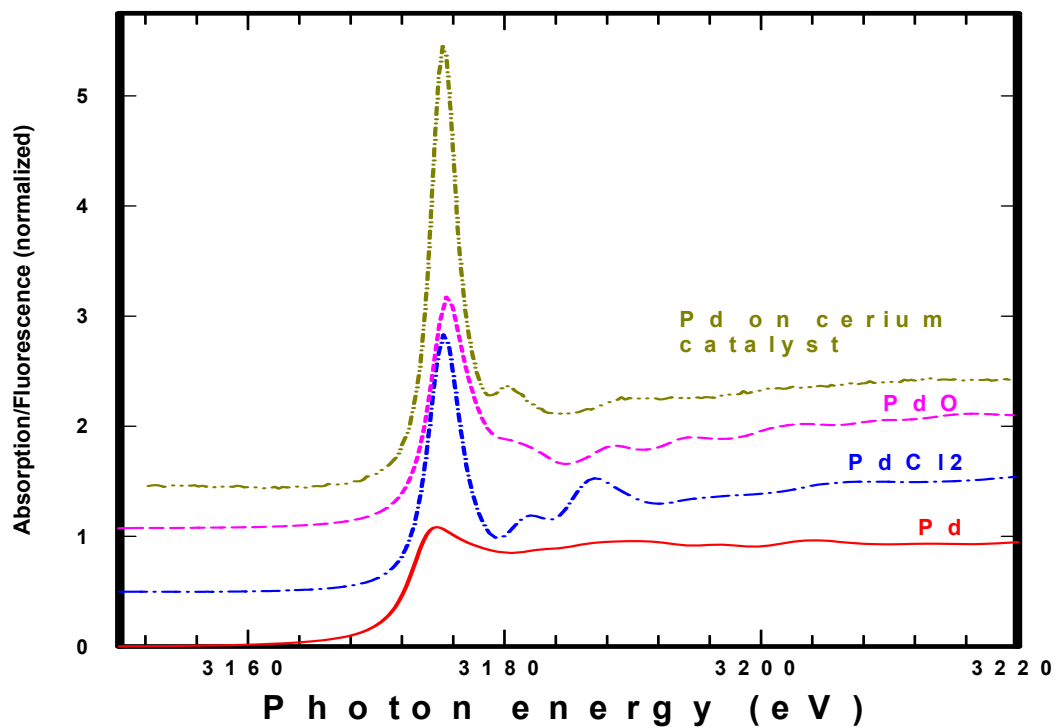


Figure 3.26: Comparison of Pd L_{III}-edge XANES spectra, 0.8 wt.% Pd/17 wt.% CeO₂/Al₂O₃ and standards, ambient conditions (PdO spectra courtesy of H. Modrow, Bonn University, Germany)

CHAPTER 4

CONCLUSIONS

It was seen that supported CeO₂ catalysts effectively catalyzed the synthesis of DIPK and MNK by the decarboxylative condensation of IBA and 3/1 HOAc/DOAc feeds, respectively. These catalysts were not as active for the IBA reaction as for MNK formation. For similar conditions, conversion of IBA was only 43% at 440 °C when compared to 52% for DOAc at a much lower reaction temperature of 400 °C. However, selectivities for the IBA reaction were good, comparable to or better than for MNK formation (~80 wt.%). The optimal temperature range for maximum yield to DIPK was 470-480 °C at WHSVs ~5. The optimal temperature range for MNK production was 400-420 °C at WHSVs ~4-6.

For MNK synthesis, there were no diffusional limitations over the size range studied. But for the IBA condensation reaction, catalyst particle size had a significant effect on the activity and selectivity of the catalyst, indicating diffusional limitations for this reaction. Conversion of IBA increased from 34% (at ~82 wt.% selectivity) to 47% (at ~90 wt.% selectivity) when the catalyst particle size was reduced from 3.18 mm to 1.27 mm. The supported CeO₂ catalysts showed little or no sign of deactivation at the end of the working day. Regeneration with air at 540 °C was sufficient to maintain long-term activity. Buildup of coke on the catalysts was observed. But it was not significant (0.062 g of coke/g of catalyst/ 24 h) and was easily removed by reactivation with air at 520 °C. Regeneration at 470 °C was essentially equivalent to regeneration at 520 °C, but regeneration at 570 °C resulted in slight loss in selectivity.

Doping of the supported CeO₂ catalyst with a transition metal such as Co or Pd (2.4 and 0.8 wt.%, respectively) was found to be beneficial for MNK synthesis. Comparing the 2.4 wt.% Co-doped catalyst with the base catalyst, it was observed that for the Co-doped catalyst the conversion was 65% compared to 54% for the base catalyst at 400 °C and ~5 WHSV; the MNK selectivity was 84 wt.%, comparable to that for the base catalyst. However when the WHSV was lowered to ~2.5, it was seen that for the Co-doped catalyst the increase in activity was negated by a decrease in selectivity leading to MNK molar yields similar to those of the base catalyst. This decrease in selectivity was mainly due to increases in C5-C7 ketones, C8-C10 ketones, dodecanones, C13-C14 ketones, DNK and heavies. At higher WHSVs (≥ 10) the conversions for both the catalysts were similar, but the selectivity for the base catalyst was slightly better (~6 wt.% higher). This was due to increased DNK produced for the Co-doped catalyst. DNK is formed by the condensation of DOAc. So it can be concluded that the addition of Co not only increases the rate of the primary acid condensation reactions, but also the rates of cracking and other condensation reactions. However by operating at an optimum WHSV of ~5, the advantage of increased activity can be utilized while minimizing the side products.

For the DIPK synthesis, doping (0.1 – 2.4 wt.%) of the supported CeO₂ catalyst with a transition metal such as Mn or Pd deactivated the catalyst but the addition of 0.8 wt.% Co increased the molar yield to DIPK. The catalysts doped with Pd deactivated especially rapidly. Of the modified (more acidic or basic) CeO₂/Al₂O₃ catalysts the 15% CeO₂/3% K₂O/Al₂O₃ catalyst showed the best activity and selectivity, although there was no advantage over the plain CeO₂/Al₂O₃ catalyst. The rest of the catalysts examined

showed much lower conversion, or selectivity, or both. This was especially true when CeO₂ was impregnated onto a more acidic support, MCM-41 mesoporous silica. The basic 20 wt.% MgO/ZrO₂ catalyst was also found to be relatively inactive.

Chemisorption studies indicate that the addition of Pd to CeO₂/Al₂O₃ does not result in complete dissolution of Pd in the CeO₂ matrix and therefore could increase the amount of reduced CeO_x through a spillover process at higher temperatures (Bensalem et al., 1995). Qualitative analysis of XANES data of the Pd- and Co-doped catalysts at room temperature, at the Pd L_{III}-edge and Co K-edge, respectively, shows that Pd is present as PdO and Co is present as a mixture of Co(II) oxide and Co(II, III) oxide. Comparison of pseudo radial distribution functions (PRDF) of the Co-doped catalyst with standards indicates a high dispersion for the Co phase. XANES data at the Ce L_{III}-edge of the 0.8 wt.% Co-doped catalyst at 420 °C in 10% H₂/N₂ atmosphere show significantly more Ce³⁺ (16-19 atom% higher than the base catalyst, depending on the computational method) when compared to the base catalyst, indicating H₂ spillover to the CeO₂ matrix. At 420 °C in He there was no difference in Ce³⁺ between doped and undoped catalysts.

Pestman et al. (1997) proposed a mechanism for acid condensation in which a ketene-like intermediate is formed by dehydrogenation, with reduction of the surface, followed by the formation of the final product by re-oxidation of the surface. Hendren and Dooley (2003) reached similar conclusions after conducting pulse reaction experiments using isotopically labeled HOAc/CCA and HOAc/DOAc feeds on supported rare earth oxides. They suggested that acid condensation on rare earth oxides occurs by way of a surface ketene-like intermediate, which couples with a surface carboxylate, eliminating CO₂ in the process. If true, increasing the dehydrogenating ability of the

catalysts should increase both activity and selectivity, up to a point where actual dehydrogenation products are formed preferentially. Partly reduced CeO₂ surfaces are very strongly dehydrogenating (Ferrizz et al., 2001), and can generate alkyl moieties as hypothesized in the “ketene” mechanism (Pestman et al., 1997). Evidence for these phenomena were also observed in this work. For MNK reaction, GC-MS analysis showed that there were also some hydrocarbons such as heptadecane, methylundecenes, undecenes, nonane and nonene (K. Dooley, 2003, personal communication). These hydrocarbons are products from the decomposition of DOAc on the catalyst surface. For IBA reaction the primary side product was isobutyraldehyde. Isobutyraldehyde is formed by reduction of IBA.

For the MNK reaction, the metal-doped (Co, Pd) catalysts showed higher activity and selectivity when compared to the base catalyst, consistent with metallic promotion of the initial dehydrogenation through stabilization of the ketene intermediate. But for the IBA reaction there was improvement with a 0.8 wt.% Co catalyst, and lower activities were observed for the Pd-doped catalyst and the higher loading Co and Mn catalysts. This suggests that the dehydrogenated intermediates in this case were too stable to react with the carboxylate. For example Pd is a well-known hydrogenation catalyst, and the reaction results indicated increased isobutyraldehyde formation for the Pd-doped catalyst. For the base catalyst there was less isobutyraldehyde formation and for the Co-doped catalyst the amount of isobutyraldehyde formed was ~3 times less than the Pd-doped catalyst.

The lower reaction rate for the IBA reaction when compared to the MNK formation is probably due to the lower number of α - hydrogens for the IBA molecule

(one) when compared to the DOAc molecule (two). Similar observations were made by Pestman et al. (1997) who observed, for acid feeds, the rate of formation of ketone to decrease as the number of α - hydrogen atoms was decreased. Removal of a α - hydrogen is needed to form the ketene-like intermediate. Steric effects due to the two bulky methyl groups attached to the α - carbon of the IBA molecule may also hinder the formation of the ketene-like intermediate and so lower the rate of the reaction for DIPK formation.

REFERENCES

- A. Auroux, A. Gervasini, *J. Phys. Chem.* 94 (1990) 6371.
- R. J. Behm, K. Christmann, G. Ertl, M.A. Van Hove, P. A. Thiel, W. H. Weinberg, *Surf. Sci.* 88 (1979) L59.
- A. Bensalem, F. Bozon-Verduraz, *J. Chem. Soc. Faraday Trans.* 91 (1995) 2185.
- P. G. Blake, G. E. Jackson, *J. Chem. Soc. B* (1968) 1153.
- P. G. Blake, G. E. Jackson, *J. Chem. Soc. B* (1969) 94.
- J. P. Brunelle, *Pure Appl. Chem.* 50 (1978) 1211.
- W.C. Child, Jr., A.J. Hay, *J. Amer. Chem. Soc.* 86 (1964) 182.
- R. Cousin, S. Capelle, E. Abi-Aad, D. Courcot, A. Aboukais, *Chem. Mater.* 13 (2001) 3862.
- R. L. Cryberg, R. M. Bimber, US Patent 4,570,021 (1986), to SDS Biotech.
- L. Dong, Y. Hu, M. Shen, T. Jin, J. Wang, W. Ding, Y. Chen, *Chem. Mater.* 13 (2001) 4227.
- J. El Fallah, S. Boujana, H. Dexpert, A. Kiennemann, J. Majerus, O. Touret, F. Villain, F. Le Normand, *J. Phys. Chem.* 98 (1994) 5522.
- R. M. Ferrizz, G.S. Wong, T. Egami, J.M. Vohs, *Langmuir* 17 (2001) 2464.
- J. M. Gatica, R. T. Baker, P. Fornasiero, S. Bernal, J. Kaspar, *J. Phys. Chem. B* 105 (2001) 1191.
- M. Glinski, J. Kijenski, A. Jakubowski, *Appl. Catal. A* 128 (1995) 209.
- M. Glinski, J. Kijenski, *Appl. Catal. A* 190 (2000) 87.
- H. He, H. X. Dai, L. H. Ng, K. W. Wong, C. T. Au, *J. Catal.* 206 (2002) 1.
- T.S. Hendren, Kinetics of catalyzed acid/acid and acid/aldehyde condensation reactions to non-symmetric ketones, MS Thesis, Louisiana State University, Baton Rouge, LA, 2001.
- T. S. Hendren, K. M. Dooley, *Catal. Today* 85 (2003) 333.

- S. Hilaire, X. Wang, T. Luo, R. J. Gorte, J. P. Wagner, *Appl. Catal. A* 215 (2001) 271.
- S. Ho, J. M. Cruz, M. Houalla, D. M. Hercules, *J. Catal.* 135 (1992) 173.
- J. Hormes, M. Pantelouris, G. B. Balazs, B. Rambabu, *Solid State Ionics* 136-137 (2000) 945.
- G. P. Huffman, N. Shah, J. Zhao, F. E. Huggins, T. E. Hoost, S. Halvorsen, J. G. Jr. Goodwin, *J. Catal.* 151 (1995) 17.
- H. Idriss, C. Diagne, J. P. Hindermann, A. Kiennemann, M. A. Barteau, *J. Catal.* 155 (1995) 219.
- T. Imanaka, T. Tarremote, S. Teranishi, in: *Proceedings of the Fifth International Congress on Catalysis, Amsterdam, 1972, North-Holland, Amsterdam, 1973, p. 163.*
- G. Kaindl, G. K. Wertheim, G. Schmiester, E. V. Sampathkumaran, *Phys. Rev. Lett.* 58 (1987) 606.
- M. Kasrai, M. E. Fleet, G. M. Bancroft, K. H. Tan, J. M. Chen, *Phys. Rev. B* 43 (1991) 1763.
- L. S. Kau, D. J. Spira-Solomon, J. E. Penner-Hahn, K. O. Hodgson, E. I. Solomon, *J. Am. Chem. Soc.* 109 (1987) 6433.
- K. S. Kim, M. A. Barteau, *J. Catal.* 125 (1990) 353.
- J.A. Knopp, W.S. Linell, W.C. Child Jr., *J. Phys. Chem.* 66 (1962) 1513.
- G. Kueper, R. Chauvistre, J. Hormes, F. Frick, M. Jansen, B. Luer, E. Hartmann, *Chem. Phys.* 165 (1992) 405.
- A. Laachir, V. Perrichon, A. Badri, J. Lamotte, E. Catherine, J. C. Lavalley, J El Fallah, L. Hilaire, F. Le Normand, E. Quemere, G. N. Sauvion, O. Touret, *J. Chem. Soc. Faraday Trans.* 87 (1991) 1601.
- S. Lippert, W. Baumann, K. Thomke, *J. Mol. Catal.* 69 (1991) 199.
- J. C. Mackie, K. R. Doolan, *Int. J. Chem. Kinetics* 16 (1984) 525.
- M. T. Nguyen, D. Sengupta, G. Raspoet, L. G. Vanquickenborne, *J. Phys. Chem.* 99 (1995) 11883.
- K. Parida, H. Kumar Mishra, *J. Mol. Catal. A* 139 (1999) 73.

- R. Pestman, R.M. Koster, A. van Duijne, J. A. Z. Pieterse, V. Ponec, *J. Catal.* 168 (1997) 225.
- S. Rajadurai, *Catal. Rev.-Sci. Eng.* 36 (1994) 385.
- S. Randery, Ceria based catalysts for asymmetric ketone production, MS Thesis, Louisiana State University, Baton Rouge, LA, 1999.
- S. D. Randery, J. S. Warren, K.M. Dooley, *Appl. Catal. A* 226 (2002) 265.
- B. Ravel, Athena version 0.8.024, 2003.
- T. Ressler, WinXAS 97 version 1.3, 1998.
- F. Sette, J. Stohr, A. P. Hitchcock, *J. Chem. Phys.* 81 (1984) 4906.
- J. Z. Shyu, W. H. Weber, H. S. Gandhi, *J. Phys. Chem.* 92 (1988) 4964.
- J. H. Sinfelt, G. H. Via, F. W. Lytle, *J. Chem. Phys.* 68 (1978) 2009.
- B. Skarman, D. Grandjean, R. E. Benfield, A. Hinz, A. Andersson, L. R. Wallenberg, *J. Catal.* 211 (2002) 119.
- A. V. Soldatov, T. S. Ivanchenko, S. Della Longa, A. Kotani, Y. Iwamoto, A. Bianconi, *Phys. Rev. B* 50 (1994) 5074.
- Y. Takahashi, H. Shimizu, H. Kagi, H. Yoshida, A. Usui, M. Nomura, *Earth. Planet. Sci. Lett.* 182 (2000) 201.
- Y. Takahashi, H. Sakami, M. Nomura, *Anal. Chim. Acta* 468 (2002) 345.
- A. Trovarelli, F. Zamar, J. Llorca, C. de Leitenburg, G. Dolcetti, J. T. Kiss, *J. Catal.* 169 (1997) 490.
- J. Wan, G. E. Thompson, K. Q. Lu, C. J. E. Smith, *J. Phys. IV* 7 (1997) C2-1181.
- X. Wang, R. J. Gorte, J. P. Wagner, *J. Catal.* 212 (2002) 225.
- T. Yamanaka, K. Tanabe, *J. Phys. Chem.* 94 (1990) 6371.
- A. Yee, S. J. Morrison, H. Idriss, *J. Catal.* 186 (1999) 279.
- X. Zhang, A. B. Walters, M. A. Vannice, *J. Catal.* 155 (1995) 290.

APPENDIX A

GAS CHROMATOGRAPHY (GC) DETAILS

Table A.1: GC Settings for IBA Product Analysis

Parameter	Setting
Injector Temperature	200 °C
Detector Temperature	200 °C
Maximum Oven Temperature	200 °C
Initial Temperature	50 °C
Ramp Rate	20 °C/min
Final Temp	190 °C
Initial Time	3 min
Final Time	12 min
Purge	ON throughout run
Methane Retention Time	1.2 min
Volumetric Flow through Column	1.9 cm ³ /min
Split Vent Rate	40 cm ³ /min
Split Ratio	21
Purge Vent Flow Rate	4.5 cm ³ /min
Column Head Pressure	225 kPa

Table A.2: Retention Times for IBA Products

Compound	Retention Time (min)
Isobutyraldehyde	1.1-1.3
Methanol	1.4-1.6
2-Pentanone + 3-Methyl-2-Butanone	1.6-1.8
Diisopropyl ketone (DIPK)	2.0-2.4
Isomers of DIPK	2.2-5.0
Propanoic Acid,2-Methyl,Anhydride	6.3-6.6
Isobutyric acid (IBA)	8.0-8.3
Heavy Ketones	8.5-

Table A.3: GC Settings for HOAc/DOAc Product Analysis

Parameter	Setting
Injector Temperature	200 °C
Detector Temperature	210 °C
Maximum Oven Temperature	200 °C
Initial Temperature	50 °C
Ramp Rate	20 °C/min
Final Temp	190 °C
Initial Time	3 min
Final Time	10 min
Purge	ON throughout run
Methane Retention Time	1.3 min
Volumetric Flow through Column	1.8 cm ³ /min
Split Vent Rate	32 cm ³ /min
Split Ratio	18
Purge Vent Flow Rate	3.5 cm ³ /min
Column Head Pressure	205 kPa

Table A.4: Retention Times for HOAc/DOAc Products using GC, Analysis of Liquid Phases

Compound	Retention Time (min)
Acetone	1.3-1.5
Methanol	1.5-1.7
C5-C7 ketones	1.7-4.5
C8-C10 ketones	4.5-7.2
Acetic acid (HOAc)	7.2-7.6
Decanaldehyde	7.6-7.8
Methyl decanoate	7.8-8.4
Methyl nonyl ketone (MNK)	8.4-9.0
Heptadecane	9.0-9.8
Dodecanones	9.8-10.8
Tridecanones	10.8-13.6
Decanoic acid (DOAc)	13.6-14.6
Dinonyl ketone	14.6-15.6
Dodecanoic acid	15.6-

Table A.5: GC Settings for HOAc/DOAc Products, Gas Phase Analysis

Parameter	Setting
Injector Temperature	150 °C
Detector Temperature	220 °C
Maximum Oven Temperature	210 °C
Initial Temperature	45 °C
Ramp Rate	20 °C/min
Final Temp	210 °C
Initial Time	5 min
Final Time	10 min
Purge	ON throughout run
Carrier Gas (He) Rate	35 cm ³ /min

Table A.6: Retention Times for HOAc/DOAc Products, Gas Phase Analysis

Compound	Retention Time (min)
O ₂	2.2
N ₂	2.4
CO	3.2
Methane	7.4
CO ₂	10.6
Water	11.8
Ethylene	15.0

APPENDIX B

MASS BALANCE CALCULATIONS AND RESULTS FOR REACTOR EXPERIMENTS

Methanol (MeOH, 99.8%) was used as an internal standard for all GC analyses. For IBA and 3/1 HOAc/DOAc feeds, ~0.1 mL of the product sample was added to 2 mL of a 2% methanol/pentane solution before GC analysis. The calibration slopes of the various compounds were calculated from the formula:

$$S_j = \frac{\text{vol}_j / \text{vol}_{\text{MeOH}}}{\text{area}_j / \text{area}_{\text{MeOH}}},$$

where S_j is the calibration slope of compound j .

Let

$$Y_j = \frac{\text{area}_j}{\text{area}_{\text{MeOH}}}$$

Then,

$$\text{wt}_j = (S_j) * (Y_j) * (\rho_j)$$

$$\text{wt}_j \% = \frac{100 * \text{wt}_j}{\sum_j \text{wt}_j},$$

where wt_j is the ratio of the weight of the compound j in the product sample taken, to the volume of MeOH added and $\text{wt}_j\%$ is the weight percent of compound j in the product sample.

The equations used to compute the conversion, selectivity, and molar yield are as follows (for the 3/1 HOAc/DOAc feed, acetic acid and acetone in the product sample were not considered in these calculations):

$$N_j = \frac{wt_j \%}{MW_j},$$

$$D = \sum_j N_j * A_j,$$

where N_j is the number of moles of product j and A_j is the number of moles of IBA/DOAc required to produce one mole of product j . For IBA feed, A_j is 1 for isobutyraldehyde, 3 for heavy ketones and 2 for the rest of the products. For 3/1 HOAc/DOAc feed, A_j is 0.5 for C5-C7 ketones, 2 for DNK and 1 for the rest of the products.

Then,

$$\% \text{ Conversion IBA / DOAc} = \frac{100 * D}{N_{\text{IBA/DOAc}} + D},$$

The weight selectivity to DIPK/MNK is given by the formula

$$\% \text{ Weight Selectivity DIPK / MNK} = \frac{100 * wt_{\text{DIPK/MNK}}}{\left(\sum_j wt_j \right) - (wt_{\text{IBA/DOAc}})}$$

The molar yield of DIPK/MNK is given by the formula

$$\% \text{ Molar Yield DIPK / MNK} = \frac{100 * N_{\text{DIPK/MNK}}}{N_{\text{IBA/DOAc}} + D}$$

The calculations based on these formulas are in Lotus 1-2-3 spreadsheets. Those spreadsheets are presented on the pages following this section.

Overall mass balances over long periods (e.g., a day) were computed as follows. For MNK reactions, the product was assumed to consist of DOAc, MNK, DNK, acetone, water and CO₂. In other words, it was assumed that DNK and acetone were the only side products (formed by the condensation of DOAc and HOAc respectively), and that there

was complete conversion of HOAc. The formulas used to arrive at these overall mass balances are as follows:

$$N_{\text{DOAc}} = \left(1 - \frac{\% \text{ Conversion DOAc}}{100}\right) * N_{\text{DOAc, feed}}$$

$$N_{\text{MNK}} = \left(\frac{\% \text{ Molar Yield MNK}}{100}\right) * N_{\text{DOAc, feed}}$$

$$N_{\text{DNK}} = \frac{N_{\text{DOAc, feed}} - N_{\text{DOAc}} - N_{\text{MNK}}}{2}$$

$$N_{\text{Acetone}} = \frac{N_{\text{HOAc, feed}} - N_{\text{MNK}}}{2}$$

$$N_{\text{Water}} = N_{\text{MNK}} + N_{\text{DNK}} + N_{\text{Acetone}}$$

$$N_{\text{CO}_2} = N_{\text{Water}}$$

Here N_j stands for number of moles of compound j .

Using these, the calculated volume of liquid product was:

$$\% \text{ Recovery} = \frac{\text{Volume of Product Collected(Actual)}}{\sum_j \frac{N_j \text{MW}_j}{\rho_j}} * 100$$

where the summation was over all of the above products except CO_2 .

Run Name: M-113

Catalyst: 20% CeO₂/Al₂O₃, Englehard, 0.42-0.84 mm (40-20 mesh) powder

Wt.% IBA, Feed: 94.06

Pretreatment: air/He@520 °C, Overnight

Feed: Isobutyric Acid

Cat. Wt., g: 0.5095

Cat. Bulk den., g/cc: 1.33

Run M-113 sample	MeOH solution, mL	Vol. rate mL/min	T °C	LHSV	P psig	Wt.% DIPK	Wt.% IBA	MOLS PRODS	%CONV. IBA	WEIGHT SEL., DIPK	MOLAR Y, DIPK	TOS h	COMMENT	WHSV
1A	2	0.043	440	6.784	0	39.90	54.56	0.80	56.50	87.82	49.10	5.50		4.84
1B	2	0.043	440	6.784	0	41.10	54.91	0.79	55.97	91.14	50.86			4.84
2A	2	0.045	440	7.082	0	40.20	56.92	0.76	54.13	93.32	50.00	9.50	air/He@540C	5.05
2B	2	0.045	440	7.082	0	39.50	57.23	0.76	53.79	92.35	49.22			5.05
3A	2	0.044	440	6.958	0	38.55	55.32	0.79	55.81	86.29	47.53	14.50		4.96
3B	2	0.044	440	6.958	0	38.07	56.89	0.75	53.89	88.32	47.62			4.96
4A	2	0.044	440	6.849	0	39.81	56.17	0.77	54.86	90.84	49.38	18.50	air/He@540C	4.88
4B	2	0.044	440	6.849	0	39.22	57.92	0.74	53.04	93.19	49.08			4.88
5A	2	0.044	430	6.906	0	28.79	64.86	0.64	46.45	81.94	36.69	23.50		4.93
5C	2	0.044	430	6.906	0	27.73	66.24	0.61	44.92	82.15	35.59			4.93
6A	2	0.042	430	6.523	0	29.04	67.98	0.57	42.51	90.71	37.90	27.50	air/He@540C	4.65
6C	2	0.042	430	6.523	0	29.08	68.54	0.56	41.88	92.42	38.05			4.65

Run Name: M-126

Catalyst: 20% CeO₂/Al₂O₃, Engelhard, 1.27 mm extrudate

Wt.% IBA, Feed: 93.99

Pretreatment: air/He@500 °C, Overnight

Feed: Isobutyric Acid

Cat. Wt., g: 0.5002

Cat. Bulk den., g/cc: 0.64

Run M-126 sample	MeOH solution, mL	Vol. rate mL/min	T °C	LHSV	P psig	Wt.% DIPK	Wt.% IBA	MOLS PRODS	%CONV. IBA	WEIGHT SEL., DIPK	MOLAR Y, DIPK	TOS h	COMMENT	WHSV
1A	2	0.042	380	3.199	0	3.42	92.79	0.12	10.19	47.44	5.11	5.50		4.74
1B	2	0.042	380	3.199	0	3.55	92.85	0.12	10.13	49.74	5.31			4.74
2B	2	0.044	390	3.412	0	5.45	86.90	0.23	18.66	41.63	7.88	9.00	air/He@520C	5.05
2C	2	0.044	390	3.412	0	5.42	88.74	0.20	16.27	48.14	7.90			5.05
3A	2	0.043	440	3.290	0	34.84	59.76	0.70	50.85	86.58	44.22	14.50		4.87
3B	2	0.043	440	3.290	0	35.18	60.84	0.69	49.81	89.83	44.79			4.87
4A	2	0.043	450	3.290	0	42.68	54.83	0.80	56.19	94.48	52.63	18.00	air/He@520C	4.87
4B	2	0.043	450	3.290	0	43.15	54.54	0.79	56.20	94.92	53.47			4.87
5A	2	0.041	460	3.161	0	46.17	46.14	0.94	64.14	85.72	55.38	23.50		4.68
5B	2	0.041	460	3.161	0	47.49	46.63	0.93	63.74	88.98	56.98			4.68
6A	2	0.045	465	3.490	0	49.41	43.88	0.98	66.35	88.04	58.47	27.00	air/He@520C	5.17
6B	2	0.045	465	3.490	0	50.43	43.73	0.99	66.59	89.62	59.47			5.17
7A	2	0.044	470	3.412	0	56.07	42.31	1.01	67.78	97.19	65.88	32.50		5.05
7B	2	0.044	470	3.412	0	56.19	42.37	1.01	67.73	97.49	66.04			5.05
8A	2	0.043	475	3.290	0	59.16	38.22	1.08	71.37	95.76	68.39	36.00	air/He@520C	4.87
8B	2	0.043	475	3.290	0	58.63	39.13	1.07	70.59	96.32	68.03			4.87
9A	2	0.043	480	3.270	0	58.40	37.84	1.09	71.72	93.94	67.36	41.50		4.84
9B	2	0.043	480	3.270	0	57.05	39.30	1.06	70.45	93.97	66.20			4.84
10B	2	0.045	485	3.490	0	57.50	37.57	1.09	71.94	92.10	66.28	45.00	air/He@520C	5.17
10C	2	0.045	485	3.490	0	56.80	38.23	1.08	71.37	91.95	65.64			5.17
11B	2	0.043	490	3.290	0	50.68	41.34	1.03	68.76	86.40	59.10	50.00		4.87
11C	2	0.043	490	3.290	0	51.09	42.37	1.01	67.72	88.65	60.06			4.87
12A	2	0.042	495	3.199	0	44.46	48.56	0.90	62.01	86.44	53.68	54.00	air/He@520C	4.74
12B	2	0.042	495	3.199	0	42.66	46.25	0.93	64.03	79.36	51.21			4.74

Run Name: M-125

Catalyst: 20% CeO₂/Al₂O₃, Engelhard, 1.27 mm extrudate

Wt.% IBA, Feed: 93.86

Pretreatment: air/He@520 °C, Overnight

Feed: Isobutyric Acid

Cat. Wt., g: 0.5009

Cat. Bulk den., g/cc: 0.64

Run M-125 sample	MeOH solution, mL	Vol. rate mL/min	T °C	LHSV	P psig	Wt.% DIPK	Wt.% IBA	MOLS PRODS	%CONV. IBA	WEIGHT SEL., DIPK	MOLAR Y, DIPK	TOS h	COMMENT	WHSV
1A	2	0.042	440	3.194	0	31.16	64.72	0.61	45.54	88.32	40.46	5.50		4.73
1B	2	0.042	440	3.194	0	31.37	65.38	0.61	44.99	90.62	40.73			4.73
2A	2	0.043	440	3.286	0	30.75	67.56	0.57	42.65	94.77	40.28	9.00	air/He@540C	4.87
2B	2	0.043	440	3.286	0	30.80	67.09	0.58	43.10	93.60	40.32			4.87
3A	2	0.042	440	3.237	0	31.83	66.07	0.59	44.14	93.82	41.53	14.50		4.79
3B	2	0.042	440	3.237	0	31.01	66.21	0.59	44.06	91.79	40.44			4.79
4A	2	0.042	440	3.237	0	29.41	65.18	0.61	45.02	84.45	38.29	18.50	air/He@540C	4.79
4B	2	0.042	440	3.237	0	29.58	65.98	0.60	44.43	86.95	38.45			4.79

Run Name: M-110

Catalyst: 20% CeO₂/Al₂O₃, Engelhard, 1.27 mm extrudate

Wt.% IBA, Feed: 100.00

Pretreatment: air@520 °C, Overnight

Feed: Isobutyric Acid

Cat. Wt., g: 23.0415

Cat. Bulk den., g/cc: 0.64

Run M-110 sample	MeOH solution, mL	Vol. rate mL/min	T °C	LHSV	P psig	Wt.% DIPK	Wt.% IBA	MOLS PRODS	%CONV. IBA	WEIGHT SEL., DIPK	MOLAR Y, DIPK	TOS h	COMMENT	WHSV
W1A	2	1.667	430	2.778	0	18.45	53.85	0.75	55.01	39.98	23.79	0.58		4.11
2E	2	1.833	430	3.055	0	16.45	82.15	0.31	25.06	92.12	23.15	1.58	Re-Run	4.53
3D	2	1.600	440	2.666	0	18.56	78.95	0.37	29.22	88.14	25.68	2.25	Re-Run	3.95
W2A	2	1.167	450	1.944	7.5	35.04	37.48	1.06	71.34	56.04	41.35	3.00	air@520C	2.88
4A	2	1.800	450	3.000	7.5	24.44	63.40	0.63	46.76	66.79	31.67	4.00	Re-Run	4.44
5A	2	1.909	450	3.182	7.5	22.23	73.63	0.45	35.10	84.33	30.24	5.00	Re-Run	4.71
6A	2	1.444	440	2.407	0	30.30	67.02	0.57	42.75	91.88	39.95	6.17	Re-Run	3.57
7A	2	1.500	440	2.500	0	35.73	64.27	0.63	46.17	100.00	46.17	7.17	Re-Run	3.70
8A1	2	1.550	440	2.583	0	40.85	56.91	0.75	53.74	94.80	51.23	8.17	Re-Run	3.83
9B	2	0.859	440	1.431	5	57.39	40.33	1.04	69.43	96.19	67.13	9.5	F.Prod.	2.12
W3B	2	1.423	440	2.372	7.5	30.15	66.35	0.58	43.70	89.61	39.48	10.5	air@537.7C	3.51
10A	2	1.500	440	2.500	7.5	31.82	65.92	0.59	44.12	93.37	41.62	11.5	Re-Run	3.70
11A	2	1.375	440	2.292	7.5	30.42	61.03	0.66	48.98	78.06	39.25	13.17	Re-Run	3.39
12A	2	1.118	440	1.863	7.5	37.84	59.89	0.70	50.58	94.34	48.19	15.33	Re-Run	2.76
13B	2	1.167	440	1.944	7.5	41.61	56.21	0.76	54.45	95.01	52.05	16.33	Re-Run	2.88
14A	2	1.250	440	2.083	7.5	44.38	53.18	0.82	57.52	94.79	54.72	17.33	Re-Run	3.09
15 1	2	1.667	440	2.778	10	38.43	55.03	0.79	55.87	85.45	47.56	18.5	air@537.7C	4.11
16A	2	1.167	440	1.944	10	66.01	32.86	1.18	75.92	98.32	74.64	19.5	F.Prod.	2.88
17B	2	1.200	440	2.000	10	58.50	33.22	1.15	75.37	87.60	66.95	20.5	F.Prod.	2.96
18A	2	1.143	440	1.905	10	67.26	29.20	1.23	78.77	95.00	75.45	21.00	F.Prod.	2.82
19B	2	1.167	440	1.944	10	65.61	32.26	1.18	76.33	96.85	74.28	22.67	F.Prod.	2.88
20B	2	1.111	440	1.852	10	68.41	29.20	1.25	79.01	95.71	75.88	23.67	F.Prod.	2.74
21A	2	1.190	440	1.984	10	71.24	25.59	1.30	81.71	95.74	78.59	25.67	F.Prod.	2.94

Run Name: M-116

Feed: Isobutyric Acid

Catalyst: 20% CeO₂/Al₂O₃, Engelhard, 1.27 mm extrudate

Cat. Wt., g: 23.0181

Wt.% IBA, Feed: 100.00

Cat. Bulk den., g/cc: 0.64

Pretreatment: air@520 °C, Overnight, HOAc feed, 8 h, air@538 °C, Overnight

Run M-116 sample	MeOH solution, mL	Vol. rate mL/min	T °C	LHSV	P psig	Wt.% DIPK	Wt.% IBA	MOLS PRODS	%CONV. IBA	WEIGHT SEL., DIPK	MOLAR Y, DIPK	TOS h	COMMENT	WHSV
1A	2	4.667	440	7.785	0	4.40	83.92	0.30	24.07	27.35	6.14	0.33	Waste	11.53
2A	2	2.667	440	4.449	0	9.28	87.04	0.24	19.47	71.61	13.25	1.00	Re-Run	6.59
3A	2	0.917	440	1.529	30	22.77	72.11	0.50	37.99	81.65	30.22	2.50	Re-Run	2.27
4A	2	0.958	440	1.599	30	33.03	61.87	0.68	49.17	86.62	41.88	4.50	Re-Run	2.37
5A	2	1.000	440	1.668	30	30.70	66.50	0.59	43.92	91.65	39.95	6.33	Re-Run	2.47
6A	2	1.000	440	1.668	30	33.53	61.69	0.66	48.66	87.53	43.07	8.00	Re-Run	2.47
7A	2	1.500	440	2.502	30	23.46	67.21	0.60	43.96	71.53	30.18	8.33	air@538C, Re-Run	3.71
8A	2	1.048	440	1.748	30	22.57	69.36	0.56	41.75	73.67	29.25	10.33	Re-Run	2.59
9A	2	1.000	440	1.668	30	24.92	69.83	0.54	40.62	82.60	32.70	11.33	Re-Run	2.47
10A	2	1.000	440	1.668	30	38.93	56.29	0.78	54.85	89.06	48.20	13.33	Re-Run	2.47
11A	2	1.056	440	1.761	30	48.78	48.08	0.91	62.58	93.95	58.59	14.83	F. Prod.	2.61
12A	2	1.067	440	1.779	30	49.55	46.65	0.93	63.67	92.88	59.56	16.00	F. Prod.	2.64
13A	2	1.222	440	2.039	30	48.38	46.46	0.95	64.19	90.35	57.55	17.00	air@538C,F.Prod	3.02
14A	2	1.130	440	1.886	30	43.66	52.56	0.84	58.42	92.04	53.31	18.50	F. Prod.	2.79
15A	2	1.143	440	1.907	30	46.27	52.33	0.84	58.44	97.08	56.71	20.24	F. Prod.	2.82
16A	2	1.143	445	1.907	30	49.29	45.99	0.96	64.73	91.25	58.33	21.50	F. Prod.	2.82
17B	2	1.222	445	2.039	30	50.69	47.06	0.93	63.45	95.75	60.77	22.50	F. Prod.	3.02
18A	2	1.111	450	1.854	30	55.58	40.44	1.05	69.63	93.33	64.41	24.00	F. Prod.	2.75
19A	2	1.133	450	1.891	30	41.00	55.36	0.78	55.50	91.83	50.86	26.50	air@538C,Re-Run	2.80
20A	2	1.048	450	1.748	30	37.54	58.22	0.74	52.91	89.85	46.86	29.17	Re-Run	2.59
21A	2	1.133	450	1.891	30	38.17	59.39	0.71	51.22	93.99	48.37	32.00	Re-Run	2.80
22B	2	1.333	450	2.224	30	22.86	73.40	0.48	36.37	85.92	30.58	34.67	air@538C,Re-Run	3.29
23A	2	1.152	450	1.921	30	24.03	72.63	0.49	37.32	87.78	32.01	37.33	Re-Run	2.85
24A	2	1.121	450	1.870	30	58.70	36.69	1.11	72.66	92.72	67.50	40.50	F. Prod.	2.77

(Run M116 cont.)

25B	2	1.154	450	1.925	30	56.94	40.75	1.04	69.16	96.11	66.50	43.17	air@538C,F.Prod	2.85
26A	2	1.154	450	1.925	30	59.25	34.77	1.14	74.32	90.84	67.55	45.50	F. Prod.	2.85
27A	2	1.125	450	1.877	30	66.80	30.52	1.21	77.80	96.14	74.99	49.00	F. Prod.	2.78
28A	2	1.147	450	1.914	30	30.33	67.73	0.56	42.10	94.00	40.02	51.67	air@538C,Re-Run	2.83
29B	2	1.143	450	1.907	30	27.06	71.45	0.50	38.27	94.78	36.08	54.33	Re-Run	2.82
30B	2	1.182	450	1.972	30	24.55	74.50	0.45	34.58	96.25	33.27	56.00	Re-Run	2.92
31A	2	1.147	450	1.914	30	21.72	72.11	0.49	37.35	77.90	29.12	58.67	air@538C,Re-Run	2.83
32B	2	1.171	450	1.954	30	17.80	81.90	0.32	25.44	98.34	25.02	63.00	Re-Run	2.89
33B	2	1.148	450	1.915	30	39.53	57.12	0.76	53.90	92.19	49.24	64.00	Re-Run	2.84
34A	2	1.196	450	1.995	30	46.49	49.00	0.89	61.50	91.15	56.37	67.00	air@538C,F. Prod.	2.95
35A	2	1.167	450	1.946	30	49.55	46.78	0.93	63.70	93.10	59.34	70.00	F. Prod.	2.88
36A	2	1.300	450	2.169	30	47.03	51.62	0.85	59.08	97.20	57.54	73.50	F. Prod.	3.21
37B	2	1.111	450	1.854	30	55.28	43.29	0.99	66.91	97.49	65.22	76.67	F. Prod.	2.75
38B	2	1.089	450	1.817	30	23.89	73.89	0.47	35.68	91.51	32.10	81.67	air@538C,Re-Run	2.69
39A	2	1.813	450	3.024	30	9.65	90.20	0.17	14.36	98.43	14.14	85.67	Re-Run	4.48
40A	2	1.206	450	2.012	30	6.67	77.28	0.40	31.44	29.35	9.13	88.67	Re-Run	2.98
41A	2	1.033	450	1.724	30	26.56	68.51	0.55	41.58	84.36	34.96	92.67	air@538C,Re-Run	2.55
42B	2	1.176	450	1.963	30	24.67	71.02	0.51	38.57	85.11	32.93	96.67	Re-Run	2.91
43A	2	0.947	450	1.580	30	24.71	71.37	0.51	38.50	86.32	32.87	100.67	Re-Run	2.34
44B	2	0.984	450	1.642	30	28.93	58.89	0.70	51.16	70.38	37.03	104.67	air@538C,Re-Run	2.43
45A	2	0.889	450	1.483	30	33.13	62.52	0.66	48.27	88.37	42.30	108.67	Re-Run	2.20
46A	2	0.895	450	1.493	30	35.01	58.86	0.72	51.73	85.08	44.31	112.67	Re-Run	2.21
47A	2	0.961	450	1.603	30	41.42	51.94	0.84	58.69	86.19	50.85	116.67	air@538C,Re-Run	2.37
48C	2	0.980	450	1.634	30	48.05	41.09	1.03	68.76	81.56	56.38	120.67	F. Prod.	2.42
49B	2	0.962	450	1.605	30	51.78	43.40	0.99	66.78	91.48	61.17	125.67	F. Prod.	2.38
50A	2	0.958	450	1.599	30	64.87	31.38	1.20	77.18	94.54	72.82	129.67	air@538C	2.37
51B	2	1.140	450	1.902	30	25.21	69.07	0.55	41.01	81.51	33.22	133.67		2.82
52A	2	0.970	450	1.618	30	13.65	83.34	0.30	23.82	81.95	19.25	139.17	air@538C	2.40

Run Name: M-121

Feed: Isobutyric Acid

Catalyst: 22.3% CeO₂/Al₂O₃, Sud-Chemie, 2.18 mm tri-lobed extrudate

Cat. Wt., g: 0.5025

Wt.% IBA, Feed: 93.61

Cat. Bulk den., g/cc: 0.44

Pretreatment: air/He@520 °C, Overnight

Run M-121 sample	MeOH solution, mL	Vol. rate mL/min	T °C	LHSV	P psig	Wt.% DIPK	Wt.% IBA	MOLS PRODS	%CONV. IBA	WEIGHT SEL., DIPK	MOLAR Y, DIPK	TOS h	COMMENT	WHSV
1A	2	0.043	440	2.230	0	30.87	63.43	0.64	47.04	84.41	39.78	5.50		4.85
1C	2	0.043	440	2.230	0	30.93	63.34	0.64	47.16	84.37	39.81			4.85
2A	2	0.042	440	2.207	0	28.73	62.61	0.66	47.99	76.83	36.83	9.00	air/He@540C	4.80
2B	2	0.042	440	2.207	0	28.12	63.69	0.64	46.87	77.44	36.20			4.80
3A	2	0.043	440	2.216	0	29.75	61.19	0.67	49.28	76.66	38.06	14.50		4.82
3C	2	0.043	440	2.216	0	28.90	60.86	0.68	49.58	73.83	36.94			4.82
4B	2	0.043	440	2.230	0	28.09	63.81	0.63	46.50	77.61	36.35	18.00	air/He@540C	4.85
4C	2	0.043	440	2.230	0	28.29	64.84	0.61	45.46	80.46	36.73			4.85
5A	2	0.042	440	2.168	0	30.41	63.22	0.64	47.04	82.68	39.32	23.50		4.72
5C	2	0.042	440	2.168	0	29.44	63.34	0.64	46.99	80.33	38.03			4.72
6A	2	0.043	440	2.230	0	29.29	61.44	0.67	49.04	75.96	37.50	27.00	air/He@540C	4.85
6C	2	0.043	440	2.230	0	28.98	62.24	0.66	48.21	76.75	37.21			4.85
7A	2	0.045	450	2.365	0	43.82	50.57	0.86	59.99	88.64	53.51	32.50		5.15
7C	2	0.045	450	2.365	0	44.53	50.07	0.87	60.52	89.18	54.19			5.15
8A	2	0.044	450	2.268	0	44.79	49.09	0.89	61.48	87.98	54.24	36.00	air/He@540C	4.93
8B	2	0.044	450	2.268	0	44.62	49.35	0.89	61.34	88.09	53.94			4.93
9A	2	0.042	450	2.207	0	41.99	53.26	0.81	57.39	89.83	51.86	41.50		4.80
9B	2	0.042	450	2.207	0	42.80	53.88	0.81	56.95	92.81	52.78			4.80
10A	2	0.043	450	2.230	0	43.99	49.97	0.87	60.64	87.93	53.46	45.00	air/He@540C	4.85
10C	2	0.043	450	2.230	0	44.32	50.17	0.87	60.43	88.96	53.95		blkg. in rectr. o/l line	4.85
11A	2	0.041	450	2.128	0	42.18	52.04	0.83	58.46	87.95	51.96	50.50		4.63
11C	2	0.041	450	2.128	0	41.40	51.54	0.84	59.08	85.43	50.72			4.63
12A	2	0.042	450	2.190	0	40.50	50.69	0.86	59.88	82.14	49.46	54.00	air/He@540C	4.77
12E	2	0.042	450	2.190	0	40.28	50.80	0.86	59.82	81.86	49.17			4.77

(Run M121 cont.)

13B	2	0.042	455	2.168	0	47.13	45.65	0.95	64.67	86.71	56.30	59.50		4.72
13D	2	0.042	455	2.168	0	47.06	45.77	0.95	64.56	86.77	56.23			4.72
14B	2	0.043	455	2.230	0	46.05	46.08	0.94	64.26	85.40	55.13	63.00	air/He@540C	4.85
14D	2	0.043	455	2.230	0	45.82	46.78	0.92	63.52	86.10	55.15			4.85
15A	2	0.041	455	2.157	0	45.92	45.25	0.95	65.01	83.87	54.80	68.50		4.69
15B	2	0.041	455	2.157	0	45.24	45.08	0.96	65.15	82.37	53.98			4.69
16B	2	0.044	455	2.268	0	45.41	46.15	0.94	64.23	84.33	54.33	72.00	air/He@540C	4.93
16C	2	0.044	455	2.268	0	45.63	46.37	0.93	63.98	85.09	54.70			4.93

Run Name: M-119

Feed: Isobutyric Acid

Catalyst: 22.3% CeO₂/Al₂O₃, Sud-Chemie, 2.18 mm tri-lobed extrudate

Cat. Wt., g: 0.5001

Wt.% IBA, Feed: 93.82

Cat. Bulk den., g/cc: 0.44

Pretreatment: air/He@520 °C, Overnight

Run M-119 sample	MeOH solution, mL	Vol. rate mL/min	T °C	LHSV	P psig	Wt.% DIPK	Wt.% IBA	MOLS PRODS	%CONV. IBA	WEIGHT SEL., DIPK	MOLAR Y, DIPK	TOS h	COMMENT	WHSV
1A	2	0.041	440	2.152	0	32.28	60.67	0.68	49.83	82.06	41.19	5.50		4.68
1C	2	0.041	440	2.152	0	32.14	60.61	0.69	50.17	81.59	40.78			4.68
2B	2	0.042	440	2.218	0	32.28	64.94	0.62	45.59	92.05	41.74	9.00	air/He@540C	4.83
2C	2	0.042	440	2.218	0	32.10	63.61	0.64	46.88	88.21	41.38			4.83
3A	2	0.042	440	2.207	0	32.19	65.56	0.60	44.61	93.47	41.97	14.50		4.80
3B	2	0.042	440	2.207	0	31.61	66.47	0.58	43.51	94.26	41.45			4.80
4A	2	0.042	440	2.218	0	31.50	65.58	0.60	44.74	91.50	40.96	18.00	air/He@540C	4.83
4B	2	0.042	440	2.218	0	30.44	67.15	0.57	42.71	92.67	40.09			4.83
5A	2	0.042	440	2.178	0	33.78	60.78	0.69	49.88	86.13	42.99	23.50		4.74
5B	2	0.042	440	2.178	0	34.55	61.33	0.68	49.25	89.36	44.13			4.74
6A	2	0.042	440	2.178	0	28.87	66.26	0.59	43.85	85.55	37.76	27.00	air/He@540C	4.74
6B	2	0.042	440	2.178	0	28.61	67.25	0.57	42.81	87.36	37.54			4.74

Run Name: M-115

Catalyst: 17% CeO₂/Al₂O₃, Sud-Chemie, 1.59 mm extrudate

Wt.% IBA, Feed: 93.75

Pretreatment: air/He@520 °C, Overnight

Feed: Isobutyric Acid

Cat. Wt., g: 0.501

Cat. Bulk den., g/cc: 0.6136

Run M-115 sample	MeOH solution, mL	Vol. rate mL/min	T °C	LHSV	P psig	Wt.% DIPK	Wt.% IBA	MOLS PRODS	%CONV. IBA	WEIGHT SEL., DIPK	MOLAR Y, DIPK	TOS h	COMMENT	WHSV
1A	2	0.042	430	3.103	0	18.18	72.17	0.48	37.04	65.34	24.48	5.50		4.79
1B	2	0.042	430	3.103	0	19.21	71.40	0.49	37.84	67.18	25.81			4.79
2A	2	0.042	440	3.062	0	28.27	64.94	0.61	45.19	80.63	36.82	9.00	air/He@540C	4.73
2B	2	0.042	440	3.062	0	27.92	66.34	0.58	43.55	82.94	36.66			4.73
3A	2	0.041	430	3.015	0	22.09	73.09	0.46	35.88	82.08	29.91	14.00		4.66
3B	2	0.041	430	3.015	0	21.86	73.26	0.46	35.64	81.77	29.64			4.66
4A	2	0.042	440	3.062	0	29.07	64.12	0.62	46.15	81.01	37.68	18.00	air/He@500C	4.73
4B	2	0.042	440	3.062	0	29.12	65.18	0.60	44.92	83.62	37.97			4.73
5A	2	0.042	420	3.062	0	15.60	77.40	0.39	30.93	69.05	21.49	23.00		4.73
5B	2	0.042	420	3.062	0	14.53	78.21	0.38	30.08	66.69	20.05			4.73
6A	2	0.042	430	3.062	0	19.01	74.64	0.44	34.04	74.97	25.93	27.00	air/He@540C	4.73
6C	2	0.042	430	3.062	0	19.80	74.11	0.45	34.78	76.47	26.89			4.73
7B	2	0.040	420	2.939	0	13.69	79.61	0.35	28.12	67.15	19.08	32.00		4.54
7C	2	0.040	420	2.939	0	13.46	79.49	0.35	28.12	65.64	18.79			4.54
8A	2	0.042	430	3.062	0	19.67	74.88	0.43	33.85	78.31	26.82	36.00	air/He@540C	4.73
8B	2	0.042	430	3.062	0	19.55	75.79	0.41	32.53	80.76	26.85			4.73

Run Name: M-117

Catalyst: 19.9% CeO₂/Al₂O₃, Sud-Chemie, 3.18 mm extrudate

Wt.% IBA, Feed: 93.74

Pretreatment: air/He@520 °C, Overnight

Feed: Isobutyric Acid

Cat. Wt., g: 0.5126

Cat. Bulk den., g/cc: 0.81

Run M-117 sample	MeOH solution, mL	Vol. rate mL/min	T °C	LHSV	P psig	Wt.% DIPK	Wt.% IBA	MOLS PRODS	%CONV. IBA	WEIGHT SEL., DIPK	MOLAR Y, DIPK	TOS h	COMMENT	WHSV
1A	2	0.044	440	3.841	0	20.56	70.11	0.51	39.24	68.78	27.50	5.50		4.85
1B	2	0.044	440	3.841	0	20.44	69.29	0.53	40.46	66.57	27.11			4.85
2A	2	0.040	440	3.553	0	20.10	66.76	0.58	43.35	60.48	26.33	9.00	air/He@540C	4.49
2B	2	0.040	440	3.553	0	19.98	68.02	0.55	41.64	62.47	26.45			4.49
3B	2	0.039	440	3.435	0	20.83	68.00	0.56	42.12	65.09	27.37	14.50		4.34
3C	2	0.039	440	3.435	0	20.85	69.28	0.54	40.87	67.87	27.46			4.34
4A	2	0.042	440	3.696	0	22.14	76.31	0.41	32.29	93.44	30.31	18.00	air/He@540C	4.67

Run Name: M-120

Catalyst: 19.9% CeO₂/Al₂O₃, Sud-Chemie, 3.18 mm extrudate

Wt.% IBA, Feed: 93.32

Pretreatment: air/He@520 °C, Overnight

Feed: Isobutyric Acid

Cat. Wt., g: 0.5018

Cat. Bulk den., g/cc: 0.81

Run M-120 sample	MeOH solution, mL	Vol. rate mL/min	T °C	LHSV	P psig	Wt.% DIPK	Wt.% IBA	MOLS PRODS	%CONV. IBA	WEIGHT SEL., DIPK	MOLAR Y, DIPK	TOS h	COMMENT	WHSV
1A	2	0.043	440	4.145	0	14.61	78.26	0.38	29.75	67.20	20.24	5.50		4.86
1B	2	0.043	440	4.145	0	14.16	76.71	0.40	31.69	60.78	19.46			4.86
2A	2	0.042	440	4.072	0	15.61	81.38	0.32	25.84	83.83	21.95	9.00	air/He@540C,	4.77
2C	2	0.042	440	4.072	0	15.26	82.76	0.30	24.31	88.48	21.53			4.77
3A	2	0.029	440	2.821	0	21.19	72.80	0.48	36.55	77.90	28.50	17.00	blk. obsd. in vapzr.	3.31
3D	2	0.029	440	2.821	0	21.20	72.00	0.49	37.62	75.71	28.34		air/He@540C	3.31
4B	2	0.040	440	3.896	0	18.44	80.01	0.35	27.78	92.24	25.69	22.50		4.57
4C	2	0.040	440	3.896	0	18.38	80.98	0.33	26.48	96.60	25.75			4.57
5B	2	0.043	440	4.145	0	16.99	75.27	0.43	33.42	68.70	23.19	26.00	air/He@540C	4.86
5C	2	0.043	440	4.145	0	17.05	77.68	0.39	30.49	76.37	23.55			4.86

Run Name: M-111

Catalyst: 15% CeO₂/3% K₂O/Al₂O₃, Engelhard, 1.27 mm extrudate

Wt.% IBA, Feed: 93.94

Pretreatment: air/He@520 °C, Overnight

Feed: Isobutyric Acid

Cat. Wt., g: 0.4986

Cat. Bulk den., g/cc: 0.69

Run M-111 sample	MeOH solution, mL	Vol. rate mL/min	T °C	LHSV	P psig	Wt.% DIPK	Wt.% IBA	MOLS PRODS	%CONV. IBA	WEIGHT SEL., DIPK	MOLAR Y, DIPK	TOS h	COMMENT	WHSV
1C	2	0.041	440	3.419	0	33.56	62.85	0.64	47.42	90.34	43.33	5.00		4.70
1D	2	0.041	440	3.419	0	33.57	62.31	0.65	47.96	89.08	43.26			4.70
2A	2	0.044	440	3.690	0	28.47	64.03	0.62	46.00	79.16	37.05	8.00	air/He@540C	5.07
2B	2	0.044	440	3.690	0	31.34	62.99	0.64	47.28	84.66	40.48			5.07
3B	2	0.043	440	3.603	0	33.78	58.47	0.72	52.06	81.34	42.74	13.00		4.95
3C	2	0.043	440	3.603	0	33.48	57.05	0.74	53.33	77.94	42.27			4.95
4A	2	0.042	440	3.513	0	30.43	56.40	0.75	53.94	69.81	38.35	17.50	air/He@540C	4.83
4B	2	0.042	440	3.513	0	31.26	54.95	0.77	55.24	69.40	39.30			4.83

Run Name: M-106/107

Catalyst: 20% MgO/ZrO₂, Engelhard, 3.18 mm extrudate

Wt.% IBA, Feed: 93.53/95.62

Pretreatment: no

Feed: Isobutyric Acid

Cat. Wt., g: 0.7079

Cat. Bulk den., g/cc: 1.085

Run M-106/107 sample	MeOH solution, mL	Vol. rate mL/min	T °C	LHSV	P psig	Wt.% DIPK	Wt.% IBA	MOLS PRODS	%CONV. IBA	WEIGHT SEL., DIPK	MOLAR Y, DIPK	TOS h	COMMENT	WHSV
1A	2	0.042	430	3.832	0	16.24	82.28	0.30	24.50	91.67	23.00	5.00		3.35
1C	2	0.042	430	3.832	0	18.47	77.68	0.38	30.15	82.74	25.63			3.35
2A	2	0.038	440	3.503	0	20.34	73.77	0.43	33.97	77.57	28.10	7.75	air/He@520C	3.06
2B	2	0.038	440	3.503	0	21.84	74.51	0.44	34.09	85.67	29.81			3.06
1B	2	0.058	440	3.164	0	13.65	75.01	0.41	32.67	54.62	18.90	5.50		4.69
1C	2	0.058	440	3.164	0	14.39	79.39	0.36	28.34	69.83	20.05			4.69
2A	2	0.062	450	3.375	0	19.05	76.80	0.39	31.05	82.13	26.40	9.50	air/He@520C	5.00
2C	2	0.062	450	3.375	0	19.00	75.87	0.41	32.11	78.71	26.23			5.00

Run Name: M-118

Catalyst: 4% CeO₂/KOH doped/ZrO₂, Engelhard, 3.18 mm extrudate

Wt.% IBA, Feed: 93.90

Pretreatment: air/He@520 °C, Overnight

Feed: Isobutyric Acid

Cat. Wt., g: 0.5059

Cat. Bulk den., g/cc: 1.78

Run M-118 sample	MeOH solution, mL	Vol. rate mL/min	T °C	LHSV	P psig	Wt.% DIPK	Wt.% IBA	MOLS PRODS	%CONV. IBA	WEIGHT SEL., DIPK	MOLAR Y, DIPK	TOS h	COMMENT	WHSV
1A	2	0.044	440	9.210	0	16.50	78.39	0.37	29.42	76.36	22.93	5.50		4.92
1D	2	0.044	440	9.210	0	15.85	79.34	0.36	28.43	76.73	22.06			4.92
2A	2	0.042	440	8.771	0	13.71	80.27	0.34	27.25	69.49	19.18	9.00	air/He@540C	4.68
2B	2	0.042	440	8.771	0	13.63	79.29	0.36	28.57	65.80	18.95			4.68
3A	2	0.040	440	8.466	0	14.61	80.05	0.35	27.58	73.24	20.41	14.50		4.52
3B	2	0.040	440	8.466	0	14.48	81.62	0.32	25.60	78.77	20.36			4.52
4A	2	0.044	440	9.356	0	12.37	78.19	0.38	29.87	56.73	17.12	18.00	air/He@540C	5.00
4B	2	0.044	440	9.356	0	12.17	78.36	0.37	29.65	56.22	16.86			5.00

Run Name: M-112

Catalyst: 11.8% PrO_{1.83}/9.8% CeO₂/Al₂O₃, 2.38 mm sphere

Wt.% IBA, Feed: 93.85

Pretreatment: air/He@520 °C, Overnight

Feed: Isobutyric Acid

Cat. Wt., g: 0.4908

Cat. Bulk den., g/cc: 0.75

Run M-112 sample	MeOH solution, mL	Vol. rate mL/min	T °C	LHSV	P psig	Wt.% DIPK	Wt.% IBA	MOLS PRODS	%CONV. IBA	WEIGHT SEL., DIPK	MOLAR Y, DIPK	TOS h	COMMENT	WHSV
1B	2	0.040	440	3.629	0	7.52	69.29	0.54	40.77	24.49	9.92	6.00		4.59
1D	2	0.040	440	3.629	0	8.87	70.01	0.53	39.97	29.57	11.74			4.59
2A	2	0.044	440	4.011	0	9.62	77.10	0.39	30.75	41.99	13.33	10.00	air/He@540C	5.07
2C	2	0.044	440	4.011	0	9.62	77.17	0.39	30.70	42.14	13.33			5.07
3A	2	0.043	440	3.965	0	10.01	83.59	0.27	22.25	60.98	14.36	15.00		5.01
3B	2	0.043	440	3.965	0	10.58	81.00	0.32	25.70	55.67	14.97			5.01
4A	2	0.042	440	3.851	0	10.03	78.80	0.35	28.17	47.29	14.10	19.50	air/He@540C	4.87
4B	2	0.042	440	3.851	0	9.33	79.34	0.35	28.09	45.15	13.04			4.87

Run Name: M-114

Catalyst: 33% CeO₂, MCM-41, 0.84 - 1.68 mm (20 – 12 mesh) powder

Wt.% IBA, Feed: 93.99

Pretreatment: air/He@520 °C, Overnight

Feed: Isobutyric Acid

Cat. Wt., g: 0.5003

Cat. Bulk den., g/cc: 0.99

Run M-114 sample	MeOH solution, mL	Vol. rate mL/min	T °C	LHSV	P psig	Wt.% DIPK	Wt.% IBA	MOLS PRODS	%CONV. IBA	WEIGHT SEL., DIPK	MOLAR Y, DIPK	TOS h	COMMENT	WHSV
1A	2	0.043	440	5.060	0	2.94	93.76	0.12	9.96	47.14	4.36	5.50		4.84
1C	2	0.043	440	5.060	0	2.64	94.13	0.11	9.40	45.02	3.92			4.84
2A	2	0.042	440	4.950	0	2.66	93.10	0.12	10.06	38.50	3.96	9.50	air/He@540C	4.74
2B	2	0.042	440	4.950	0	2.98	92.30	0.14	11.84	38.76	4.40			4.74
3A	2	0.045	440	5.400	0	1.21	94.03	0.11	9.28	20.24	1.80	15.00		5.17
3B	2	0.045	440	5.400	0	1.14	94.61	0.10	8.51	21.08	1.70			5.17
4A	2	0.043	440	5.092	0	0.99	96.64	0.06	5.35	29.33	1.49	18.50	air/He@540C	4.87
4B	2	0.043	440	5.092	0	0.83	96.48	0.06	5.54	23.59	1.25			4.87

Run Name: M-124

Catalyst: 17% CeO₂/0.8% Co/Al₂O₃, Sud-Chemie, 1.59 mm extrudate

Wt.% IBA, Feed: 93.91

Pretreatment: air/He@520 °C, Overnight

Feed: Isobutyric Acid

Cat. Wt., g: 0.501

Cat. Bulk den., g/cc: 0.6136

Run M-124 sample	MeOH solution, mL	Vol. rate mL/min	T °C	LHSV	P psig	Wt.% DIPK	Wt.% IBA	MOLS PRODS	%CONV. IBA	WEIGHT SEL., DIPK	MOLAR Y, DIPK	TOS h	COMMENT	WHSV
1C	2	0.044	440	3.203	0	36.92	61.74	0.67	48.90	96.50	47.15	5.50		4.95
1D	2	0.044	440	3.203	0	37.10	60.14	0.70	50.77	93.07	46.86			4.95
2C	2	0.041	440	3.015	0	36.90	60.71	0.69	49.96	93.90	46.94	9.00	air/He@540C	4.66
2D	2	0.041	440	3.015	0	36.24	61.67	0.68	49.11	94.55	46.15			4.66
3C	2	0.045	440	3.307	0	39.36	59.38	0.71	51.43	96.88	49.68	14.50		5.11
3D	2	0.045	440	3.307	0	39.07	59.20	0.72	51.69	95.74	49.21			5.11
4A	2	0.040	440	2.939	0	32.29	66.62	0.58	43.60	96.74	42.19	18.00	air/He@540C	4.54
4B	2	0.040	440	2.939	0	31.98	66.63	0.59	43.67	95.84	41.73			4.54
5B	2	0.042	440	3.109	0	35.29	62.58	0.66	48.03	94.29	45.23	23.50		4.80
5C	2	0.042	440	3.109	0	34.61	62.48	0.66	48.11	92.24	44.36			4.80
6A	2	0.043	440	3.184	0	34.82	63.03	0.65	47.42	94.19	44.83	27.00	air/He@540C	4.92
6B	2	0.043	440	3.184	0	34.63	62.77	0.65	47.65	93.03	44.58			4.92

Run Name: M-127

Catalyst: 17% CeO₂/0.1% Co/Al₂O₃, Sud-Chemie, 1.59 mm extrudate

Wt.% IBA, Feed: 94.20

Pretreatment: air/He@520 °C, Overnight

Feed: Isobutyric Acid

Cat. Wt., g: 0.5013

Cat. Bulk den., g/cc: 0.6136

Run M-127 sample	MeOH solution, mL	Vol. rate mL/min	T °C	LHSV	P psig	Wt.% DIPK	Wt.% IBA	MOLS PRODS	%CONV. IBA	WEIGHT SEL., DIPK	MOLAR Y, DIPK	TOS h	COMMENT	WHSV
1A	2	0.042	440	3.060	0	23.79	72.19	0.48	37.13	85.56	31.98	5.50		4.73
1B	2	0.042	440	3.060	0	23.92	72.33	0.48	37.01	86.45	32.15			4.73
2B	2	0.045	440	3.338	0	22.75	72.67	0.48	36.64	83.25	30.61	9.00	air/He@540C	5.16
2C	2	0.045	440	3.338	0	22.21	71.57	0.50	38.07	78.09	29.65			5.16
3A	2	0.046	440	3.353	0	23.17	74.70	0.44	34.24	91.58	31.48	14.50		5.18
3B	2	0.046	440	3.353	0	22.99	73.44	0.47	35.84	86.56	31.00			5.18
4A	2	0.047	440	3.427	0	21.09	75.68	0.42	32.96	86.73	28.84	18.00	air/He@540C	5.30
4C	2	0.047	440	3.427	0	21.22	74.27	0.45	34.72	82.48	28.79			5.30

Run Name: M-131

Catalyst: 17% CeO₂/2.4% Co/Al₂O₃, Sud-Chemie, 1.59 mm extrudate

Wt.% IBA, Feed: 93.94

Pretreatment: air/He@500 °C, Overnight

Feed: Isobutyric Acid

Cat. Wt., g: 0.5016

Cat. Bulk den., g/cc: 0.6136

Run M-131 sample	MeOH solution, mL	Vol. rate mL/min	T °C	LHSV	P psig	Wt.% DIPK	Wt.% IBA	MOLS PRODS	%CONV. IBA	WEIGHT SEL., DIPK	MOLAR Y, DIPK	TOS h	COMMENT	WHSV
1A	2	0.041	440	3.022	0	25.31	71.45	0.49	37.89	88.63	33.95	5.50		4.67
1C	2	0.041	440	3.022	0	25.12	71.28	0.50	38.06	87.46	33.69			4.67
2B	2	0.044	440	3.262	0	23.07	71.93	0.49	37.31	82.17	31.02	9.00	air/He@500C	5.04
2C	2	0.044	440	3.262	0	21.87	72.52	0.48	36.60	79.59	29.51			5.04
3B	2	0.045	440	3.320	0	25.98	70.46	0.51	39.08	87.96	34.67	14.50		5.13
3C	2	0.045	440	3.320	0	24.86	70.95	0.50	38.49	85.55	33.26			5.13
4A	2	0.040	440	2.971	0	25.70	70.39	0.52	39.20	86.80	34.26	18.00	air/He@540C	4.59
4B	2	0.040	440	2.971	0	25.45	71.34	0.50	38.05	88.80	34.11			4.59
5A	2	0.044	440	3.211	0	25.82	67.07	0.57	42.83	78.41	33.97	23.50		4.96
5B	2	0.044	440	3.211	0	25.12	67.21	0.56	42.53	76.61	33.14			4.96
6A	2	0.042	440	3.058	0	26.30	67.51	0.56	42.29	80.96	34.69	27.00	air/He@540C	4.72
6B	2	0.042	440	3.058	0	25.98	68.56	0.54	41.13	82.63	34.43			4.72

Run Name: M-132

Feed: Isobutyric Acid

Catalyst: 17% CeO₂/0.8% Mn/Al₂O₃, Sud-Chemie, 1.59 mm extrudate

Cat. Wt., g: 0.5017

Wt.% IBA, Feed: 94.08

Cat. Bulk den., g/cc: 0.6136

Pretreatment: air/He@500 °C, Overnight

Run M-132 sample	MeOH solution, mL	Vol. rate mL/min	T °C	LHSV	P psig	Wt.% DIPK	Wt.% IBA	MOLS PRODS	%CONV. IBA	WEIGHT SEL., DIPK	MOLAR Y, DIPK	TOS h	COMMENT	WHSV
1B	2	0.040	440	2.970	0	22.85	73.99	0.45	35.02	87.88	30.97	5.50		4.59
1C	2	0.040	440	2.970	0	21.95	75.20	0.43	33.58	88.50	29.92			4.59
2A	2	0.043	440	3.145	0	22.07	76.79	0.40	31.71	95.12	30.29	9.00	air/He@520C	4.86
2C	2	0.043	440	3.145	0	20.81	78.21	0.38	29.99	95.53	28.75			4.86
3A	2	0.041	440	3.028	0	21.22	76.45	0.41	31.92	90.13	29.17	14.50		4.68
3B	2	0.041	440	3.028	0	21.44	76.77	0.40	31.71	92.29	29.44			4.68
4B	2	0.044	440	3.261	0	22.07	76.67	0.41	31.85	94.63	30.28	18.00	air/He@520C	5.04
4C	2	0.044	440	3.261	0	21.22	77.63	0.39	30.69	94.86	29.24			5.04
5B	2	0.050	440	3.669	0	20.43	77.25	0.39	31.02	89.79	28.16	23.50		5.67
5C	2	0.050	440	3.669	0	19.55	77.47	0.39	30.88	86.76	26.92			5.67
6B	2	0.044	440	3.261	0	19.31	77.42	0.39	30.92	85.51	26.59	27.00	air/He@520C	5.04
6C	2	0.044	440	3.261	0	18.48	78.24	0.38	29.79	84.91	25.59			5.04

Run Name: M-133

Catalyst: 17% CeO₂/2.4% Mn/Al₂O₃, Sud-Chemie, 1.59 mm extrudate

Wt.% IBA, Feed: 93.94

Pretreatment: air/He@500 °C, Overnight

Feed: Isobutyric Acid

Cat. Wt., g: 0.5003

Cat. Bulk den., g/cc: 0.6136

Run M-133 sample	MeOH solution, mL	Vol. rate mL/min	T °C	LHSV	P psig	Wt.% DIPK	Wt.% IBA	MOLS PRODS	%CONV. IBA	WEIGHT SEL., DIPK	MOLAR Y, DIPK	TOS h	COMMENT	WHSV
1A	2	0.042	440	3.093		17.67	77.47	0.39	30.83	78.42	24.35	6.00		4.78
1B	2	0.042	440	3.093		17.38	78.85	0.37	29.10	82.17	24.11			4.78
2A	2	0.047	440	3.434		17.13	80.15	0.34	27.32	86.30	23.97	9.00	air/He@520C	5.31
2B	2	0.047	440	3.434		17.49	80.20	0.34	27.46	88.34	24.42			5.31
3A	2	0.041	440	3.030		13.68	83.46	0.29	23.20	82.73	19.43	14.50		4.68
3B	2	0.041	440	3.030		13.76	82.77	0.30	24.04	79.85	19.49			4.68
4A	2	0.044	440	3.271		13.51	83.23	0.29	23.45	80.57	19.18	18.00	air/He@520C	5.05
4C	2	0.044	440	3.271		13.18	84.66	0.27	21.68	85.95	18.82			5.05
5A	2	0.042	440	3.066		1.82	96.28	0.06	5.42	48.98	2.76	23.50		4.74
5B	2	0.042	440	3.066		1.78	96.50	0.06	5.22	50.81	2.69			4.74
6B	2	0.041	440	3.019		1.94	96.18	0.06	5.44	50.82	2.95	27.00	air/He@520C	4.66
6C	2	0.041	440	3.019		1.92	96.59	0.06	5.11	56.41	2.92			4.66

Run Name: M-123

Catalyst: 17% CeO₂/0.1% Pd/Al₂O₃, Sud-Chemie, 1.59 mm extrudate

Wt.% IBA, Feed: 93.46

Pretreatment: air/He@520 °C, Overnight

Feed: Isobutyric Acid

Cat. Wt., g: 0.4995

Cat. Bulk den., g/cc: 0.6136

Run M-123 sample	MeOH solution, mL	Vol. rate mL/min	T °C	LHSV	P psig	Wt.% DIPK	Wt.% IBA	MOLS PRODS	%CONV. IBA	WEIGHT SEL., DIPK	MOLAR Y, DIPK	TOS h	COMMENT	WHSV
1C	2	0.033	440	2.457	0	26.30	65.39	0.61	44.92	76.01	34.19	5.50		3.80
1D	2	0.033	440	2.457	0	25.75	66.75	0.58	43.42	77.45	33.69			3.80
2B	2	0.033	440	2.457	0	20.86	67.42	0.56	42.28	64.02	27.55	8.00	air/He@540C	3.80
2C	2	0.033	440	2.457	0	21.32	69.47	0.53	40.22	69.85	28.31			3.80
3B	2	0.043	440	3.194	0	16.13	76.66	0.40	31.62	69.13	22.21	13.00		4.93
3C	2	0.043	440	3.194	0	17.50	72.46	0.48	36.78	63.53	23.56			4.93
4B	2	0.041	440	3.024	0	16.23	77.10	0.40	31.19	70.87	22.35	16.00	air/He@540C	4.67
4C	2	0.041	440	3.024	0	15.75	76.95	0.40	31.56	68.33	21.62			4.67
5A	2	0.042	440	3.127	0	16.20	72.96	0.46	35.67	59.90	22.04	21.50		4.83
5B	2	0.042	440	3.127	0	16.39	69.36	0.53	40.03	53.48	21.86			4.83
6B	2	0.043	440	3.179	0	14.43	82.99	0.29	23.68	84.79	20.48	25.00	air/He@540C	4.91
6C	2	0.043	440	3.179	0	14.58	82.65	0.30	24.04	84.03	20.68			4.91

Run Name: M-122

Catalyst: 17% CeO₂/0.8% Pd/Al₂O₃, Sud-Chemie, 1.59 mm extrudate

Wt.% IBA, Feed: 93.85

Pretreatment: air/He@520 °C, Overnight

Feed: Isobutyric Acid

Cat. Wt., g: 0.5001

Cat. Bulk den., g/cc: 0.6136

Run M-122 sample	MeOH solution, mL	Vol. rate mL/min	T °C	LHSV	P psig	Wt.% DIPK	Wt.% IBA	MOLS PRODS	%CONV. IBA	WEIGHT SEL., DIPK	MOLAR Y, DIPK	TOS h	COMMENT	WHSV
1D	2	0.042	440	3.108	0	15.47	78.62	0.37	29.38	72.35	21.44	6.25		4.80
1E	2	0.042	440	3.108	0	15.86	79.55	0.35	28.22	77.52	22.08			4.80
2A	2	0.044	440	3.221	0	12.70	79.02	0.36	28.74	60.55	17.68	9.00	air/He@540C	4.98
2C	2	0.044	440	3.221	0	12.27	79.86	0.35	27.87	60.93	17.10			4.98
3A	2	0.043	440	3.129	0	15.68	73.90	0.45	34.79	60.10	21.36	14.50		4.83
3B	2	0.043	440	3.129	0	15.91	74.26	0.45	34.66	61.80	21.60			4.83
4A	2	0.040	440	2.980	0	11.45	80.31	0.34	27.03	58.15	16.06	18.00	air/He@540C	4.60
4B	2	0.040	440	2.980	0	11.24	82.01	0.31	24.87	62.46	15.88			4.60
5B	2	0.042	440	3.108	0	17.23	75.10	0.43	33.63	69.18	23.49	23.50		4.80
5C	2	0.042	440	3.108	0	17.20	76.51	0.41	32.04	73.23	23.58			4.80
6C	2	0.042	440	3.067	0	12.30	81.67	0.31	25.14	67.08	17.40	27.00	air/He@540C	4.74
6A	2	0.042	440	3.067	0	12.30	82.25	0.30	24.58	69.31	17.41			4.74

Run Name: M-128

Catalyst: 17% CeO₂/0.8% Pd/Al₂O₃, Sud-Chemie, 1.59 mm extrudate

Wt.% IBA, Feed: 93.81

Pretreatment: air@520 °C, 4 h, H₂@450 °C, 4 h, He@450 °C, Overnight

Feed: Isobutyric Acid

Cat. Wt., g: 0.5018

Cat. Bulk den., g/cc: 0.6136

Run M-128 sample	MeOH solution, mL	Vol. rate mL/min	T °C	LHSV	P psig	Wt.% DIPK	Wt.% IBA	MOLS PRODS	%CONV. IBA	WEIGHT SEL., DIPK	MOLAR Y, DIPK	TOS h	COMMENT	WHSV
1B	2	0.040	440	2.935	0	12.77	81.78	0.32	25.50	70.12	17.95	5.50		4.53
1C	2	0.040	440	2.935	0	12.86	82.51	0.31	24.57	73.55	18.15			4.53
2A	2	0.041	440	3.010	0	10.57	85.15	0.26	20.97	71.17	15.14	9.00	air/He@520C	4.65
2B	2	0.041	440	3.010	0	10.65	84.32	0.27	22.13	67.92	15.18			4.65
3B	2	0.043	440	3.144	0	12.39	81.90	0.31	25.18	68.44	17.46	14.50		4.86
3C	2	0.043	440	3.144	0	12.20	83.05	0.29	23.78	72.01	17.28			4.86
4A	2	0.043	440	3.144	0	7.96	87.05	0.22	18.52	61.47	11.50	18.00	air/He@520C	4.86
4C	2	0.043	440	3.144	0	7.88	87.00	0.22	18.55	60.66	11.39			4.86
5B	2	0.040	420	2.904	0	7.59	89.17	0.19	15.63	70.06	11.08	23.50		4.49
5C	2	0.040	420	2.904	0	7.58	88.52	0.20	16.60	66.00	11.02			4.49
6A	2	0.044	420	3.261	0	6.40	89.44	0.18	15.36	60.59	9.34	27.00	air/He@540C	5.04
6B	2	0.044	420	3.261	0	6.43	90.39	0.17	13.97	66.97	9.45			5.04
7B	2	0.041	440	3.036	0	11.46	83.37	0.29	23.50	68.93	16.23	32.50		4.69
7C	2	0.041	440	3.036	0	11.48	84.38	0.27	22.06	73.52	16.37			4.69
8B	2	0.043	450	3.144	0	13.61	82.04	0.31	25.17	75.77	19.15	36.00	air/He@540C	4.86
8C	2	0.043	450	3.144	0	13.38	82.47	0.30	24.25	76.30	18.96			4.86

Run Name: M-139

Catalyst: 18.4% CeO₂/Al₂O₃, Sud-Chemie, 3.18 mm extrudate

Wt.% DOAc, Feed: 48.87

Pretreatment: O₂@500 °C, Overnight, HOAc@410 °C, 4.75 h, O₂@520 °C, Overnight

Feed: 3/1 HOAc/DOAc

Cat. Wt., g: 25.1558

Cat. Bulk den., g/cc: 0.8

Run M-139 sample	MeOH solution, mL	Vol. rate mL/min	T °C	LHSV	P psig	Wt.% MNK	Wt.% DOAc	MOLS PRODS	%CONV. DOAc	WEIGHT SEL., MNK	MOLAR Y, MNK	TOS h	COMMENT	WHSV
1C	2	1.677	440	3.199	30	66.01	0.62	0.51	99.31	75.77	74.83	03.50		3.85
1D	2	1.677	440	3.199	30	64.65	1.04	0.51	98.83	74.70	73.38			3.85
3A	2	1.667	440	3.180	30	67.28	0.90	0.51	98.99	77.54	76.46	11.50	O ₂ @ 520C	3.83
3B	2	1.667	440	3.180	30	66.46	0.00	0.53	100.00	74.59	73.76			3.83
4A	2	1.718	440	3.277	30	59.53	0.00	0.50	100.00	70.13	69.74	12.50		3.94
4B	2	1.718	440	3.277	30	60.90	2.28	0.50	97.43	71.52	69.57			3.94
5A	2	1.502	440	2.866	30	60.26	3.88	0.50	95.66	71.99	68.18	16.50		3.45
5B	2	1.502	440	2.866	30	62.38	0.48	0.52	99.47	70.78	69.51			3.45
6B	2	1.806	440	3.447	30	66.44	0.00	0.52	100.00	76.23	75.37	23.00	O ₂ @ 520C	4.15
6C	2	1.806	440	3.447	30	65.17	0.40	0.53	99.57	73.31	72.04			4.15
7A	2	3.168	440	6.045	30	68.05	3.05	0.48	96.46	83.20	79.96	27.00		7.27
7B	2	3.168	440	6.045	30	71.50	0.84	0.51	99.05	82.48	81.47			7.27
8A	2	3.310	440	6.316	30	71.37	0.87	0.52	99.04	80.80	79.11	34.50	O ₂ @ 520C	7.60
8B	2	3.310	440	6.316	30	73.58	0.31	0.52	99.66	83.74	83.00			7.60
9B	2	3.259	440	6.218	30	75.19	1.18	0.50	98.64	88.36	87.25	41.50		7.48
9C	2	3.259	440	6.218	30	72.44	0.80	0.50	99.08	85.22	84.22			7.48
10B	2	3.498	440	6.675	30	68.51	0.00	0.50	100.00	80.84	79.80	46.00	O ₂ @ 520C	8.03
10C	2	3.498	440	6.675	30	68.10	0.37	0.51	99.58	79.62	78.05			8.03
11A	2	1.612	400	3.076	30	69.41	1.46	0.49	98.30	84.12	81.97	51.50		3.70
11B	2	1.612	400	3.076	30	70.70	0.38	0.51	99.57	82.86	81.53			3.70
12B	2	1.543	400	2.944	30	75.90	1.75	0.48	97.93	92.44	90.72	57.58	O ₂ @ 520C	3.54
12C	2	1.543	400	2.944	30	73.70	2.51	0.48	97.06	90.30	87.48			3.54
13A	2	1.998	400	3.813	30	73.66	1.48	0.50	98.31	87.50	85.34	63.08		4.59
13B	2	1.998	400	3.813	30	73.75	3.20	0.49	96.35	88.72	85.16			4.59
14A	2	1.856	400	3.542	30	71.01	4.01	0.49	95.47	85.86	81.05	69.50	O ₂ @ 520C	4.26
14C	2	1.856	400	3.542	30	72.08	1.57	0.49	98.17	87.12	84.70			4.26

(Run M139 cont.)

15A	2	3.205	400	6.116	30	59.68	7.18	0.40	90.65	87.18	78.63	75.00		7.36
15C	2	3.205	400	6.116	30	62.82	7.66	0.42	90.37	88.49	79.85			7.36
16A	2	3.387	400	6.462	30	55.69	14.83	0.38	81.43	87.37	70.54	81.17	O ₂ @ 520C	7.77
16C	2	3.387	400	6.462	30	56.76	14.08	0.38	82.28	88.43	72.26			7.77
17B	2	3.422	400	6.530	30	55.79	12.66	0.36	83.18	90.34	74.99	86.67		7.86
17D	2	3.422	400	6.530	30	56.68	14.48	0.38	81.73	88.74	72.35			7.86
18A	2	3.428	400	6.540	30	54.40	21.65	0.37	74.63	87.23	64.52	92.92	O ₂ @ 520C	7.87
18C	2	3.428	400	6.540	30	53.26	23.79	0.36	72.36	87.29	62.60			7.87
19A	2	2.609	420	4.459	30	71.60	0.52	0.51	99.42	82.87	81.35	97.92		5.99
19C	2	2.609	420	4.459	30	69.19	0.00	0.51	100.00	80.93	79.66			5.99
20B	2	2.682	420	4.584	30	72.69	0.41	0.52	99.54	83.05	81.35	103.42	O ₂ @ 520C	6.16
20C	2	2.682	420	4.584	30	72.90	1.13	0.52	98.75	83.68	81.47			6.16
21B	2	2.540	420	4.340	30	69.29	0.48	0.49	99.43	83.48	82.13	109.42		5.83
21C	2	2.540	420	4.340	30	70.85	0.51	0.50	99.41	84.09	82.56			5.83
22C	2	2.717	420	4.643	30	70.63	0.44	0.50	99.50	84.03	82.49	115.00	O ₂ @ 520C	6.24
22D	2	2.717	420	4.643	30	73.18	0.00	0.52	100.00	84.28	83.10			6.24
23B	2	2.932	420	5.011	30	68.99	3.20	0.51	96.45	81.51	77.27	121.00		6.73
23C	2	2.932	420	5.011	30	68.03	4.93	0.51	94.65	80.49	74.68			6.73
24B	2	2.662	420	4.550	30	71.23	1.96	0.49	97.75	85.93	82.96	126.75	N ₂ @ 420C	6.11
24C	2	2.662	420	4.550	30	69.35	3.47	0.49	96.09	83.71	79.17			6.11
25A	2	2.713	420	4.636	30	68.80	4.74	0.48	94.59	85.29	79.44	132.75		6.23
25B	2	2.713	420	4.636	30	69.76	4.08	0.50	95.46	83.91	78.58			6.23
26B	2	2.588	420	4.423	30	70.68	5.92	0.50	93.59	84.24	77.45	138.25		5.94
26C	2	2.588	420	4.423	30	70.07	7.36	0.50	92.11	84.18	76.05			5.94
27A	2	2.588	420	4.423	30	64.21	9.70	0.45	88.96	84.73	73.98	138:15	N ₂ @ 420C	5.94
27B	2	2.588	420	4.423	30	63.72	11.18	0.45	87.50	84.07	72.09		Grab sample	5.94
28A	2	2.574	420	4.399	30	66.10	10.89	0.45	87.60	87.92	76.16	142.75	Grab sample	5.91
28B	2	2.574	420	4.399	30	63.52	12.90	0.44	85.54	85.56	72.04			5.91
29A	2	2.574	420	4.399	30	56.09	15.68	0.40	81.56	83.36	66.73	144.25		5.91
29C	2	2.574	420	4.399	30	53.13	16.63	0.38	79.72	83.71	65.57			5.91
30B	2	2.468	420	4.218	30	56.65	16.19	0.40	81.02	84.45	67.20	149.50	Grab sample	5.67
30C	2	2.468	420	4.218	30	55.57	18.82	0.40	78.42	83.75	64.45			5.67
31A	2	2.468	420	4.218	30	58.73	14.75	0.41	82.70	85.67	69.72	149.50	N ₂ @ 420C	5.67
31B	2	2.468	420	4.218	30	56.72	19.05	0.40	78.15	85.65	65.81			5.67

(Run M139 cont.)

32A	2	2.557	420	4.369	30	54.74	13.48	0.36	82.13	89.82	73.43	155.00		5.87
32B	2	2.557	420	4.369	30	51.76	11.89	0.34	83.14	89.64	74.27			5.87
33C	2	2.551	420	4.360	30	52.84	21.52	0.37	74.87	84.67	62.41	161.00	Grab sample	5.86
33D	2	2.551	420	4.360	30	52.39	24.41	0.37	72.24	84.81	60.30			5.86
34A	2	2.551	420	4.360	30	55.92	24.39	0.38	72.65	88.21	63.45	161.00	O ₂ @ 470C	5.86
34C	2	2.551	420	4.360	30	54.57	22.73	0.37	73.93	86.72	63.34			5.86
35A	2	2.684	420	4.587	30	61.94	8.52	0.47	90.54	78.46	69.56	165.00		6.16
35C	2	2.684	420	4.587	30	64.14	4.91	0.49	94.47	79.06	73.19			6.16
36A	2	2.606	420	4.454	30	64.72	0.47	0.43	99.37	88.14	87.41	169.00	O ₂ @ 570C	5.98
36B	2	2.606	420	4.454	30	68.91	1.37	0.46	98.31	88.19	86.35			5.98
37B	2	2.849	420	4.868	30	62.86	8.42	0.47	90.63	79.53	70.73	173.00		6.54
37C	2	2.849	420	4.868	30	61.73	6.53	0.46	92.45	79.45	72.18			6.54
38B	2	2.623	420	4.483	30	66.86	4.52	0.48	94.85	82.48	76.99	177.00	O ₂ @520C	6.02
38C	2	2.623	420	4.483	30	64.72	6.71	0.48	92.53	80.37	72.90			6.02
39A	2	2.623	420	4.483	35	61.77	5.57	0.48	93.64	77.83	71.40	181.00		6.02
39C	2	2.623	420	4.483	35	63.82	4.83	0.49	94.56	78.43	72.68			6.02
40A	2	2.554	420	4.365	35	64.98	3.74	0.48	95.69	80.56	75.72	185.00	N ₂ @420C	5.86
40B	2	2.554	420	4.365	35	65.75	6.02	0.48	93.21	81.77	75.06			5.86
41A	2	2.623	420	4.483	35	64.23	10.79	0.47	88.21	82.02	71.06	189.00		6.02
41C	2	2.623	420	4.483	35	62.49	13.90	0.46	85.13	81.09	67.65			6.02
42A	2	2.554	420	4.365	35	65.82	7.76	0.47	91.29	83.33	74.70	193.00	N ₂ @420C	5.86
42B	2	2.554	420	4.365	35	64.92	9.33	0.47	89.65	82.75	72.84			5.86

Run Name: M-137

Catalyst: 17% CeO₂/Al₂O₃, Sud-Chemie, 1.59 mm extrudate

Wt.% DOAc, Feed: 48.87

Pretreatment: air/He@500 °C, Overnight

Feed: 3/1 HOAc/DOAc

Cat. Wt., g: 0.5004

Cat. Bulk den., g/cc: 0.6136

Run M-137 sample	MeOH solution, mL	Vol. rate mL/min	T °C	LHSV	P psig	Wt.% MNK	Wt.% DOAc	MOLS PRODS	%CONV. DOAc	WEIGHT SEL., MNK	MOLAR Y, MNK	TOS h	COMMENT	WHSV
1B	2	0.045	400	3.311	0	44.61	29.47	0.32	64.87	83.36	53.79	7.00		5.19
1C	2	0.045	400	3.311	0	46.11	29.68	0.32	64.85	85.66	55.26			5.19
2A	2	0.047	400	3.433	0	38.43	39.81	0.27	54.07	83.82	44.86	9.50	air/He@520C	5.39
2D	2	0.047	400	3.433	0	38.54	39.83	0.27	54.22	83.56	44.81			5.39
3A	2	0.042	400	3.066	0	25.99	45.84	0.19	42.09	79.83	33.22	15.00		4.81
3B	2	0.042	400	3.066	0	26.27	45.50	0.19	42.45	80.08	33.62			4.81
4B	2	0.045	400	3.328	0	20.53	51.07	0.16	34.67	77.61	26.57	18.50	air/He@540C	5.22
4C	2	0.045	400	3.328	0	20.43	52.47	0.15	33.72	78.26	26.11			5.22
5A	2	0.040	400	2.978	0	29.90	41.92	0.22	47.40	80.84	37.96	24.00		4.67
5B	2	0.040	400	2.978	0	28.63	45.07	0.21	44.95	79.51	35.37			4.67
6A	2	0.045	400	3.328	0	29.93	42.13	0.22	46.98	81.92	38.10	27.50	air/He@540C	5.22
6B	2	0.045	400	3.328	0	28.12	44.46	0.21	44.89	79.42	35.26			5.22
7A	2	0.041	400	3.018	0	44.87	25.26	0.30	67.37	87.59	58.64	33.00		4.73
7B	2	0.041	400	3.018	0	45.00	27.40	0.31	66.24	85.16	56.09			4.73
8A	2	0.042	400	3.066	0	40.09	33.98	0.29	59.14	83.28	48.77	37.00	air/He@540C	4.81
8B	2	0.042	400	3.066	0	42.99	31.25	0.30	62.00	85.92	52.90			4.81
9A	2	0.043	400	3.188	0	34.88	39.44	0.25	52.45	81.96	42.55	42.50		5.00
9C	2	0.043	400	3.188	0	36.65	37.43	0.26	54.89	82.27	44.69			5.00
10A	2	0.043	400	3.153	0	34.70	40.40	0.25	51.64	82.25	42.02	46.00	air/He@540C	4.95
10B	2	0.043	400	3.153	0	35.33	39.76	0.26	52.78	81.29	42.45			4.95
11A	2	0.045	400	3.311	0	33.28	37.94	0.25	53.01	79.42	41.71	53.00		5.19
11B	2	0.045	400	3.311	0	35.25	35.90	0.26	55.23	81.54	44.48			5.19
12A	2	0.042	400	3.066	0	36.08	38.54	0.26	53.90	81.89	43.66	55.00	air/He@540C	4.81
12C	2	0.042	400	3.066	0	36.07	39.97	0.26	53.16	81.48	42.77			4.81
13G	2	0.086	400	7.430	0	17.90	34.59	0.11	36.02	92.82	33.50	60.50		9.98
13I	2	0.086	400	7.430	0	17.23	29.48	0.11	38.99	92.14	36.09			9.98

(Run M137 cont.)

14D	2	0.021	400	1.841	0	54.79	19.93	0.38	76.62	85.34	65.03	65.00	air/He@540C	2.47
14E	2	0.021	400	1.841	0	53.29	22.24	0.37	74.29	84.57	62.33			2.47
15C	2	0.040	350	3.477	0	11.61	37.40	0.08	25.74	90.85	23.32	70.50		4.67
15D	2	0.040	350	3.477	0	12.28	35.18	0.08	27.86	91.59	25.47			4.67
16A	2	0.046	375	3.938	0	23.09	42.09	0.15	37.36	93.19	34.78	74.50	air/He@540C	5.29
16D	2	0.046	375	3.938	0	20.44	46.19	0.13	32.52	93.19	30.21			5.29

Run Name: M-138

Catalyst: 17% CeO₂/0.8% Pd/Al₂O₃, Sud-Chemie, 1.59 mm extrudate

Wt.% DOAc, Feed: 48.87

Pretreatment: air/He@500 °C, Overnight

Feed: 3/1 HOAc/DOAc

Cat. Wt., g: 0.5000

Cat. Bulk den., g/cc: 0.6136

Run M-138 sample	MeOH solution, mL	Vol. rate mL/min	T °C	LHSV	P psig	Wt.% MNK	Wt.% DOAc	MOLS PRODS	%CONV. DOAc	WEIGHT SEL., MNK	MOLAR Y, MNK	TOS h	COMMENT	WHSV
1A	2	0.042	400	3.109	0	51.42	18.95	0.34	75.70	88.96	66.72	5.50		4.88
1B	2	0.042	400	3.109	0	51.70	21.51	0.34	72.90	90.99	65.93			4.88
2A	2	0.041	400	3.021	0	45.90	25.74	0.29	66.37	92.13	60.67	9.00	air/He@520C	4.74
2C	2	0.041	400	3.021	0	44.89	25.63	0.30	66.58	89.91	59.21			4.74
3B	2	0.042	400	3.068	0	45.88	24.99	0.30	67.22	91.03	60.91	15.00		4.81
3C	2	0.042	400	3.068	0	40.86	29.96	0.27	61.21	88.45	53.53			4.81
4B	2	0.042	400	3.068	0	42.30	29.55	0.28	62.00	89.77	55.04	18.00	air/He@520C	4.81
4C	2	0.042	400	3.068	0	43.53	28.47	0.28	63.16	91.00	56.99			4.81
5B	2	0.042	400	3.109	0	44.64	21.29	0.28	69.73	92.60	64.21	23.50		4.88
5C	2	0.042	400	3.109	0	46.79	19.46	0.29	72.27	93.73	67.46			4.88
6B	2	0.044	400	3.210	0	45.87	18.39	0.29	72.86	94.36	68.49	27.00	air/He@520C	5.03
6C	2	0.044	400	3.210	0	43.71	23.60	0.27	66.65	94.03	62.48			5.03
7A	2	0.042	400	3.068	0	38.63	33.66	0.25	56.41	90.45	50.61	32.50		4.81
7C	2	0.042	400	3.068	0	37.77	35.45	0.25	54.47	90.74	49.08			4.81
8E	2	0.042	400	3.068	0	37.73	32.53	0.25	57.00	89.36	50.46	36.00	air/He@520C	4.81
8F	2	0.042	400	3.068	0	35.21	37.46	0.24	51.97	88.78	45.66			4.81

Run Name: M-135

Catalyst: 17% CeO₂/2.4% Co/Al₂O₃, Sud-Chemie, 1.59 mm extrudate

Wt.% DOAc, Feed: 48.87

Pretreatment: air/He@500 °C, Overnight

Feed: 3/1 HOAc/DOAc

Cat. Wt., g: 0.5001

Cat. Bulk den., g/cc: 0.6136

Run M-135 sample	MeOH solution, mL	Vol. rate mL/min	T °C	LHSV	P psig	Wt.% MNK	Wt.% DOAc	MOLS PRODS	%CONV. DOAc	WEIGHT SEL., MNK	MOLAR Y, MNK	TOS h	COMMENT	WHSV
1B	2	0.043	400	3.167	0	48.31	24.47	0.34	70.24	84.80	59.44	5.83		4.97
1C	2	0.043	400	3.167	0	48.72	29.25	0.34	66.99	83.62	55.62			4.97
2A	2	0.042	400	3.100	0	45.30	32.62	0.32	63.03	83.13	51.94	9.00	air\He@520C	4.86
2B	2	0.042	400	3.100	0	48.44	30.29	0.33	65.39	86.48	56.01			4.86
3B	2	0.042	400	3.067	0	49.97	28.17	0.34	67.71	86.29	57.95	15.00		4.81
3C	2	0.042	400	3.067	0	48.17	29.21	0.34	66.67	84.34	55.62			4.81
4B	2	0.044	400	3.272	0	44.11	35.56	0.32	60.81	82.11	49.17	18.00	air\He@520C	5.13
4C	2	0.044	400	3.272	0	44.64	33.74	0.32	62.03	82.96	50.84			5.13
5A	2	0.107	400	7.853	0	19.94	47.73	0.14	33.34	85.50	28.17	22.42		12.32
5C	2	0.107	400	7.853	0	20.74	47.99	0.14	33.60	87.16	29.04			12.32
6A	2	0.021	400	1.578	0	62.37	8.17	0.51	91.47	67.84	65.86	26.25	air\He@520C	2.47
6C	2	0.021	400	1.578	0	62.92	9.09	0.50	90.51	74.18	66.45			2.47
7B	2	0.042	350	3.067	0	10.15	56.44	0.07	17.98	83.71	14.93	27.42		4.81
7C	2	0.042	350	3.067	0	10.71	54.35	0.07	18.94	85.89	16.16			4.81
8A	2	0.043	375	3.136	0	29.82	43.87	0.20	43.97	88.51	38.53	31.42	air\He@520C	4.92
8B	2	0.043	375	3.136	0	30.35	42.37	0.20	45.32	88.40	39.63			4.92

VITA

Arvind K Bhat was born in 1973, to Venkatesh and Asha Bhat, in Udupi, India. He completed his high school education in Mangalore. He was accepted by the Karnataka Regional Engineering College, Mangalore University, India, into the chemical engineering program and earned a Bachelor of Engineering degree in 1995. Upon graduation he worked for five years, first as a process engineer with Grasim Industries Ltd. and later as a senior engineer with Essar Oil Ltd. In 2001, he entered the Graduate Program at Louisiana State University in Baton Rouge, Louisiana. This thesis completes his requirements to receive the degree of Master of Science in Chemical Engineering.